ÇUKUROVA UNIVERSITY
INSTITUTE OF NATURAL AND APPLIED SCIENCES

PhD THESIS

Mohamed HUSSEIN

THE USE OF INTER-SPECIFIC PROTEIN COMPLEMENTATION APPROACH TO UNDERSTAND THE ROLE OF LOCALISED REPLICATION IN PLANT VIRUS CELL-TO-CELL TRANSPORT THROUGH PLASMODESMATA

DEPARTMENT OF PLANT PROTECTION

ADANA-2022

ABSTRACT

PhD THESIS

THE USE OF INTER-SPECIFIC COMPLEMENTATION APPROACH TO UNDERSTAND THE ROLE OF LOCALISED REPLICATION IN PLANT VIRUS CELL-TO-CELL TRANSPORT THROUGH PLASMODESMATA

Mohamed HUSSEIN

ÇUKUROVA UNIVERSITY
INSTITUTE OF NATURAL AND APPLIED SCIENCES
DEPARTMENT OF PLANT PROTECTION

Supervisor : Assoc. Prof. Dr. Muharrem A. KAMBEROĞLU
Assoc. Prof. Dr. Jens TILSNER
Year: 2022, Pages: 153
Jury : Assoc. Prof. Dr. Muharrem A. KAMBEROĞLU
: Prof. Dr. Saadettin BALOĞLU
: Prof. Dr. Gülşen SERTKAYA
: Prof. Dr. Miray SÖKMEN
: Assoc. Prof. Dr. Bahri Devrim ÖZCAN

The only way for plant viruses to spread through their hosts is transport of viral genomes through plasmodesmata (PD) with the aid of virus-encoded movement proteins (MPs), which can target and open PD and bind nucleic acids. This transport typically happens early during infection, when viral genomes are not yet abundant, in order to escape non-cell-autonomous defence signalling and mobile RNA silencing. However, none of the MPs characterised to date show any sequence specificity, raising the question whether transport is selective and how this occurs. The RNA virus, Potato virus X targets some of its replication sites to the entrances of plasmodesmata (PD), where it may insert newly synthesized viral RNA directly into the channels (co-replicational movement). Complementation of movement by ectopic MPs is widespread amongst plant viruses and provides a way to dissect the mechanism and significance of localised replication. In this study, PVX-based plasmid vector is constructed by modifying it to express the 30K MP of Tobacco mosaic virus, instead of its cognate triple gene block (TGB) proteins, which are responsible for cell to cell transport of PVX. Using a new, highly sensitive RNA imaging system based on the high-affinity RNA binding protein Csy4 which can track viral genomes within PD, it is shown that PVX with in cis movement complmentation, nonetheless, is still capable of forming PD-associated replication sites, suggesting that MPs may recruit viral replicases non-specifically through mutual interactions with the same RNA molecule(s) or host proteins.

Key Words: PVX, Confocal microscopy, Complementation, Cell-to-cell movement

ÖZET

DOKTORA TEZİ

PLAMODESMATA YOLUYLA HÜCREDEN HÜCREYE BİTKİ VİRÜS TAŞINMASINDA LOKALİZE REPLİKASYONUN ROLÜNÜN ANLAŞILMASI İÇİN TÜRLER ARASI PROTEİN TAMAMLAMA STRATEJİSİNİN KULLANIMI

Mohamed HUSSEIN

ÇUKUROVA ÜNİVERSİTESİ
FEN BİLİMLERİ ENSTİTÜSÜ
BİTKİ KORUMA ANABİLİM DALI

Danışman : Doç. Dr. Muharrem A. KAMBEROĞLU
Doç. Dr. Jens TILSNER
Year: 2020, Page: 153
Jüri : Doç. Dr. Muharrem A. KAMBEROĞLU
: Prof. Dr. Saadettin BALOĞLU
: Prof. Dr. Gülşen SERTKAYA
: Prof. Dr. Miray ARLI SÖKMEN
: Doç. Dr. Bahri Devrim ÖZCAN

Bitki virüslerinin konukçuda yayılmasının tek yolu, plamodesmata (PD)'yı hedefleyebilen ve açabilen ve nükleik asitleri bağlayabilen virüs kodlu hareket proteinleri (MP) yardımıyla viral genomların PD'dan geçiş yaparak taşınmasıdır. Bu taşınma tipik olarak, hücre dışı otonom savunma sinyalizasyonu ve mobil RNA susturma işleminden kaçmak için viral genomların henüz bol olmadığı enfeksiyonun erken döneminde gerçekleşir. Bununla birlikte, bugüne kadar karakterize edilen MP'lerin hiçbiri herhangi bir dizi özgüllüğü göstermemekte, bu da taşımanın seçici olup olmadığı ve nasıl olduğu sorusunu gündeme getirmektedir. Genomu RNA olan virüsler arasında yer alan Patates X virüsü, replikasyon alanlarından bazılarını, yeni sentezlenmiş viral RNA'yı doğrudan kanallara yerleştirebilecekleri plazmodesmata girişlerine yöneltmektedir (eş replikasyonal-hareket). Ektopik MP'ler tarafından hareketin tamamlanması bitki virüsleri arasında yaygın bir olaydır ve lokalize replikasyonun mekanizmasını ve önemini incelemek için bir yol sağlar. Bu çalışmada, PVX'in hücreden hücreye taşınmasından sorumlu olan üçlü gen bloğu (TGB) yerine, Tütün mozayik virüsü'nün 30K hareket proteinini ifade etmek üzere modifiye edilen PVX-temelli plasmid vektör oluşturulmuştur. PD içindeki viral genomları takip edebilen yüksek afiniteli RNA bağlayıcı protein Csy4'e dayanan yeni, oldukça hassas bir RNA görüntüleme sistemi kullanılarak, PVX in PD-ilişkili replikasyon yerleri oluşturduğu gösterilmiştir. Bu sonuç, MP'lerin, aynı RNA molekülü/molekülleri veya konukçu proteinler ile karşılıklı etkileşimler yoluyla viral replikazları spesifik olmayan bir şekilde bir araya getirdiğini düşündürmüştür.

Anahtar Kelimeler: PVX, konfokal mikroskopi, tamamlama, Hücreden hücreye hareket

EXTENDED ABSTRACT

Animal cells communicate through signal transmitted in their membranes, that are adherently continuous. However, plant cells have their membranes separated with rigid cell walls except at intervening nanopores known as plasmodesmata (PD), to facilitate intercellular communication. Whereas plant cell walls contribute to apoplastic transmission of some signal factors, which is mainly for short range distance, most of signals controlling developmental and physiological processes is facilitated with symplastic transmission via PD. These PD, that can be found branched or in groups, are membranous intercellular channels, allowing continuousness of ER and plasma membranes between contiguous plant cells. A desmotubule, evidenced to be an ER-connector penetrating within PD, participates mainly in lipophilic signal transmission and divides the PD into two narrow subchannels with protein rings or spokes linked both plasma membranes to desmutuble, that are thought to contribute in PD gating through their constriction, and, hence, control the transport of macromolecules passing through not only based on their sizes but also on their membrane association ability.

Many molecular tools and disciplines of sciences are used to help understand this dynamic tiny membranous organelle, including confocal microscopy, protein tagging, and plant virology. Tobacco mosaic virus (TMV) and Potato virus X (PVX) are two viruses that made a significant impact on our understanding of PD. They are proteinous particles enclosing a piece of (+ sense) ssRNA. Once these RNA strands are introduced into the cell, the messages they carry can be directly translated, and viral proteins, attacking cell machineries, are launched on virus multiplication and spread.

The first message read on the PVX genomic RNA (gRNA) is to clone itself via expressing the 5 prime ORF into a replicating enzyme (165kD), which is an RNA-dependent RNA polymerase RdRp of viral origin. At the onset of RdRp expression, it recognizes certain sequencing or configuration stem loops on the

vRNA template strand to execute on replicating it, we refer to this process as co-translational replication. Transcribing RNA in the cytoplasm of the robust cells seems so alien. Therefore, viruses conceal and compartmentalize their RNA replication in sub-cellular membrane-bound compartments, resulting in virus replication complexes, in their infected cells. These complexes are considered sites/factories of replication and found associated with rearranged host membranes sheltering viral genomes with the help of other viral and host proteins.

Other viral proteins indispensable for virus movement are encoded from intermediates vRNAs during PVX replication: coat protein CP (P27) from sub-genomic RNA1 (sgRNA1), and the triple gene block (TGB) encoded three proteins; TGBp1 (P25) from sgRNA2, and TGBp2-3 (P12 and P8, respectively) from sgRNA3. Associated with sever virus infection is the development of cytoplasmic and perinuclear virus inclusion bodies, their function was not known for years that they were solely depicted as X-bodies. The infected cells are directed to express for the virus. However, the viral proteins are not directly excessively increased in number upon infection. They are rather gradually de novo synthesized, emphasizing a metabolic state difference in the recent and late infected cells. At the infection edge, where virus has not yet fully colonized the cell nor has directed it for overproduction of viral proteins, a degree of interaction between viral proteins at their very diluted concentrations as small as femto-molar in unit can still be facilitated for successful virus establishment. As such, quantitative studies of PVX encoding proteins have been studied at different biological life time of the virus as early as 1 hpi and Jens lab has recently described a linkage between the movement and replication virus factors that are spatially enclosed within cap structures near PD orifices at the recently infected cells or complexed together within peri-nuclear or cytoplasmic x-bodies at later stages of infection. Here we show the role of PVX-proteins and their localization in their ectopic expression and their possible recruitment factor as encoded during the virus infection.

All viral infection processes require the expression of viral proteins. Some of the proteins transcribed/translated from one virus can fulfil their function also in the context of infection by another unrelated virus. This complementation is well established among many plant virus movement proteins (MP), which assist in the transport of plant viruses between cells via small nanopores in their walls, known as plasmodesmata (PD). At least one MP of all plant viruses can show nuclic acid binding ability. That with the assistance of MPs, plant viral genomes exit the living cell where they replicate to commence further infections in the following cells they enter. However, this binding ability with their cognate viral RNA (vRNA) is sequence non-specific, i.e. any MP can complement the movement of many unrelated viral genomes. How do then the MPs pick up their viral cargo, especially that the virus movement occurs at the early infection state when vRNAs are in scarce level compared to cellular RNA? In plants, viruses move their genomes in different travelling forms complexing them with viral and cellular proteins.

At the leading edge of PVX-infection, where virus progenies are actively moving cell-to-cell, Tilsner et al. (2013) have recently found that viral replication 'factories' can become anchored directly at the entrances of plasmodesmata inside endoplasmic reticulum–derived membranous caps. Inside these caps occurs a series of events, resulting in the co-replicational insertion of nascent vRNA into the PD channels; to facilitate vRNA progeny spread without having to travel through the cytoplasm where it may be attacked by cellular defense mechanisms such as RNA silencing.

His model has emphasized the localized virus replication through close spatial links between vRNA-replicating enzyme complex and virus movement proteins near the PD orifices. Some other cellular factors can enhance these links. The PVX-TGBps function to compartmentalize replication complexes at PD for localized RNA synthesis, contributing to the species-specificity of plant virus RNA cell-to-cell movement through close spatial links between replication and movement of the virus near the PD orifices. TGBps-deficit PVX mutants were shown to be

incapable of moving between cells; complementing with 30K, another movement protein encoded from TMV, was, however, able to rescue the virus. I questioned how co-replicational virus transport may be possible in such situations, where non-cognate replication proteins and MPs have to cooperate for transport. In a PVX expression vector, we, therefore, swapped the coding regions of TGBps with 30K resulting in an infecting virus -this swapped virus is termed as JTM003- able to both replicate and move between a few cells, which allows tracking the subcellular localization of the PVX replicase in the absence of TGBps at the infection border. Ectopic expression of GFP-tagged replicase in the context of the swapped virus (JTM003) infection showed the localization of the replicase inside cap structures next to the PD. Moreover, by using RNA live-imaging system, these cap structures were found to be rich in the naked vRNA as well, indicating a recruitment of replication complex occurs in them. However, the TGBs are all gone in JTM003, so that leaves only vRNA or host proteins to mediate the recruitment of replication sites to PD by TMV 30k.

The coupling of movement and replication at the PD is an accepted model by Tilsner (2013) to account for the preferential transport of viral, rather than cellular RNA by sequence-non-specific MPs. In Potato virus X (PVX), the subject of my study, the PD targeting is mediated by the triple gene block (TGB) movement proteins. However, it remains unclear how they recruit replication complexes to PD. In this study, PVX is modified in a reverse genetics system, where the TGBs responsible for the PVX movement are deleted and replaced with the TMV movement protein (30K). Tagging with fluorescent proteins of the virus replicase and using in vivo RNA imaging techniques, viral replication complexes can be detected in terms of this movement complementation system. Movement-deficient PVX can only produce bright fluorescent single cells since the virus can still replicate even though it cannot move. As expected, the TMV 30K has assisted in the movement of the TGB1-3-truncated PVX but to only a maximum of one-to-two cell boundaries. Probably the infection of TGBp1-deficient virus is blocked by the

cellular RNA silencing machinery, and the virus could not move further due to the loss of the TGBp1, which acts as an RNA silencing suppressor protein. However, bombardment of this virus movement complementation system into tissue already ecotopically expressing 19K silencing suppressor develops some bigger viral lesions. The virus in those big lesions has crossed an average of 10 cell-boundaries, demonstrating the successful co-complementation of the PVX lacking TGBp1-3 by TMV30k-MP together with 19K.

PD-associated cap structures are analysed to contain both vRNA progenies and replicases of this PVX construct that is modified to express the 30K MP instead of its cognate TGB, indicating that co-compartmentalisation of replication and movement may happen non-specifically either by a mutual interaction with common host proteins or via the binding to the same vRNA molecules.

ACKNOWLEDGEMENTS

To start off I should acknowledge God for giving me reasons and guiding me throughout my experiment and thesis work. All praise be to Him; Allah, our self-sufficient. “Pay thanks to the man who has done a favor for you” said by His beloved prophet Muhammed –peace and blessings be upon him-, I therefore have to thank firstly my Turkish supervisor Assoc. Prof. Dr. Muharrem Arap KAMBEROĞLU for his patience and unlimited efforts to draw guidelines for my thesis work so as to be done on time. I have also a due acknowledgement to Assoc. Prof. Dr. Jens TILSNER for giving me space in his laboratory to work for my thesis experiment and welcoming me during my stay in Scotland. “Rise for the teacher in due reverence, A teacher is akin to an apostle.” My sincere gratitude to my dearest Jens, who I will always consider to be my teacher. His PhD student, David BURNETT was giving me a very helpful hand and advices that developed my thesis work a lot, Thank you David. In addition, I want to thank Graham, Wendy, Alison, Sean, and Sarah from James Hutton Institute for all of their help and wise counsel. I also acknowledge Prof. Dr. Sadettin BALOĞLU the group leader of plant virology laboratory and all other professors working in the plant protection department at Cukurova University. I owe a debt of gratitude and respect to my friends, classmates, lab partners, lab technicians, and other lab assistants. Thank you to the Institute of Graduate Research and Science for accepting my thesis and foremost to Mr. Yusuf DEMIRÖZ for removing any monotony for any paperwork done through his office. To my parents, sibilings and other family members for their continuous encouragement, I owe you all my kind respect and thanks.

CONTENTS **PAGE**

LIST OF TABLES **PAGE**

LIST OF FIGURES **PAGE**

SYMBOLS AND ABBREVIATIONS

30K : The TMV movement protein
a.a. : Amino acid
ABP : Actin-binding proteins/adaptors
ADF2 : Actin-depolymerizing factor 2
ATM1 : *Arabidopsis thaliana* myosin 1
ATP : Adenin triphosphate
BDM : Butanedione monoxime
BFA : Brefeldin A
BSMV : Barley stripe mosaic virus
BYV : *Beet yellows virus*
CCT : chaperonin-containing TCP-1
CfMV : Cocksfoot mottle virus
CLS : Confocal laser scanning microscopy
CMV : *Cucumber mosaic virus*
CP : Coat protein
CP : Coat protein
CytB : Cytochalasin B
CytD : Cytochalasin D
dpi : days post inoculation
EID : Emerged infectious diseases
ER : Endoplasmic reticulum
ER : Endoplasmic reticulum
gat1 : gfp arrested trafficking
GC : Closed Gate
GFLV : *Grapevine fanleaf virus*
GO : Gate Open
gRNA : genomic RNA

GSL	: Glucan-synthase-like
GTP	: Guanin triphposphate
Hsp70h	: Heat shock protein 70 homologue
hTalin	: Human talin
IF	: Intermediate filament
ise1	: Increased size exclusion limit
LatB	: Latrunculin B
MAP	: MT-associated proteins
MCS	: Membrane contact site
MF	: Microfilaments
MOs	: Microorganisms
MP	: Movement protein
MT	: Microtubules
N-protein	: Nucleopcapsid protein of TSWV
NCAP	: Non-cell-autonomous protein
NCAPs	: Non-cell-autonomous proteins
NCATFs	: Non-cell-autonomous transcription factors
NET1A	: NETWORK 1A
nt	: Nucleotide
NTR	: Nontranslated region
OAS	: Origin of assembly
ORF	: Open reading frames
P12 kDa	: The PVX TGBp2
P126 kDa	: The TMV replicase
P25 kDa	: The PVX TGBp1
P30 kDa	: The TMV
P8 kDa	: The PVX TGBp3
PAPK	: Plasmodesmal associated kinase
PD	: Plasmodesmata

PDCBs : PD callose-binding proteins
PDLP : PD-located proteins
PLRV : *Potato leaf roll virus*
PLS : Plasmodesmal localization signal
PM : Plasma membrane
PM : Plasma membrane
PMTV : *Potato mop-top virus*
PVA : Potato virus A
PVX : *Potato virus X*
PVY : Potato virus Y
R : Protein-mediated resistance
RdRNA pol. : RNA-dependent RNA polymerase
RdRP : RNA-dependent RNA polymerases
REM : Remorin
RL : Rod-like
RNA : Ribonucleic acid
RNP : Ribonucleoprotein
ROS : Reactive oxygen species
RSV : *Rice stripe virus*
RTN : Reticulons
SA : Salicylic acid
SAR : Systemic acquired resistance
SEL : Size exclusion limit
SEL : Size exclusion limit
SL : Stem–loop secondary RNA structures
smRNAs : Small RNAs
SMV : *Soybean mosaic virus*
ssRNA : Single-stranded ribonucleic acid
STP : Single-tailed particles

subgRNA : subgenomic RNA
TEM : Transmission electron microscopy
TEV : *Tobacco etch virus*
TGB : Triple gene block
TMV : *Tobacco mosaic virus*
tsTMV : temperature sensitive TMV mutant
TSWV : *Tomato spotted wilt virus*
TSWV : *Tomato spotted wilt virus*
TuMV : *Turnip mosaic virus*
TVCV : *Turnip vein clearing virus*
VLP : Virus like particles
VRC : Virus replication complexes
VRC : Viral replication complex
vRNA : Viral ribonucleic acid

1. INTRODUCTION

The systemic and local accumulation of viruses in plants is related to the speed of viral cell-to-cell movement and understanding it at the molecular level would extend to implementing new antiviral approaches. In plants, viruses move their genomes in different travelling forms complexed with viral and cellular proteins and regulated under several distinct host cellular trafficking pathways (Heinlein, 2015). All plant viruses need to move cell-to-cell through narrow cell-membrane-lined pores known as plasmodesmata (PD), traversing the cell wall barriers. This is a crucial infection step, and a real bottleneck (as only few genomes initiate infection in the next cell), so potentially a good target for antiviral crop protection strategies, if we understood it better (Rodrigo et al., 2014). The genomes of the majority of plant viruses consist of ribonucleic acids (RNAs), encode few proteins, and are specifically encapsidated within virally encoded coat protein (CP). Unlike animal and human viruses, they also encode additional protein(s) that aid in their movement between the cell-walled host cells. These movement proteins (MPs) are encoded from a single gene entity, as in Tobacco mosaic virus (TMV), or from several overlapping gene blocks, as in Potato virus X (PVX); some can function alone while other require an ancillary/helper protein(s) where CP is indispensable for local movement (Lucas, 2006; Tilsner et al., 2014; Kellmann, 2001). Of all known plant viruses, at least one MP's main function is to move between plant cells via targeting and modifying the PD and exhibiting cooperative binding affinity to single-stranded ribonucleic acids (ssRNAs) in a sequence nonspecific manner. In the infection context, MPs are thought to attach co-translationally to their viral RNAs (vRNAs) in the proximity and deliver them into the PD. From there, and during an early event of infection they export the vRNAs to the next cell, before they lose that capability as subsequent degradation of the MP has been observed at later infection stages (Heinlein, 2015; Tilsner et al., 2014). The transport of MPs between cells can be in their simple manner or complexed form: either alone or combined with the RNA as

a ribonucleoprotein (RNP) complex (e.g. TMV 30 kDa MP) or together with the CP in a partially or fully assembled virion complex (e.g. PVX TGBp1-3) (Heinlein, 2015; Tilsner et al., 2014; Kellmann, 2001; Lucas, 2006). Early studies of MPs showed their interchangeable activity that they are able to complement the cell-to-cell trafficking of unrelated viruses, and independent on the infection. A question is to be posed about how the MPs can fetch their viral cargo in the infected cells, or how they can discriminate the RNA of the viral origin from the cellular one. This could be explained through close spatial links between replication and movement of the virus (Tilsner and Oparka, 2012). In infected cells, the infectious (+) vRNAs are likely complexes with their replicating enzymes, move and replicate in association with the endoplasmic reticulum (ER). These viral replication complexes (VRC) may aggregate into virus factories and fill in the cell space with many virus progenies that are seen at later stages of infections. However, at the leading edge of infection, even as the virus RNA titer is much lower than the cellular RNAs, it still crosses the cell-to-cell PD channels to spread intercellularly. Recent in vivo studies of the TMV-30K (Levy et al., 2015) and PVX-TGB (Tilsner et al., 2013) proteins have shown their association with the VRCs, forming subcellular co-compartments that anchor next to the PD at early infection stages. This suggests that co-compartmentalisation might contribute to the species-specificity of plant virus RNA cell-to-cell movement. Anchoring of these early VRCs next to the entrances of PD may also permit newly produced viruses to be inserted into the PD channel directly from the replicating enzymes, without the vRNA traveling through the cytoplasm (Tilsner et al., 2013) where it could be attacked by cellular defense mechanisms such as RNA silencing. Since it is generally assumed that MP are doing the targeting to PD, not the replication proteins, this additional function of MP recruiting the VRC to PD may therefore accomplish certain specificity by developing some compatibility between the sequence-non-specific RNA binding MPs and virus encoded-replication proteins, that are highly specific binders to their cognate viral genome.

We suggest in this study that direct interaction between the viral replication enzyme protein and one of the MP components is not necessary for the successful transport of its cognate viral genome as an MP-containing complex (Fig. 1.B). We believe that the co-binding of these two different proteins to the same RNA molecule, destined to be anchored near the PD (in Fig. 1.A) will instead be the crucial factor determining which RNA is preferred in cell-to-cell tranport. That explains why viral rather than cellular RNAs are trafficked by various MPs, that show no signs of any sequence-specificity.

The main objective of this study is to establish a complementation movement system where localized PD-replication is examined. If the protein:protein interaction was the one recruiting the replicase to PD, we would expect that the recombinant PVX with 30k replacing TGB would not be able to recruit replicase to PD. Without localised replication, the speed of movement might be reduced. In order to test this, a complementation experiment is conducted where non-cognate movement and replication proteins are involved. It will be studied using live-cell imaging at the leading edge of infection in *Nicotiana benthamiana* leaves. Infectious clones will be constructed by replacing the TGB1/2/3 movement proteins of PVX with the single 30k movement protein of TMV. Parallel experiments will attempt to visualize the active PVX RNA dependent RNA polymerase (RdRNA pol.). This will also add to the analysis of how the virus recruits its replication complexes subcellularly to interact with MP during infection. The RNA replicase of an infectious PVX construct will be tagged by the insertion of different fluorescent proteins including large GFP and small iLOV, or alternatively small peptide tags that can be recognized by fluorescent reporter constructs.

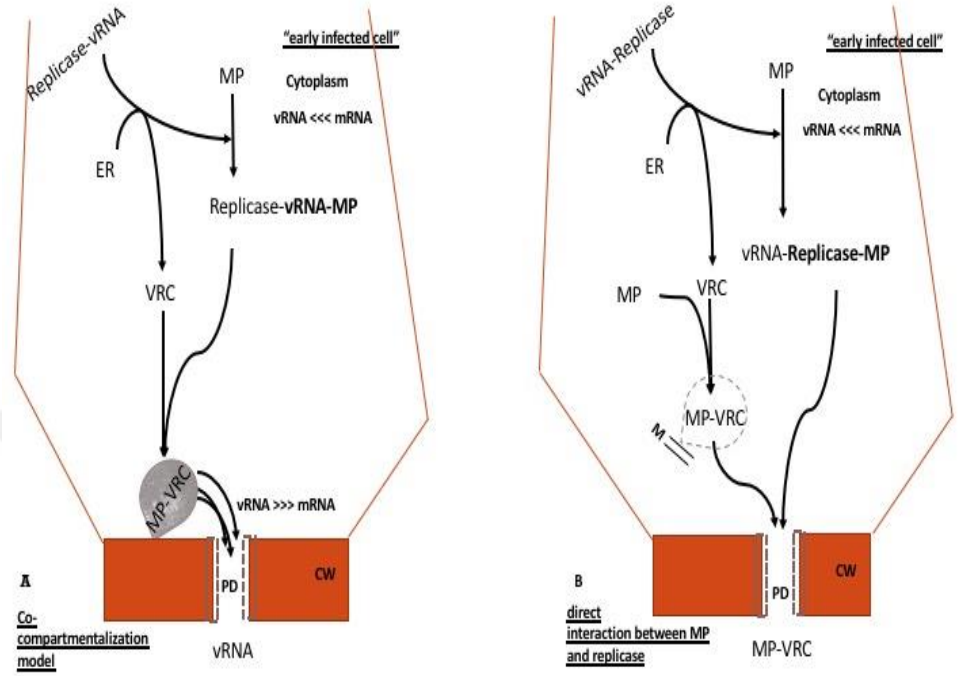

Figure 1.1. Two simplified models of plant virus RNA intercellular transport

Two simplified models are proposed in this study to describe the species specificity during plant virus RNA intercellular transport via pores traversing the plant cell wall (CW), termed as plasmodesmata (PD). Viral movement proteins (MPs) encoded from plant virus RNA (vRNA) can dilate PD (dashed rectangle) and target them with the viral cargo captured through A) their non-sequence-specific binding ability to RNA that is also bound by the viral replicase (Replicase-vRNA-MP) or B) a possible protein-protein interaction with the vRNA-encoded replicase which in turn travels with the vRNA specifically associated with it (vRNA-Replicase-MP). Both of the models refer only to the vRNA being limited in abundance compared with cellular messenger RNA (mRNA) (vRNA <<<< mRNA), a typical situation at early stages of infection when virus movement occurs. Model A applies for the MPs indirectly recruiting the replicases, both of which bind to the same vRNA, and having the nascent viral progeny localized in caps (grey circle)

next to the PD and synthesized in their vicinity for directional trafficking between the cells (co-compartmentalization model). These replicating enzymes associated with the endoplasmic reticulum (ER) as virus replication complex (VRC) can travel through different pathways inside the cell till they anchor with the help of the co-translation of viral gene(s) for MP at the PD orifices where viral replication products are then inserted and exported intercellularly. However, in model B, the virally encoded replicases bind specifically to the viral genomes they are encoded from, and are hypothesized to interact directly with the MPs for the virus cellular trafficking. The specificity of binding between replicases and MP will assure the transport of vRNA as an MP-containing-VRC complex (MP-VRC). Therefore, it indicates that the co-compartmentalisation may not need to happen (dashed circle) unless it is an inevitable corollary of the virus life cycle. It will not thereupon be necessarily recruited at the PD but probably somewhere else (the double lines M: internal membranes) and in this case it is likely that a further intracellular mechanism for transport from this site of replication to the PD will have to precede the virus cell-to-cell movement steps.

2. BACKGROUND AND LITERATURE REVIEW

2.1. Drivers of Viral Pathogen Pollution in Plants

The climatic change puts the crop production in risk, influencing the global food security and plant biodiversity. This risk is exacerbated by the increasingly severe virus epidemics, which is also a direct or indirect consequence of diverse climate change parameters (as regards the assessments of the impact of climate alterations on the plant virus epidemics, refer to Table 1 in Jones, 2016). The adaptive evolution of plant viruses when confronted with complex environments accounts for their throughout spread and possible cause of newly emerged diseases. As a consequence of this and the other drivers of viral pathogen pollution, nearly half of the reported plant emerged infectious diseases (EID) are caused by plant viruses, posing them as one of the major threats to both cultivated and wild vegetation (Lefeuvre et al., 2019; Anderson et al., 2004). The plant viruses can be considered as obligatory generalist parasites, that can invade and colonize in a wide range of plant hosts and cause disease by diverting plant host machineries allowing their own expansion within the host (García-Arenal et al., 2013; Bera et al., 2018). However, these host plants do not passively surrender to the invasion, some have evolved intricate antiviral resistance mechanisms to mitigate the impact of the infection by the restriction of virus load augmentation and movement displacement. RNA-silencing and protein-mediated resistance (R) pathways of the host in response to viral invasion are the two major strategies to counter the risk of virus infections in plants. As a counteract response, some viral proteins are evolved to help the virus escape these defense levels of host surveillance and allow its systemic accumulation (Paudel and Sanfaçon, 2018). Central to the local and systemic virus infection in plants is the speed of viral cell-to-cell movement and understanding it at the molecular level would extend to implementing new antiviral approaches (Rodrigo et al., 2014).

2.2. Understanding the Movement Inside the Cell

2.2.1. Relative Plant Cell Movement

Unlike animal cells, plant cells are commonly known to be immobile, thanks to the interlinked network of cellulosic microfibers that create rigid cell walls to support the plant cells and prevent any form of cell sliding. There shall be certain mechanisms creating some weakening points in the wall rigidity to allow the cell expansion during plant cellular growth and development (Bidhendi and Geitmann, 2016). Cell motility in plants has been only reviewed when parts of the cell are relatively changing the position compared to other cells. This relative movement of plant cells is briefly discussed in Lev-Yadun, 2015, 2001. In which case the growing cell can also intrude other groups of cells as well-known as the "**intrusive growth**" in most vascular plants. In a plant tissue, the penetration of their self-cells during the intrusive growth is distinguished from the invasion of a foreign pathogenic or symbiotic cell by a mechanism that has to be furtherly elaborated (Lev-Yadun, 2001; Lev-Yadun, 2015).

2.2.2. Plant Cytoskeleton

Most eukaryotic animal cells may move, usually/typically in the form of a crawl, by using the internal force produced by the **cytoskeleton** system (Ananthakrishnan and Ehrlicher, 2007). Some cells, however, have a mechanical motor in protrusions of the outside to propel and achieve a faster swimming movement; vascular plants do not require such cells, except for some plant sperm (Southworth and Cresti, 1997). In plants, the cytoskeleton is a crucial dynamic factor in a variety of cyto-biological processes. Most significantly, it controls the intracellular movement and positioning of proteins, vesicles and organelles inside the cell, which is correlated with how the cell responds to external abiotic (light, for example) and biotic (pathogens, for example) stimuli (Takemoto and Hardham, 2004; Porter and Day, 2016). Microtubules (MT), microfilaments (MF, also called actin filament), and intermediate filament (IF) are three biopolymers that make up

the cytoskeleton. MT (stiff tubule, 25 nm in diameter) and MF (semi-flexible filament, 5 - 9 nm in diameter, several micrometers long), the main components of the plant cytoskeleton, are networks of filamentous proteins made up of compact and globular tubulin (molecular weight of ~50 kDa) and actin (molecular mass of 42 kDa) subunits, respectively, plus other associated proteins like the molecular motor protein: kinesin and myosin. Although they vary in terms of rigidity and composition, they share some important properties, such as being polar, treadmill and capable of exerting forces upon polymerization (Kost and Chua, 2002). Each filament is polarized because one of its ends, the leading or plus/barbed end, grows asymmetrically, 10 times faster than the other, the lagging or minus/pointed end. They can also disassemble at the one growing end very quickly and according to the cell needs, and this dynamic instability and other dynamic characteristics including nucleation (the formation of a new filament), polymerization (the addition of subunits at the plus end that results in lengthening), depolymerization (the removal of subunits at the minus end that results in shortening) and treadmilling (the increase of the filament length at one end is countered by the shrinkage at the other end) are shaped by several cytoskeleton-associated proteins and directed by the hydrolysis and binding of GTP and ATP, which associate with MT-tubulin and MF-actin monomers, respectively (Reddy, 2001; He et al., 2020).

Cells have many proteins to regulate the stability, crosslinking, capping, severing, and degradation of the cytoskeleton filaments. The **motor proteins**, for instance, are a group of cytoskeleton-associated proteins that can convert chemical energy stored in the cytoskeleton into mechanical energy employed in the intracellular transport of a variety of molecules or cellular structures. They act as "vehicles," using the cytoskeleton as "tracks," and ATP as "fuel" to transport their "cargo" inside the cell. In plants, two motor proteins are identified: myosins (actin-based motors) and kinesins (microtubule-based motors). These molecular motors move along the cytoskeleton filaments in a directed manner (Reddy, 2001). In order to replace the dynein animal motor, which is lacking in plants, plants have expanded

their kinesins, constituting 10 of the 14 recognized kinesin subfamilies. The bulk of these kinesins belong to subfamilies 7 and 9 (Gicking et al., 2018; Ali and Yang, 2020). However, of the 35 different myosin classes, there are just two myosin classes in land plants: class XI has fewer members and myosin VIII makes up the majority (Tominaga and Nakano, 2012). At its N-terminus, myosin has a head motor domain that binds with the actin filament and hydrolyzes ATP to transport a cargo specifically connected to a long, rod-like tail structure at its C-terminus in the direction of the filament's plus end, that extends outwards to the periphery. Similar to this, kinesins include head and tail domains, and the motor domain of a conventional kinesin is located at the amino-terminal and often directed toward the MT-plus end. In addition, numerous plant kinesins have been found to have carboxyl-terminal motor domains that move in the direction of the MT-minus end. The motor domains of these motile kinesins are metabolically/enzymatically active with ATP- and microtubule-binding sites. Kinesins with a centrally positioned motor domain often depolymerize microtubules from the ends rather than moving, however (Reddy, 2001; Nebenführ and Dixit, 2018). Microtubule-kinesins are in charge of moving heavy intracellular cargo, such as during the formation of a new cell wall, while the actin-myosin system is predominantly in charge of most of the transport in the cell, as well as the long-distance movements like the cytoplasmic streaming of many organelles (Geitmann and Nebenführ, 2015; Niehl et al., 2013). It should be noted, however, that cross-talks between the two cytoskeletal components exist (as reviewed by Collings, 2008; Schneider and Persson, 2015).

Some plant cytoskeleton components are associated with **plasmodesmata** (PD), cytoplasmic connections that unite plant cells, and this increases their capacity for transporting their cargo between cells. The immunolabelling patterns shows that Arabidopsis thaliana myosin (ATM1, the first gene to be cloned from myosin VIII in plants) was localized in PD. Similar studies demonstrated that myosin-like proteins, as well as actin and actin-like proteins, are PD-localized. PD is, however, more weakly labeled by tubulin-specific antibodies than the cytoplasm, and it doesn't

appear that microtubules move onto the PD gaps (Blackman and Overall, 1998). Through desmotubules, constricted tubular membranous structures that span cell-membrane-lined PD channels, plant cells are connected to their cortical endoplasmic reticulum (ER). Early PD studies using transmission electron microscopy (TEM) provided 2-dimensional images of an ultrastructural component spirally arranged around the desmotubule of PD that was later proposed to be actin-derived (Overall and Blackman, 1996; White and Barton, 2011). Furthermore, actin and myosin are both connected to ER domains in plant cells, suggesting that they might be also involved in controlling intercellular transport through the desmotubule conduit, the ER-continuum throughout the tissues (Chen et al., 2021). The little area of cytoplasm between the plasma membrane and desmotubule is where the cytoskeletal elements of PD are most likely to be located. Additionally, molecules moved into this cytoplasmic sleeve may be controlled by cytoskeletal activity at the neck regions of PD, with a size exclusion limit (SEL) of 36-67 kDa (Stadler et al., 2005). Many data suggest that actin-myosin cytoskeletal machinery is closely associated with membrane contact sites between ER and the cell membrane, and together with other tethering proteins, they connect the desmotubules to the enclosing plasma membrane. This cytoskeletal tethering of the desmotubule to the plasma membrane will obviously further constrict the cytosolic path and ultimately regulate PD gating (being more permeable) and dilating (being more open). The integrity and assembly of the PM-desmotubule network are compromised by the degradation of actin filaments at the PD, raising the PD size exclusion limit (Chen et al., 2021). When actin filaments are disrupted by depolymerizing treatments like latrunculin B (LatB) or cytochalasin D/ or B (CytD or CytB), or by the actin-binding proteins profilins, PD is dilated and, more generally, intercellular trafficking is increased. Applying the actin-stabilizing agents phalloidin provided evidence that PD is constricted by the actin cytoskeleton. 2,3-Butanedione monoxime (BDM), an ATPase inhibitor of myosin that increases the stability, by preventing the depolymerization, of actin

filaments, causes the PD to constrict and reduces its permeability (White and Barton, 2011; Aaziz et al., 2001). It is also supported by the decrease in PD permeability that occurs when native myosins are disrupted in cells that overexpress myosin tails (Geng et al., 2015). Cell-cell conductivity is unaffected by treatment with the microtubule inhibitor colchicine (Krasavina et al., 2001). Nevertheless, the linkage of the non-cell-autonomous (NCAP) transcription factor SHOOT-ROOT (SHR) protein, in its mobile form with Kinesin G (KinG) motor to the PD leads to the hypothesis that microtubules are indirectly involved in the intercellular trafficking by transferring their cellular cargo into the PD (Spiegelman et al., 2018). Actin targeting to the PD is regulated by formins and NETWORK 1A (NET1A) proteins, among other unknown endogenous PD-located proteins (PDLPs) that function as plant-specific actin-binding proteins/adaptors (ABP) (Diao and Huang, 2021; Sun et al., 2019).

The involvement of cytoskeleton in plasmodesmata-mediated trafficking have also arisen from the studies on **virus movement** in plants. Many plant viruses replicate and move in a linked manner in association with the cellular endomembrane (mostly ER) and cytoskeleton system (mostly actin). During infection, plant viruses hijack the actin or microtubule cytoskeleton and exploit it as a means of transportation to get to their sites of replication, from whence they send their offspring to the PD to spread intercellularly. Both of the arrival to their replication sites by the incoming and the PD-targeting by the outgoing plant viruses are cytoskeleton-dependent.

The movement proteins (MP), encoded by plant viruses to assist in the virus cell-to-cell movement by targeting and altering PD function, interact with actin filament or actin-associated protein at one point of the virus life cycle (Niehl and Heinlein, 2011). Although **TMV** MP (P30 kDa), for example, is primarily associated with MT, the function of this association in cell-to-cell movement is not fully understood because MT inhibitors do not have an impact on the spread of the TMV infection; MF inhibitors do (Kawakami et al., 2004). In addition to TMV P30, that

is colocalized, though to a lower extent, with the MF (McLean BG, et al., 1995), the TMV replicase (P126 kDa; Harries et al., 2009) traffics along the MF in an ER-mediated manner and inside PD (Liu et al., 2005). Interestingly, only after it has entered the PD, the TMV P30 becomes capable of severing the PD-MF to increase the PD SEL (Su et al., 2010). Myosins XI (XI-2 and K) are required for the intra- (and, subsequently/consistently, also inter-) cellular trafficking of both the TMV MP and VRC along the actin-ER system, whereas myosins VIII (VIII-2 and B) assist the accumulation of MPs into PD, or are otherwise retained at the plasma membrane (PM). Furthermore, TMV replicase 126 kDa, a component and a size regulator of the TMV ER-associated VRCs, is affected by myosin XI-2 but not by myosin XI-K or VIII, which in turn changes the level of vRNA accumulations (Amari et al., 2014).

The coat protein (CP), as well as the virion, of the **PVX** bind to the MT and are able to outcompete the plant-specific MT-associated proteins (MAP) for the MT binding, according to in vitro investigations by Serazev et al., (2003). According to numerous reports, the triple gene block (TGB) proteins encoded by the virus are necessary for the virus's ability to travel between cells because of their interaction with MF (Harries et al., 2009). Confocal images show the actin-association of the distribution and localization of the PVX TGBp1 (P25; Tilsner et al., 2012), TGBp2 (P12; Ho-Jong et al., 2005) and TGBp3 (P8; Krishnamurthy et al., 2003). In early infected PVX-cells, P25 induces rod-like (RL) structures, that provide to its function in the virus cell-to-cell movement. These RL are inhibited by LatB, but not with the MT-inhibitor Oryzalin, as compared with the control dimethyl sulfoxide (an optical clearing agent with enhanced fluorescence emission) DMSO-treated samples (Yan et al., 2012). A perinuclear big inclusion body, also known as an X-body historically, is induced by the virus during advanced stages of PVX-infection. It is considered as a virus factory that is altered by other viral and host factors, including actin filaments, to compartmentalize the infection inside the cell (Tilsner et al., 2012). The ability of the ER-associated PVX-replicas to interact with the cytoskeleton is still unclear, and considerable research remains to be done.

Numerous studies summarized in (Table 2.1.) have been investigating the interactions between viral components and cytoskeleton and/or cytoskeleton-related proteins/structures, that result in intra- and/or intercellular movement of viruses like Tomato spotted wilt virus (TSWV), Soybean mosaic virus (SMV), Potato mop-top virus (PMTV), Turnip vein clearing virus (TVCV), Tobacco etch virus (TEV), Cucumber mosaic virus (CMV), Beet yellows virus (BYV), Grapevine fanleaf virus (GFLV), Rice stripe virus (RSV) and turnip mosaic virus (TuMV).

Table 2.1. Nature of interaction with cytoskeleton filaments by some plant viruses (see review by Harries et al., 2010).

Virus component	Cytoskeleton component	Viral-cytoskeletal interaction	Ref.
TSWV Nucleopcapsid (N-)protein	Actin Myosin	The N-protein form mobile, cytoplasmic ER-associated viral inclusion bodies that interact with MF in a myosin-dependent manner.	Feng et al., 2013
SMV The P3 protein (Virulence factor with a putative role in virus replication and movement)	Soybean actin-depolymerizing factor 2 (ADF2)	P3 is proposed to be directed into the MF for movement via its interaction with the MF component ADF2 and it also localizes in *Nicotiana benthamiana's* cytomembrane and cytoskeleton.	Lu et al., 2015
PMTV TGBp2 and TGBp3	F-actin filaments	Colocalization of the TGBp2/3 mobile granules and F-actin filaments, which are expected to move along ER and perinuclear membranes, is achieved by labelling the F-actin binding domain of human talin (hTalin) in plant cells.	Haupt et al., 2005

Table 2.1 continue

TVCV P30 kDa (MP)	F-actin-containing nuclear filaments	TVCV MP accumulates in the nucleus, interacts with nuclear structures containing F-actin filaments, and also co-localizes with histone H2B.	Levy et al., 2013
TEV P3 (a putative role in virus replication and movement)	Actin filaments	After P3 localizes on ER, it forms punctate inclusions in association with Golgi apparatus, that travel along actin filaments and colocalize with replication vesicles.	Cui et al., 2010
CMV MP	Actin filaments	The actin filaments are severed and capped by CMV MP, which increases the PD SEL and aids in cell-to-cell trafficking.	Su et al., 2010
BYV Heat shock protein 70 homologue (Hsp70h)	Actin microfilaments	The PD-targeted Hsp70 forms motile granules that travel in cytoplasm via actomysin active transport system.	Prokhnevsky et al., 2005
	Myosin class VIII	Dominant negative inhibition of host myosins shows that the PD targeting of Hsp70 depends on the tail cargo-binding activity of myosin VIII, but not XI.	Avisar et al., 2008
	Microtubule	The Hsp70h viral protein (P65 kDa) binds with the MT in vitro.	Karasev et al., 1992
		The deforming of the PD by the GFLV MP is secretory-dependent, as the tubule formation and MP localization are interrupted in brefeldin A (BFA)-treated cells. The	Laporte et al., 2003

Table 2.1 continue

		distribution of GLVP MP-derived vesicles requires the MT, which might switch to the default MF pathway when MT are depolymerized. Moreover, GLVP MP colocalizes with KNOLLE, that mediates cell plate formation during cell division.	
RSV NSvc4	actin-myosin VIII system	The PD-targeted RSV NSvc4 traffics along ER-to-Golgi secretory pathway in an actin myosin-VIII dependent manner.	Yuan et al., 2011
TuMV 6 kDa	actin-myosin system	The TuMV 6 kDa protein forms ER-derived vesicles that contain viral replication machinery and targets the chloroplast via the actomyosin transport system.	Wei et al., 2010
		The TuMV-induced 6kDa-tagged vesicles align with the MF, and the TuMV-infected cells that have been infiltrated with MF-inhibiting drugs are less able to generate viruses and restrict virus movement.	Cotton et al., 2009
	myosin XI-2 and XI-K	The MF/myosin XI (XI-2 and XI-K) transport system, but not myosin VIII, is involved in the trafficking of the TuMV virus.	Agbeci et al., 2013

Because of their molecular properties, both of the cytoskeleton protein fibers function not only as a static support for the cell structures but also as a dynamic scaffolding that coordinates organelles movement and organization inside the cell. Both actin filaments and microtubules can have the ability to direct their cargo towards PD, a route that most viruses hijack on infecting plant cells.

2.3. Deciphering the Movement Out of the Cell

2.3.1. Plasmodesmata: The Gateway

Plant cells are surrounded by a semipermeable plasma membrane that is sandwiched between two plant cells by a cellulosic cell wall. Cell walls provide extracellular matrix connecting the plant cells together and act as a barrier, allowing the passive transport of only molecules of small size less than 10^4 dalton (10 kDa); macromolecules like viruses and other plant invading microorganisms (MOs) are sieved out (Brett and Waldron, 1990). Any molecule that leaves the cell and travel through the plant tissues must follow the symplastic or apoplastic route. The cell walls with the intercellular spaces and the xylem are all parts of the apoplast (Figure 2.1) (Farvardin et al., 2020). However, the entire living component of the cells within a tissue is the symplasm, which has a continuous cytoplasm flowing through cytoplasmic annuli in the cell walls, or the **plasmodesmata** (PD). Primary PD originate between sister-cells during cytokinesis, but secondary PD form at a later stage after cytokinesis on the existing walls and can also communicate non-sister cells. **PD structures** are dynamic because they are frequently modified during the course of a plant's life. Nevertheless, a typical PD has an ER-derived core, the desmotubule, encased in a cytoplasmic sleeve that is bound by the plasma membrane (PM) and cell walls of the two connected cells (Figure 2.2) (Sevilem et al., 2015). Early PD studies using transmission electron microscopy (TEM) provided 2-dimensional images of an **ultrastructural** component spirally arranged around the desmotubule of PD that was later proposed to be actin-derived. Actin filaments are essential components of the PD; when they are destroyed, the PD opens, but when

they are stabilized, the PD may close (Sager and Lee, 2014). Neck constrictions around the outer region of some PD are noticed in some cells, participating in opening and closing the orifices, with noticeable collar-like sphincters structures that may act as turgor-dependent valves to delimit the direction and speed of sysmplastic movement into the cytoplasmic sleeve (Olesen, 1979). The cytoplasmic annulus appears to be partitioned by the PD proteins into distinct microchannels that function as molecular sieves allowing the passage of molecules of a diameter on the order of **3-4nm** (Lucas, 2006). That and other conductivity regulatory factors (Figure 2.3.) set a size exclusion limit (SEL) on PD permeability (Sun et al., 2019). There may be varying size exclusion limits for plasmodesmata in different cells and tissues, during various developmental stages, and in various environmental conditions (Table 2.2.) (*Rim et al., 2011*). However, a molecule's size (nm) and shape (Stroke radius), not its weight (kDa), can be used to estimate how permeable it is to a nanochannel like the PD that is 30 nm wide and 100 nm long (Dashevskaya et al., 2008; Lucas, 1995). With that said, the intercellular trafficking is commonly controlled in all types of PD by the deposition of a water-insoluble polysaccharide molecule called **callose** (β-1,3-glucan) at the neck area, which reversibly constricts the pores (Figure 2.4.) (Sevilem et al., 2015). The deposition is dynamic and involves lipid metabolism into the PD membrane microdomains (Bayer et al., 2014). These two enzymes β-1,3-glucan/callose synthases (favors the synthesis) and β-1,3-glucanases (favors the degradation) control the callose turnover, and they as well as another PD callose-binding proteins (PDCBs) have been localized at PD neck region. Callose is produced to shut the PD in response to both biotic and abiotic stresses such as pathogen infection and injury. That defensive mechanism is tightly linked to formation of salicylic acid (SA), a systemic acquired resistance (SAR)-inducer, that also triggers the callose synthase activity (Dong et al., 2008). Viruses develop evasive tactics in order to avoid the callose-induced closure of the PD. For instance, the TMV P30 facilitates its mobility by possibly recruiting the -1,3 glucanases to prevent the callose deposition (Epel, 2009). The PVX TGBp2 may interact with this

enzyme inadvertently by means of TGB2-interacting proteins (TIP1, TIP2, and TIP3) that have been isolated and demonstrated to associate with the β-1,3, glucanase (Fridborg et al., 2003; Iglesias and Meins, 2000). Given that PD is where callose is largely present, it can be used as a specific PD-marker, and the callose staining with the histochemical aniline blue can directly mark PD in the cells under light and fluorescent microscopy. The proteins involved in callose metabolism will very certainly localize to the PD and will also participate in controlling its permeability. Glucan-synthase-like (GSL) proteins GSL7, GSL8 and GSL12, plasmodesmal-localized β-1,3-glucanase (PDBG) PDBG1, PD callose binding (PDCB) proteins, a GPI-anchor, PDLPs, ER-associated calreticulin and a reversibly glycosylated polypeptide associated with Golgi and PD (RGP2) are all examples of PD-associated cellular proteins that regulate PD transport by mediating callose metabolism. Some viruses facilitate their trafficking via PD in a callose-independent way, by severing **actin filaments** within. Two modes may then describe the PD-gating inside the cell, as understood from PD-Virus research: by decreasing the callose deposits levels and/or by destabilizing the PD actin filaments (Figure 2.6) (Sager and Lee, 2014).

A number of plasmodesmal associated kinase (PAPK) are identified in the cytoplasmic sleeve and participate in the activation by phosphorylation of many NCAPs. Reticulons (RTN), a group of membrane-shaping proteins that mainly plays a role in the curvature of the ER, have been identified in the PD proteome of Arabidopsis (Tilsner and Kriechbaumer, 2022). Remorin (REM) are a group of membrane raft proteins that are also located in the PD, and in some way or another, they play a role in controlling its permeability. REM can bind to the PVX TGBp1 and hinder the virus movement. They may serve as a docking platform for the PVX retention in the PD, inhibiting its exit. It is yet unclear how REM affects the PD permeability (Eckard, 2009). Furthermore, some other non-PD-resident proteins are screened and characterized to be involved in the PD cell-to-cell communication (Figure 2.3) (Sun et al., 2019; Ueki and Citovsky, 2014).

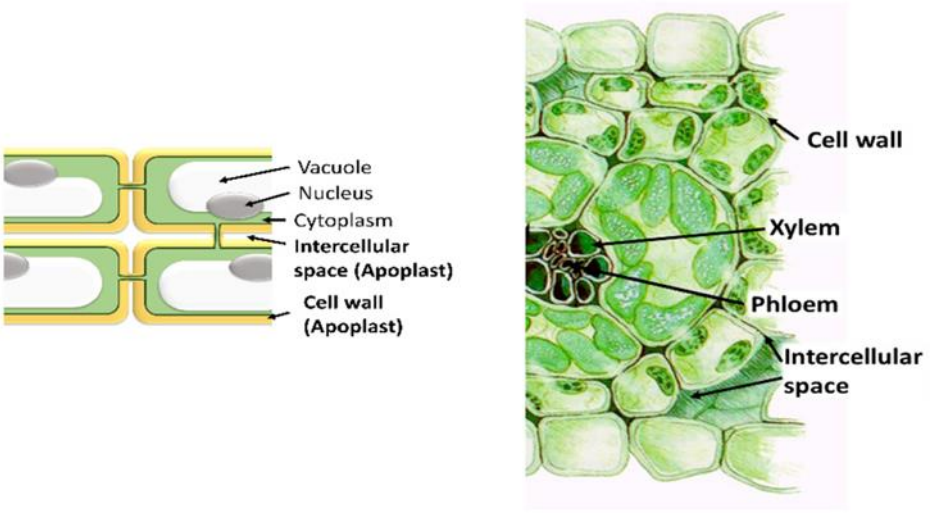

Figure 2.1. Diagram illustrating the composition of the apoplast, cell walls (in yellow) and intercellular space (on the right), and the xylem tissue (on the left; Farvardin et al., 2020)

Table 2.2. The SEL of PD on various tissues of the Arabidopsis root through non-targeted symplastic movement of different-sized non-cell-autonomous transcription factors (NCATFs; Rim et al., 2011).

Arabidopsis root Tissue	**PD SEL**
Undifferentiated tissues around the meristem	Larger than 54 kDa
Young tissues	Between 27 and 54 kDa
Mature nonvascular tissues	Less than 54 kDa

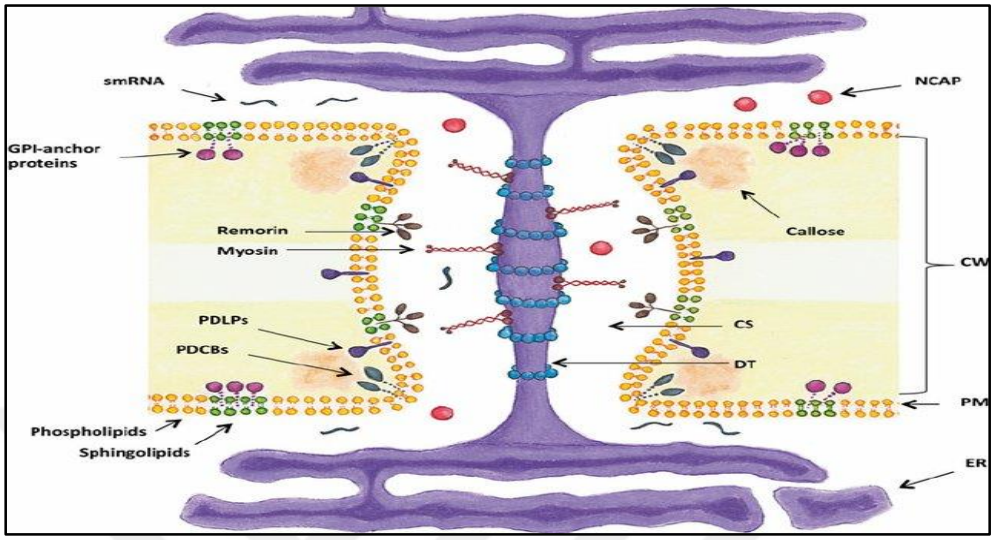

Figure 2.2. Diagram illustrating the ultrastructure of a plasmodesmata (PD, 30-40 nm wide), the nanochannels that travers the cell walls (CW) connecting the cytoplasm of two neighboring cells via an endoplasmic reticulum (ER)-based tube called desmotubule (DT, 2 nm wide) that runs along the channel. PD orifice is controlled by the callose turnover at its neck area. The cytoplasmic sleeve (CS, 6 nm wide) filling the area between the plasma membrane (PM) lining the inner side of the channel, and the DT is the trafficking route of most of the passing molecules that mainly function in developmental or defensive mechanisms such as non-cell-autonomous proteins (NCAPs) and small RNAs (smRNAs). ER membrane inside the PD is an alternative route for the transmembrane-domain containing proteins. Small molecules can cross cells via ER lumena. Remorins, myosin, GPI-anchor proteins, callose-binding proteins (PDCBs), and PD-localized proteins (PDLPs) are part of the PD proteome. Remorins and GPI-anchor proteins are raft-associated proteins that found enriched in sterol/sphingolipid- containing microdomains of PM (Sevilem et al., 2015).

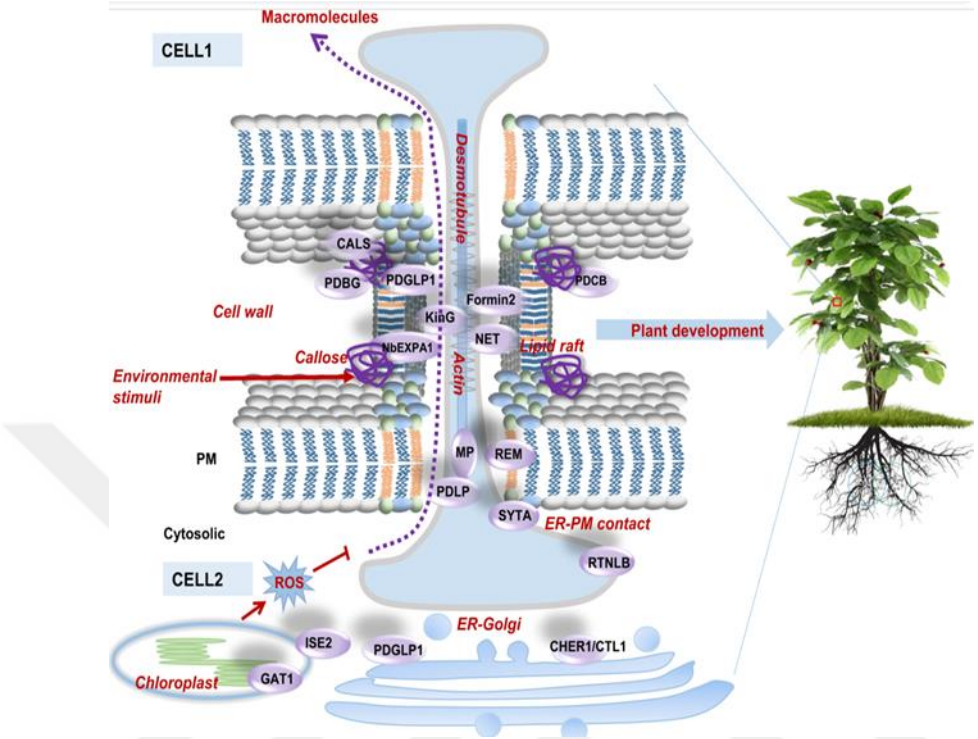

Figure 2.3. Cellular factors that regulate the PD symplastic conductivity. The gating of PD has been shown to be affected by various environmental and developmental signals (Sun et al., 2019).

Contrary to the apoplastic free non-selective movement via intercellular spaces, which involves the adsorptive capacity of the cell walls and transporter proteins anchored in the cell membrane, the intercellular symplastic movement is controlled by the PD via **two primary routes**: targeted and non-targeted (Brunkard et al., 2013). The cytoplasmic sleeve in the PD allows the non-targeted movement of small (less than 40 kDa), soluble (not membranous bound) molecules without having to modify the PD or interact with its associated proteins. The passive diffusion of the GFP, 27 kDa, is a good example of such a mode. By altering their inner diameter, PD can control what diffuses through their channels. Targeted movement, however, involves macromolecules that transport via PD membranes; the desmotubules, or the encasing PM (Figure 2.5). Likewise is the PDLP, which is secreted from golgi

vesicles and is then considered to be diffused laterally in the PM before being finally anchored/localized in the PD PM (Gallagher et al., 2014). Lipids and transmembrane proteins, that are created by the ER membranes, can travel across cells by way of the desmotubule membranes. However, the desmotuble lumena can only transport very small ER-lumenal proteins with a SEL up to 10.4 kDa (Barton et al., 2011; Martens et al., 2006). Proteins that are larger than the PD SEL can also be trafficked when they are targeted to the PD by changing the shape of the PD (i.e. dilating its SEL). The majority of plant viruses evolve to move intercellularly by promoting these movement proteins (Gallagher et al., 2014; Lucas and Lee, 2004).

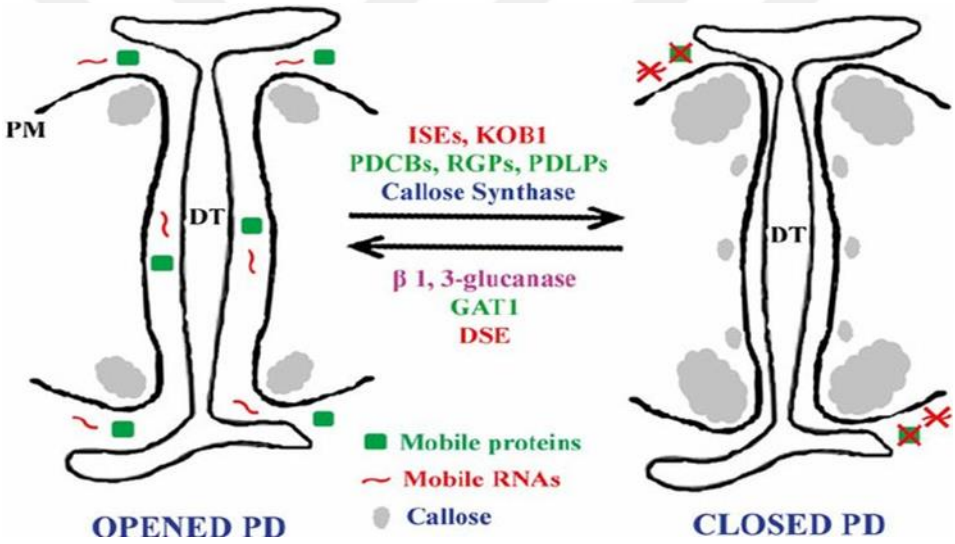

Figure 2.4. Diagram showing the reversible PD-associated callose deposition and how it controls the PD permeability. Closed PD allows no trafficking; open PD by dilating does, but to a certain SEL (Sevilem et al., 2015).

Non-targeted intercellular movement

- This passive free diffusion of molecules that has the ability to pass through these nanopores does not involve any PD targeting motifs nor an interaction with functional PD-located proteins.
- Movement is restricted based on the size. Molecules larger than PD SEL, such as RNP both endogenous and pathogen-derived, cannot move freely between cells.
- Different physiological parameters regulate this symplastic pathway. For example, callose deposition around the PD neck area reduces the PD SEL. Also spoke-like proteins that connect the desmotuble to the PD-PM can narrow the cytoplasmic annulus and control the PD permeability by changing its SEL (Chen et al., 2021).
- Metabolite like soluble solutes, sucrose and macromolecules up to 40 kDa can move freely when the PD gate is open (Gate Open; GO). Closed Gate (GC) prevents any trafficking above 800 Da SEL. This pathway is modeled as **GO/GC.**

Targeted intercellular movement

- This controlled movement involves a reversible interaction with PD membranes and its associated proteins, that results in shaping PD structure for the favor of movement. The interaction is selective tan being free to diffuse.
- Targeting to the PD is a key point in such a mode, and the Interaction with the PD machinery is a must.
- Targeted dilating of the PD, which in most of cases are temporarily/transiently, will allow their passage even when they are

considered over-SEL-sized molecules (once thought to be impassable). For example, viral movement proteins (such as of CMV and TMV) dilate the PD by targeting, severing and capping the MF inside the PD (Su et al., 2010). Deformation of the PD can also occur by tubule-forming MP upon their interactions with PD-located protein (PDLP; Laporte et al., 2003). The KNOTTED1 (KN1) is the first transcription factor noticed to be capable of targeting and dilating the PD, and moving itself through with its mRNA (Lucas et al., 1980).

- Transcription factors, NACP (e.g. KNOTTED1) and most viral movement proteins can only pass through after carefully targeting the PD for a dilation through some protein-protein interaction.

With very few exceptions, all the transcription factors are **signal proteins** trafficking within the plant in a symplatic way through the PD (reviewed in Fernandez-Calvino et al., 2011). If these factors are above the SEL of the PD, how will they then allow themselves to flow through the PD? The proteins may need to be refolded and unfolded by chaperonin-containing TCP-1 (CCT) before they can be able to move through the PD. The chaperon-dependent protein trafficking was reported in KNOTTED1 (KN1; Xu et al., 2011) and tobamovirus movement (Fichtenbauer et al., 2012). Loss-of-function mutations have identified numerous transcription factors that are involved directly or indirectly in the callose deposition to aid their trafficking between cells. LEAFY (LFY; a plant-specific transcription factor involved in flower formation) has been found to reduce defense against bacteria by interfering with the flg22-induced callose depositions and other flg22-induced defense genes (Winter et al., 2011). There are numerous proteins that are crucial for plasmodesmal transport yet do not localize to plasmodesmata. Mitochondrial and choloroplast metabolism can regulate the regulation of SA biosynthesis and subsequently callose deposition. Mutant screening has identified genes regulating PD permeability, such as the mitochondrial RNA helicase that

increases the SEL (named, therefore, as increased size exclusion limit; ise1) or the plastid thioredoxin that reduces the PD transport (named, therefore, as gfp arrested trafficking; gat1). Their reaction to mitochondrial reactive oxygen species (ROS) and plastic superoxide can also influence how well the PD functions (reviewed in Brunkard et al., 2013; Gallagher et al., 2014). Numerous transcription factors have the ability to move from cells where they are produced to cells where they will function. The organizational system of transportation of these Non-Cell-Autonomous Proteins (NCAP) contributes to the supracellular nature of the PD (Lucas and Lee, 2004)

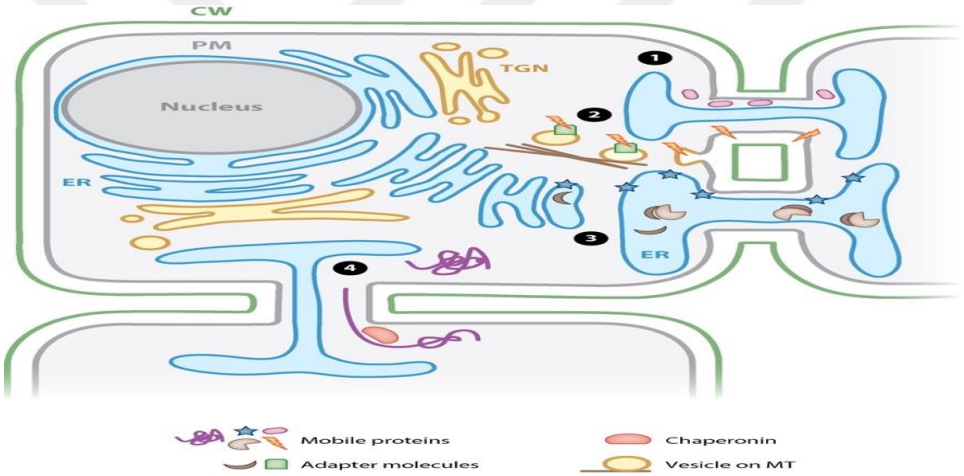

Figure 2.5. Different ways of endogenous proteins trafficking through PD. 1) Targeted symplastic movement via the cytoplasmic sleeve (CS), 2) Lateral diffusion through the plasma memebrane (PM), 3) Small molecules can pass within the ER-lumena of the desmutubule and 4) Chaperon-mediated transport requires certain folding/unforlding of the mobile protein (Gallagher et al., 2014).

A competition with these endogenous **NCAPs** on accessing the host cellular trafficking pathways has been likely a preceding event in any viral infection context on plant cells. Only in compatible hosts, viruses are able to “hijack” one of these trafficking pathways to reach the PD of the infected cell and then spread infection to

its neighboring cells before its own antiviral defense signal does. PD is, therefore, considered to be a very crucial infection route for the plant viruses that they have devolved mechanisms to mediate the PD structure and functions in order to facilitate the spread of their own. Of all the virus-encoded proteins, MP have been found to be the main factor in the **PD-mediated virus trafficking**. They interact directly with the PD proteins (Figure 2.6.). The MP of TMV (Olesinski et al., 1996), Potato leaf roll virus (PLRV; Kronberg et al., 2007) and Tomato spotted wilt virus (TSWV; Rinne et al., 2005) have reduced the accumulation of callos near PD orifices. TMV has developed different phenotyping and impaired cell-to-cell movement when infecting plant tissues overexpressing the RGP2, a 400 kDa plasmodesmata-associated protein, that probably blocks the passage of the cytoplasmic sleeve (Zavaliev et al., 2010). Upon phosphorylation of P30 by the plasmodesmal associated kinase (PAPK), the TMV loses its function to gate the PD but still retain its ability to bind NA (Waigmann et al., 2000). Certain viruses undermine the integrity of the PD by modifying its cytoskeleton components, allowing bigger molecules to pass (see section 2.1.2. Plant cytoskeleton). RTN3 and RTN6 interact with various MPs and propably play a role in the viral movement (Tilsner and Kriechbaumer, 2022). With the difference in the numbers of the MP encoded by the virus, viruses adapt differently with the PD and develop different transport strategies. TMV encodes a single MP (P30) that binds vRNA, dilates the PD and move as vRNA:P30 RNP complex. The P48 kDa MP of Cowpea mosaic virus (CPMV) is its only viral protein responsible for movement by forming a tubule inside the PD channel, allowing the virus particles to pass through it (Figure 2.6., Figure 2.7) (Pouwels et al., 2004). PVX encodes three MPs from three overlapped genes, named triple gene blocks (TGB), they all collectively aid in the virus movement. The largest is TGBp1 and has multiple functions; it can bind RNA, dilate PD and has a silencing suppressing ability with an NTPase/RNA helicase domain. The PD-targeting ability of the TGBp1 associates only with the other two proteins. TGBp2 and TGBp3 are smaller transmembrane proteins that reside in ER and play a role in the virus

intracellular trafficking into PD. PVX CP is necessary for the virus movement, but does not target, per se, the PD or increase its SEL. During the infection, the TGBp2-induced, ER-derived vesicles recruit TGBp3, and these granular vesicle complexes bind the TGBp1 with its viral cargo to PD. The infectious moving unit as a vRNA complexed with TGBp1 and protected by the CP (in a virion or non-virion/virion-like form) moves through the PD in association with the fluid ER/desmotubule membrane (Heinlein 2015a; Tilsner et al., 2014; Benitez-Alfonso et al., 2010; Lucas, 2006).

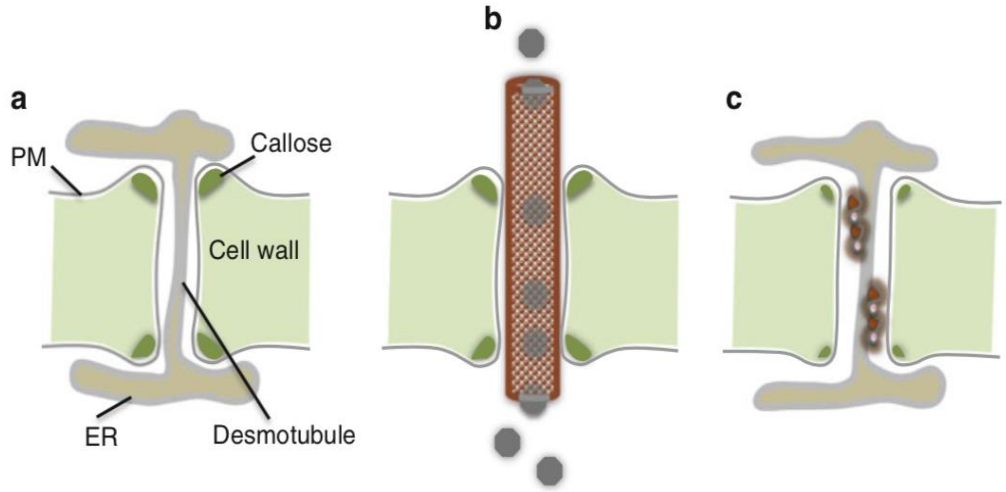

Figure 2.6. Plasmodesmata (PD)-mediated Virus trafficking. a) Simple PD with continuity of plasma membrane (PM) and endoplasmic reticulum (ER) between cells. Desmotubule is the ER-integral structure of the PD b) Modified PD with an interruption in the ER continuity, by viruses that form tubule replacing the ER-desmotubule inside the PD. c) Gated-PD with an increased SEL by viruses that may target certain PD-localized proteins decreasing the callose deposits levels or interfering with PD-associated actin (Heinlein, 2015a).

2.3.2. Movement Proteins: The Nonspecific N.A. binders

Plant virus particles are too big to simply diffuse through the nanochannels of the PD, without having to modify PD in a way that the host cell may employ to traffic

its endogenous macromolecules. The now-known fact that the viral genome already contains information necessary for the movement of the virus was established 50 years ago, when the temperature sensitive (ts) mutant of TMV that was restricted to the site of infection was shown to have had a point mutation in the ORF encoding the 30kDa protein. The fundamental studies on TMV that led to the discovery of the movement protein concept are reviewed in Lucas, 2006. Viruses are always vying for the cellular transport pathways that are also employed by the antiviral defense system. This imposes a **bottleneck** effect that particularly reduces the number of individual viral genomes traveling between plant cells and it is most likely that viruses start cell-to-cell movement at the very beginning of infection (Gutiérrez et al., 2012).

Movement proteins (MP) are non-structural, plant-virus specific proteins that are pivotal for the spread of infection between cells but dispensable for virus replication. They can have their functions distributed among several proteins or encoded as a single MP. Although MPs from different plant virus families have very different molecular and sequence features, at least one MP from each plant virus will share the same **functional qualities**, such as the ability to bind nucleic acids, target and dilate the PD (see section 2.2.1.) and move between cells (autonomously, i.e. self-movement; being able to move between cells on its own in the absence of other viral RNA/factors (Sheshukova et al., 2020).

MP can bind N.A. (RNA over DNA; SS over DS) in a sequence nonspecific manner, and show interchangeable activity that they are able to complement the cell-to-cell trafficking of unrelated viruses, and independent on the infection. Complementation is a general aspect displayed by MPs of most plant viruses. In Latham and Wilson 2008, Table 1 lists all the reported complementation experiments, with the first column focusing on movement **complementation**. Although MP lack the specificity to distinguish between their cognate RNA cargo and others, they are still able to spread at early infection state when their cognate vRNA is rare and cellular RNA is abundant. There must be some mechanism other

than nucleotide-specific RNA binding by MPs that provides the specificity. Probably, interactions are taking place between MP, the "carrier," and other viral/host components to ensure the transport of infection, or "the cargo."

In the infection context, MPs are simply thought to attach co-translationally to their viral RNAs (vRNAs) in their proximity and deliver them into the PD. That is consistent with the hypothesis of the peripheral compartmentalization of the viral replication complexes (VRC) associated with the MP. MPs that are very weak nucleic acid binders may provide virus **transport specificity** by associating with CP that have a strong affinity for their cognate vRNA, and these viruses are always moving between cells as CP-containing vRNPs (Chowdhury and Savithri, 2011). In the movement systems of several plant viruses, MPs often associate with or assist in the formation of viral replication complexes, and spatial links between MPs (which show no specificity) and replicase enzymes (which are highly specific to their cognate genome) will most likely facilitate efficient and specific transport of the infection (Tilsner and Oparka, 2012).

There is virtually no knowledge of transport specificity. Nevertheless, the MP:vRNA **binding** may occur in cooperative high affinity manner, and these complexes will come in extended thread-like or globular compact structures (Lucas, 2006). Lim et al., 2008 shows that *Barley stripe mosaic virus* (BSMV) movement complexes contain exclusively vRNA, demonstrating a virtual degree of transport specificity by the MP.

The capacity of viral MPs to localize to PD and spread to next cells is primarily dependent on their ability to "hijack" the numerous pathways that the host cell uses to transfer endogenous proteins to PD (Figure 2.5.). Pathways like either through the lateral mobility of the ER and/or PM or via the secretion delivery to the plasma membrane (PM), that both show symplastic continuity inside PD, are utilized for the intracellular trafficking of a number of viruses (Tilsner et al., 2014). Consistent with this, one component of most known MP are transmembrane or membrane-associated domains. **ER** is scaffolded with actomysin system, and the PD

targeting of most viruses is disrupted by drugs that inhibit that system, indicating that viruses are most likely depending on the ER/actin network for **targeting the PD**. Microtubule, though is not a major component of the PD, may participate in the cell-to-cell movement of the virus replication complexes (VRCs) that use MT as anchoring sites for replication (as simplified for TMV model in Figure 2.7. by Pitzalis and Heinlein, 2018). PD targeting is not very well understood as the PD components are yet not fully elucidated, but PDLP kinases are defined to be the MP-receptor and key factor in the tubule formation of GFLV and other tubule-forming viruses (Amari et al., 2010). Similar to the plasmodesmal localization signal (PLS) of the NCAP KN1 (Kim I, et al., 2005), the genetic analysis of the TMV P30 shows three domains accountable for the MP targeting to PD, though they do not extend to neighboring cells or localize/insert in the PD cavity as the full length P30 MP (Liu Y, et al., 2020).

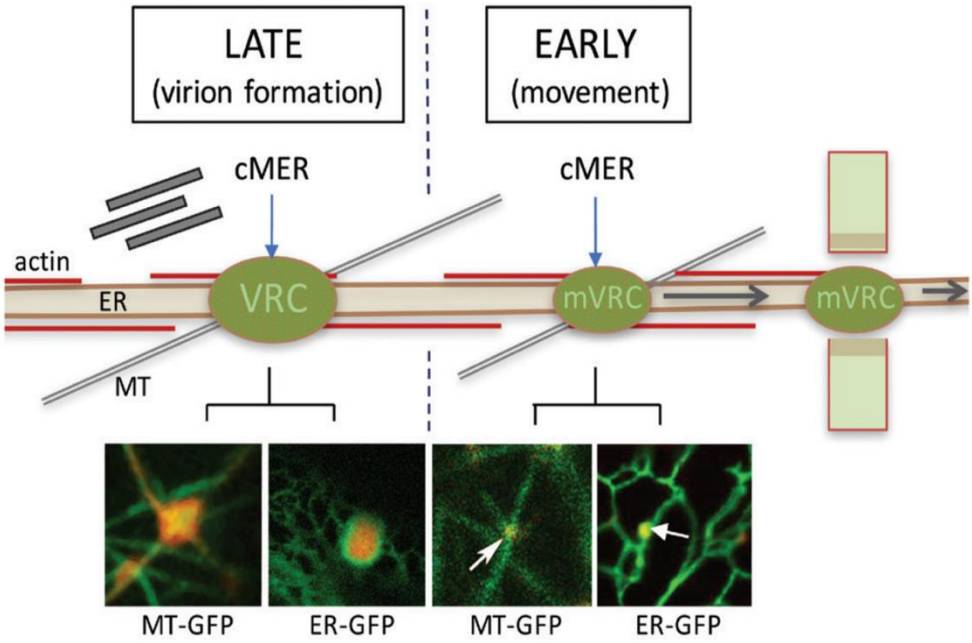

Figure 2.7. Targeting of viral replication complex (VRCs) to the cortical microtubule-associated ER sites during late and early TMV infection. At early infection, VRC are mobile (mobile VRC or mVRC) along the MT tracks till it can be detached at intersections of the cortical MT with ER-actin system, or the cortical microtubule-ER associated sites (cMER), to move along the ER-actin system through PD. At late infection stages, MT are involved in the subsequent degradation of the MP and the anchoring of large VRC, or X-body (Image from Pitzalis N and Heinlein M, 2018).

Only cells at the spreading front of infection are where the virus is actively moving, since subsequent degradation of the MP or inactivation by cellular kinases is reported at late infection. Inactive MP by phosphorylation are still PD-localized but no longer able to increase SEL. The MP-induced dilation of the PD is transient (unlike TMV, continuous MP accumulation has been shown for some other viruses throughout the course of infection) and restricted to the infection front, and proposed to be possible by a direct interaction of the MP with the PD components, or indirectly by influencing factors like callose metabolic enzymes or PD-associated proteins

(PDAPs) to regulate the PD and increase the SEL. Recent studies are focusing now on the importance of the membranes of the PD functions, and ER-PM contact sites, putative tethers are identified to be interacting with the MPs (Reagan and Burch-Smith, 2020). Table 1 reviewed by Dorokhov et al.,2019 shows the PDAP and their association with the cellular endogenous proteins and MP in dilating the PD.

The studies on the MP **dynamics** provides insights on how transport unit (RNP or virion) undergoes certain modifications to permit the formation of movement-competent but also infectious complexes. The phosphorylation by membrane-localized PD kinases of the TMV MPs in their moveable vRNP destabilizes the complex and it becomes feasible to the translation machinery (i.e. infectious) upon their exit of the PD into the next cell (Karpova et al., 1999). Also, the TGBp1 association with the 5'end of the PVX RNA in their moving virion destabilizes CP coat, allowing the co-translational disassembly of the virion and the infection to continue in the cell it enters (Atabekov et al., 2000).

Despite the fact that it has been shown that they may use different pathways and mechanisms for virus transport, it is still possible to distinguish between a number of **different MP types** (see Table 2.4.). The **30K** TMV superfamily members encode single MP for the intercellular trafficking of the virus. It also includes all the MP that penetrate tubule in the PD and move as virions. Additional proteins may be required to increase the efficacy and efficiency of the transport. Because the CMV 3a:RNP is less stable and not completely protected against RNase, CMV in infected cells may move as a complex of the 3a:RNP and CP. It's possible that CP plays a part in the vRNP's increased stability and enhanced RNA binding affinity. Support for this comes from the fact that CMV 3a CP-independent mutants that are also movement-competent have higher RNA binding affinity than their wild type, suggesting that they may use this property to make up for the absence of CP. However, the loss of requiring the CP by CCMV is considered an adaptation to some form of host response rather than an evolutionary preference of the virus to make the movement between cells simpler (Sasaki et al., 2005).

Three functionally distinct viral polypeptides, encoded from one evolutionarily conserved genetic element with three overlapping ORF, are all essential to secure intracellular trafficking of the viral components to PD. These triple gene block (**TGB**)-containing viruses vary in how the two main hordei- and potex-like types of TGB proteins work (Tilsner et al., 2014; Benitez-Alfonso et al., 2010; Lucas 2006). The need of the CP for the potexvirus cell-to-cell movement distinguishes the two types most significantly. The role of the CP in the cell-to-cell movement of PVX is demonstrated to be dependent on TGB-system as a result of the successful TMV P30 complementation to the cell-to-cell movement-defective PVX CP mutants (Fedorkin et al., 2001). The TGBp1 is the largest PVX MP and the main component responsible for the movement, as it can bind RNA in a sequence nonspecific manner, dilate PD and move between cells. TGBp2 and 3 are smaller ER-transmembrane proteins that can target the TGBp1 to PD. Whereas BSMV (hordeivirus) moves as vRNP (vRNA complexed with TGBp1), the PVX (potexvirus) is proposed to move as a TGBp1-5'-associated virion or CP-containing-non-virion complex. The PVX TGBp1, due to its NTPase and/or RNA helicase activity, plays a role in destabilizing the moving PVX virion allowing the release of RNA for translation in the receiving cell (i.e. a translation activator). It is a multifunctional protein that, in addition to its role in the virus movement by increasing PD SEL, may also inhibit RNA silencing and improve translation. However, the BSMV TGBp1 contains an expanded N-terminal with an additional high-affinity RNA binding domain, which counteracts the need for CP to safeguard the viral genome during movement.

Table 2.2. Different types of Movement Proteins found in plant viruses. Groups here are for simplicity: Group 1 includes viruses that require only single MP for virus trafficking. Group 2 viruses encode single MP, but they require for their local spread another protein, mainly the CP, which may not function here in the virion assembly. Group 3 is the tubule-forming viruses. They move through PD as virions, and in addition to the single MP they encode, they require the structural viral protein CP for the virion assembly. Members of that group (e.g. caulimovirus) may also require a contact between the MP and CP mediated by a virion-associated protein (VAP). All double-stranded, monopartite DNA viruses move through PD as tubule-formers. DNA viruses having single-stranded multipartite genome fall, however, in group 4 and their MP plus a host nuclear shuttle protein (NSP) are essential for the transfer of the DNA virus through dilated PD. The last group comprises viruses that encode multiple genes for their local intercellular spread. There doesn't seem to be a specific ORF for encoding a MP in members of the Potyvirus genus. However, genomes of some other viral genera contain an evolutionarily conserved genetic element of two (double gene block or DGB) or three (triple gene block or TGB) overlapping ORF that have been implicated in the virus movement. The closteroviral movement system contains the most components (5 viral movement genes or the quintuple gene module).

Group	Genus	Virus	MP(s)	Ancillary proteins	moving form
1 Require only single MP	Tobamovirus	TMV	30 kDa	–	vRNP extended thread like
2 Encodes single MP but require an additional viral protein for local spread	Bromovirus	CCMV (dicot-adapted) BMV (monocot-adapted)	3a 3a	– CP	vRNP vRNP CP:3a:vRNA
	Cucumovirus	CMV	3a	CP	vRNP CP:3a:vRNA
3 Tubule-forming viruses	Comovirus	CPMV	48 kDa	CP	Virion (see figure 2.7)
	caulimovirus	CaMV	P1	CP + VAP	virion
4 Requires NSP	Begomovirus	BDMV/SLCV	BC1	BV1	DNA+MP+NSP

Table 2.3 continue

5 Encodes more than one gene	Carmovirus	(MNSV and TCV),	DGBp1+ DGBp2	–	vRNP
	Potyvirus	TEV/BCMNV/ LMV	HC-Pro + CP	CI	modified virion
	Hordeivirus	BSMV **Hordei-like**	TGBp1 + TGBp2 + TGBp3	–	vRNP
	Potexvirus	PVX/ WClMV **Potex-like**	TGBp1 + TGBp2 + TGBp3	CP	modified virion
	Closterovirus	BYV	6k, Hsp70h, 64k, CP, CPm	–	Modified virion

2.4. Linking Virus Movement to Replication

Plant viruses, as obligate parasites, cause infection by modifying the endomembrane system of their host cells in order to replicate and move. The major modifications in the membranes are stimulated probably as a result of the increment of foreign proteins inside the cell (Hong and Ju, 2017). Among these viral proteins, the RNA-dependent RNA polymerases (RdRP) can adapt membranes of many organelles (such as the endoplasmic reticulum (ER), chloroplast outer membrane, vacuolar membranes, mitochondria, nuclear envelope, or peroxisomes) to harbor host- and virus-encoded cofactors in a viral replication complex (VRC) and form, in some cases, vesicles that sustain genome replication in a **microenvironment** where replication factors are concentrated, and replication intermediates are protected (Heinlein, 2015b; Hong and Ju, 2017). Inside the infected plant cells, the ER was considered the site of replication of many RNA viruses including TMV (Más and Beachy, 1999) and PVX (Linnik et al., 2013; Bamunusinghe et al., 2009), and these ER-associated VRC are also found colocalized with their respective MPs (Liu and Nelson, 2013; Tilsner et al., 2012).

TMV has a positive-sense, single-stranded RNA encoding for the 126kDa and 183kDa replicase proteins that are translated directly from the genomic RNA (gRNA) with the same initial codon, and for the 30 kDa MP and the 17.5kDaCP proteins that are translated from subgenomic RNA (subgRNA; Buck, 1999; Liu and Nelson, 2013; Ishibashi and Ishikawa, 2016). Whereas the virus genome encodes for two interacting replicases that can be separately isolated from infected plants, the virus can less sufficiently replicate in protoplasts with only the 180kDa replicase (Ishikawa and Okada, 2004), which is observed to be efficiently increasing the replication rate, when expressed together (at a ratio of about 10-20:1) with the other 126kDa replicase (Ishibashi and Ishikawa, 2016; Ishikawa and Okada, 2004). Moreover, since the 126kDa replicase protein traffics along actin-supported ER (dos Reis Figueira et al., 2002), it is suggested to be involved together with the 30kDa MP in the cell-to-cell movement, though its role in this is still unknown (Guenoune-Gelbart et al., 2008; Hirashima and Watanabe, 2001). The ER modifications that are associated with virus infection are structured in a membrane bound complex that contains, in addition to some host factors, 183- and 126kDa replicases, MP and vRNA, and travels them to transit near PD, where infectious TMV can be easily trafficked to neighboring uninfected cells (Levy et al., 2018; Guenoune-Gelbart et al., 2008).

The 30kDa MP does not integrates but associates with the ER periphery (Peiró et al., 2014) that with the help of some cytoskeletal components diffuses through the membranes towards and through PD. The movement of 30K protein through PD implicates the TMV vRNA progenies and the replicase protein as well (during infection, 126kDa is found in PD but doesn't target it by itself), indicating that the TMV spreads in the mobile form of intact VRC rather than in the simple form of MP:vRNA complex (Kawakami et al., 2004). The PD recruitment of the TMV replicase may involve a direct or indirect interaction with the MP, raising spatial links between movement and replication (Tilsner and Oparka, 2012). However, a direct interaction with 126kDa/183kDa replicase is less concerned as a

result of the successful complementation of different TMP MP strains. It is most likely that 30kDa MP interacts, binds or localizes to the where the replication occurs (Reagan and Burch-Smith, 2020; Heinlein, 2015b). Replication of TMV occurs as bound/associated with the cortical-ER membranes in close contacts with the PM, as well as the MP30 that interacts with the same membrane contact site (MCS) components forming "peripheral" punctate (early VRCs) adjacent to PD (Heinlein, 2015b). Anchoring of TMV VRC from the coricta-ER to the PM and subsequently to the PD involves SYTA/1 receptors, that recruit the 30kDa to PD in an endocytic way (Lewis and Lazarowitz, 2010), and thus play a role in the formation of these early PD-localized VRC (Levy and Tilsner, 2020; Levy et al., 2015). The model proposed by Levy and Tilsner , 2020 of anchoring the virus replication to PD during cell-to-cell Tobamovirus movement by the MCS near the PD is a possible explanation to the specificity required to permit the molecular flux of virus spread as early as 0-4h after infection.

The **PVX** RNA has five open reading frames (ORFs), and at the 5'end, the 165 kDa RNA-dependent RNA polymerase or simply the replicase gene (ORF1) is the first to be translated in the infected cell directly from the genomic RNA. This protein, the only viral-encoded protein required for replication, has three domains that are all necessary for virus replication, namely methyl transferase, helicase, and polymerase. At the 3′ end of genomic RNA, the PVX coat protein gene (ORF 5) is preceded by three overlapping ORFs (2, 3 and 4) encoding the triple gene block (TGB) proteins which, together with CP, are required for cell-to-cell spread of the PVX, yet dispensable for replication (discussed in brief in section 2.3.2.). Although these TGBps (1,2 and 3) are not essential for replication, they may assist in the transport of replication complexes towards PD. TGBp2/3 complexes induce ER-vesicle formation, target TGBp1, move and anchor near the PD. These TGBp2/3-induced vesicles are found to harbor the replicase, and ribosome as well, thus it can be considered viral replication sites, however TGBp2/3 mutations which inhibit these vesicles' movement are unlikely to affect virus replication. This may mean that

these vesicles are not the replication-competent membranes that harbor the site of replication, but rather are more likely anchoring replicase for transit to PD (Tilsner and Oparka, 2012). TGBp2/3 vesicles are motile during the early infection and reside in punctate caps in front of the PD. These caps are remodeled ER membranes that harbor ribosomes, in addition to the replicase and vRNA, hence considered a PD-localized smaller VRC. The recruitment of replicase into these caps is not yet known. This Co-replicational insertion (compartmentalization of the early developed (at early infection) PVX VRCs next to the entrances of PD by the TGBps) may also permit newly produced viruses to be inserted into the PD channel directly from the replicating enzymes, i.e. without the viral RNA traveling through the cytoplasm where it may be attacked by cellular defense mechanisms such as RNA silencing (Figure 2.8.) (Tilsner J, et al., 2013). At the late infection, these TGBp2/3-induced ER-granules form bigger inclusion bodies, where the TGBp1 plays a structural role in the formation of these bodies, switching its movement ability to assist in organizing the virus accumulation inside the cell (Tilsner et al., 2012). As such, quantitative studies of PVX encoding proteins have been studied at different biological life time of the PVX virus as early as 1 hpi, and Tilsner et al. (2012; 2013) have described a linkage between the movement and replication virus factories that are spatially enclosed within cap structures near PD orifices at the recently infected cells or complexed together within peri-nuclear X-bodies at later stages of infection.

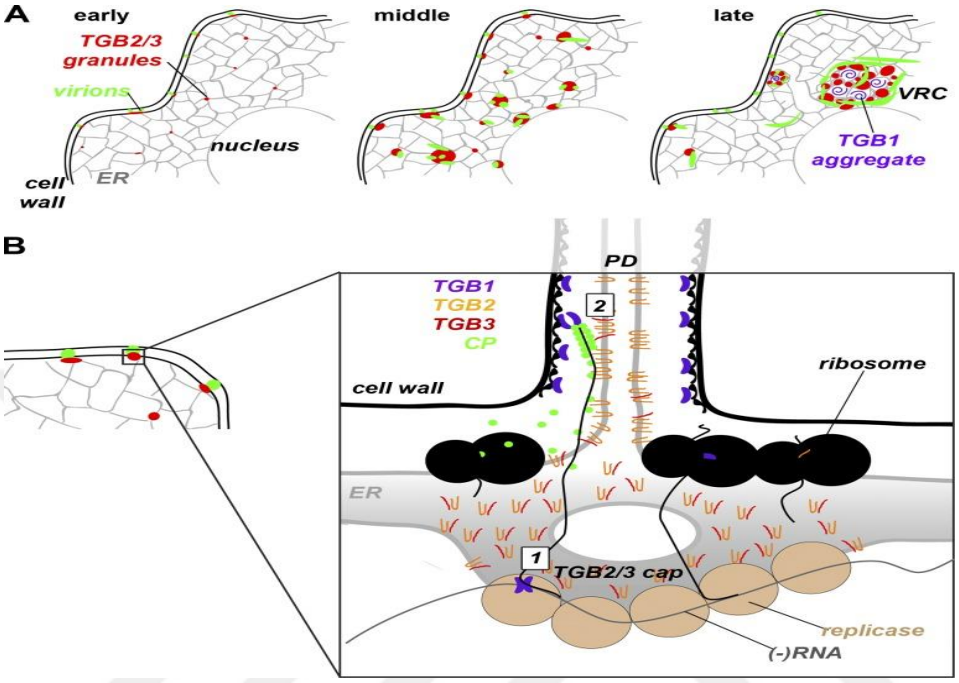

Figure 2.8. Diagram illustrating the cap structure of the PD-localized replication in recent PVX-infected cells (Tilsner et al., 2013)

The role of PVX-proteins and their localization in their ectopic expression and their possible recruitment factor as encoded during the virus infection is summerized below:

TGBp1

- In vitro, it can interact with CP (protein-protein interaction) and also binds in a moderate co-operative manner with in vitro prepared vRNA. The protein also tends to oligomerize from both N- and C-terminal ends, forming aggregates of homodimers or homooligomers (Leshchiner et al., 2008)
- In planta, FP-fusions show cytoplasmic aggregates, with no PD localization (**TGBp1 does not target PD by itself**). When it is co-

expressed with the other TGBp2 and TGBp3 proteins altogether (i.e. TGBp2/3 complex), it is inserted into the PD (at 1-2dpi; **TGBp1 is recruited inside the PD cavity; the recruitment is infection independent by the TGBp2/3 complex**) and found in cytoplasmic ER-granules (at 2-3dpi; **TGBp1 is also recruited along ER-derived granules; the recruitment is infection independent by the TGBp2/3 complex**). However, it cannot recruit CP into PD, even in the presence of the other TGBp2/3 complex.

- At early infection (1-2 dpi), it binds vRNA and interacts with the CP of the CP-coated vRNA. It co-localizes with the CP of the PVX virion inside the PD cavity and in cap structures at the cytoplasmic orifice of the PD (**TGBp1** can thus **recruit CP into the PD only in the infection context**).
- At late infection (2-3 dpi), it forms "beaded sheets" aggregates, switching its movement function to act more as a scaffold to the components of the virus factories. These beaded sheets are surrounded by large actin cables inside the core of the X-body (Tilsner et al., 2012).

TGBp2

- In vitro, it can interact with CP (protein-protein interaction) and also form hetero-oligomers with TGBp3.
- In planta, only C-terminal FP-fusion (with and without unfused versions) show its tubular ER-residence and the formation of ER-derived granules at 2-3 dpi. However, this quietly changes at the very low expression levels at as early as 21hpi, and it localizes in front of the PD orifice (i.e. **TGBp2 can first target PD and form peripheral punctae known as caps before they can induce the ER-granules**

formation) as well as inside the PD cavity, though very faintly, from the constricted ER-desmotuble. Only when it is co-expressed with the other TGBp3, they can recruit TGBp1 to the punctate caps as well as to the ER-derived granules. The TGBp2 alone does not directly interact with the CP as it fails to bring the cytoplasmic FP-CP aggregates into PD caps or ER-derived granules.

- At early infection (1-2 dpi), it, together with TGP3 (see above), can target TGBp1 with its CP-bound vRNA into PD and in punctae aligned with PD. Peripheral ER-remodeling by the TGBp2 is recognized in these punctae to also contain the replicase and naked vRNA, and thus these cap structures are later proposed to be early VRCs.
- At late infection, the ER-induced granules accumulate on the ER surrounding the TGB1 aggregates, within the X-body (Tilsner et al., 2012).

TGBp3

- In vitro, it can form hetero-oligomers with TGBp2.
- In planta, only N-terminal FP-fusion is found resident/localized in the ER but cannot induce ER to form vesicles/granules. However, this quietly changes in the presence of the unfused TGBp3, where small motile punctae are recognized in the ER-cortex and at the periphery in front of the PD, with this PD-targeting ability amplified when coexpressed with the TGBp2 (i.e. **TGBp3, in its native/unfused form, can target PD and forms caps, but with an increased rate in the TGBp2/3 complex form**).
- At early infection (1-2 dpi), it can target the PD and is found in peripheral ER-modified caps. It also jointly with TGBp2 can insert

TGBp1 with its CP-bound vRNA into these PD-localized caps, which in association with replicase and other host factors develop into early PD-localized VRCs.

- At late infection (2-3 dpi), TGBp3-associated granules gather around coated and uncoated vRNA, with naked vRNA whorls in the middle and virions at the edges of a big viral factory or X-body (Tilsner et al., 2012).

Replicase

- In planta, the expression of the replicase with its c-terminal domain replaced with FP (truncated, FP-fused replicase) has been aggregated inside the nuclei, with no sign of PD or ER localization even after the co-expression with the TGB proteins and CP (i.e. **recruitment of replicase into VRC is infection dependent**).
- At early infection (1-2 dpi), it forms peripheral VRCs with labeled vRNA, arranged in the form of punctate hotspots in the small caps but as whorls inside bigger ones (PVX replicates as early as it moves in PD-localized caps).
- At late infection (2-3 dpi), replicase and other replication-associated proteins are notably structured in big viral compartments, accumulated around ER-granules membranes, and encircled with vRNA. As a result, the X-body develops to offer a secure, significant replication site (Tilsner et al., 2012).

CP

- In vitro, the c-terminus of the CP associates with TGBp1 motif IV (due to its RNA helicase activity), only when the complex is mediated by the vRNA, as the **CP–TGBp1 complexes are insoluble** (non-functional; Karpova et al., 2006). The in vitro assembly from the 59-nucleotide (nt) 5'end of PVX RNA and CP leads to a head-shaped virus like particles (VLP), that are untranslatable in cell-free translation system. However, single-tailed particles (STP) are created when TGBp1 attaches to the terminal CP of these head structures, and these particles are more easily translated in vitro and in vivo. The intercellular movement of the in vitro-assembled non-virion STPs proves that **encapsidation is not a requirement** for the PVX spread (Karpova et al., 2006). Unlike TMV that have sequence specific packaging signal or origin of assembly (OAS), PVX require cis-acting sequences (Kwon et al., 2005) and/or stem–loop secondary RNA structures (SL) (Petrova et al.2015) for binding to the PVX CP and to initiate the in vitro assembly. These SL1 are identified within **the 5' nontranslated region** (NTR) of the PVX gRNA and found to be crucial for the **CP recognitio**n forming in vitro-assembled virus-like particles (Cho and Kim 2012) as well as for the **vRNA accumulation (**Miller et al., 1998**)**.
- In planta, the expression of the N-terminal FP-fusion of CP has shown cytoplasmic aggregates, with no sign of PD or ER localization even after the co-expression with the TGB proteins (i.e. **recruitment of CP into PD by the TGBp1 is infection dependent**).
- At early infection (1-2 dpi), it is only found as localized inside the PD but not in front of the PD (most likely upon translation, **CP is immediately inserted from caps into the PD channel**). But behind the

infection front, caps containing CP/CP-containing RNP can be seen (see figure 7D in Tilsner et al., 2013). Mutations that truncate the entire CP result in movement defective PVX mutants. Cell to cell movement of these PVX with fully-truncated CP mutants is recovered at different rates when co-expressed with plasmids encoding TMV P30k, PVX CP, Cocksfoot mottle sobemovirus CfMV CP, but not BYV CP, Potato virus A potyvirus PVA CP or Potato virus Y potyvirus PVY CP. Though the successful complementation, trans-encapsidation is not noticed between these two unrelated viruses. Surprisingly, PVX CP mutants lacking the last 10 amino acid (a.a.; Tilsner et al., 2013) or 18 a.a. (Fedorkin et al., 2001) are being able to form virions, yet incapable of cell-to-cell movement. Complementation of these PVX with c-terminal truncated CP mutants with PVA genome (Fedorkin et al., 2000) or plasmids encoding PVY CP, PVX CP, CfMV CP, BYV CP, PVA CP and PVY CP has increased the size of infection to levels closer to the PVX with wild CP (Fedorkin et al., 2000; Fedorkin et al., 2001). Though the successful complementation with the wild PVX CP, PD-localization of the CP is not observed at the infection front (Tilsner et al., 2013). Fused TGBp1 are incapable of inserting CP into the PD, when they are ectopically co-expressed with PVX lacking the TGBp1, and P19 (a silencing suppressor to compromise suppressing activity lost when TGBp1 is removed). Accumulation of the CP into PD may be interrupted with the modification of the helicase activity of TGBp1 upon fusion. That is supported by a similar experiment with the unfused TGBp1 that shows an entire leaf infection spread with PD-localized CP at the infection fronts (Tilsner et al., 2013). Intriguingly, when PVX with defective CP mutants (marked by GFP) are **co-moved** with PVX with defective TGBp1 mutants (marked by GUS), the CP-mutants have restored the PVX movement to exceed 30–50 cells marked by GFP

signal, more movement than is seen when these same mutants are even complemented by plasmid encoding the PVX wild CP, which is recorded on the round of 8–10 cells (Fedorkin et al., 2000). Indicating that TGBp1 is the one orchestrating the process by recruiting the CP (gene/protein?) into the movement system and that the CP has just an associated role in completing that process. The behavior of the PVX with defective CP mutants (marked by GFP) in addition to wild PVX (with a tagged vRNA not the CP to avoid superinfection exclusion) would be interesting to observe the competition of TGBp1s from different sources on the CP.

- At late infection (2-3 dpi), circles of non-encapsidated vRNA produced in the middle of the X-body are assembled within and accumulate in cages along edges of the X-body facing the cytoplasm (Tilsner et al., 2012).

3. MATERIALS AND METHODS

3.1. Plasmid Constructs

Potato virus X (PVX), the subject of my study, was modified in a reverse genetics system, where the viral RNA (in cDNA form) has been inserted onto a suitable plasmid expressing the viral genome after being introduced into plant cells to start the infection, and tagged with fluorescent proteins to detect infected cells/tissue under CLS microscopy (Figure 3.1.).

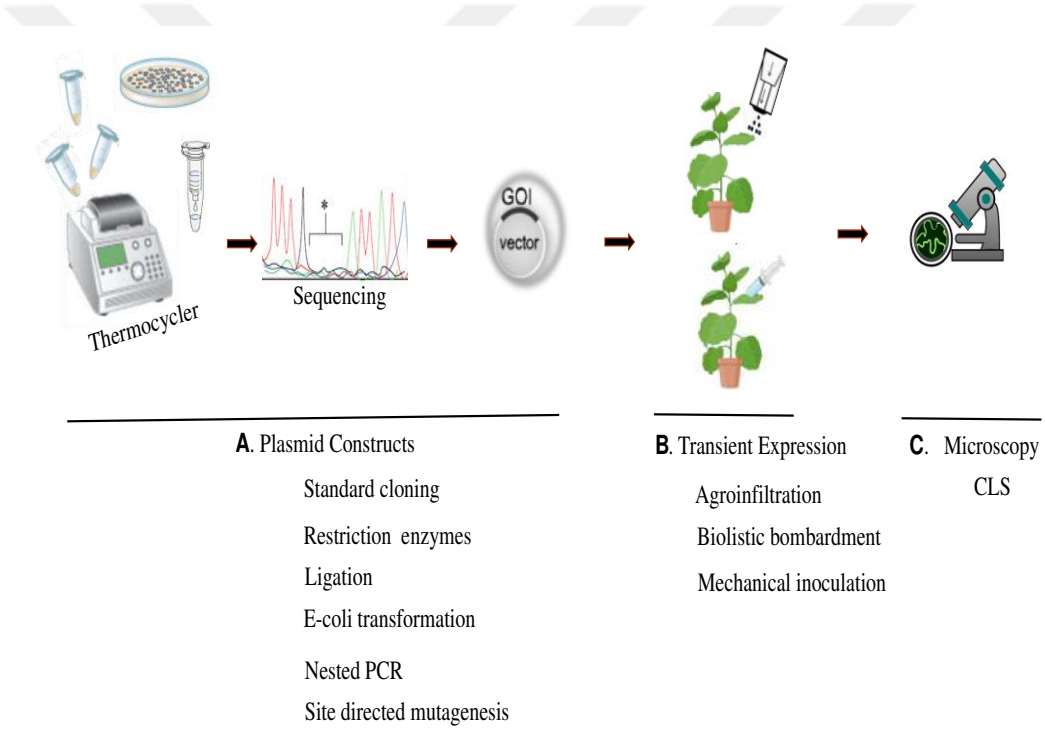

Figure 3.1. Schematic representation of the work of study. A) the plasmid construction using different cloning techniques. After sequence verification, B) the plasmids are introduced into the plant materials either by agroinfiltration or biolistic particle bombardment. C) The subcellular localization of the virus is analyzed under confocal laser scanning (CLS) microscopy.

3.1.1. p35S.PVX.deltaTGBs.30K.4xCsy4.DsRED-2A-CP

Using restriction free cloning (NEBuilder HiFi DNA Assembly Cloning Kit from New England Biolabs), p35S.PVX.deltaTGBs.30K.4xCsy4.DsRED-2A-CP (or JTM003) construct is successfully assembled as three PCRs followed by NEBuilder overlapping reaction.

a. PCR amplifying the p35S.PVX backbone

Recommended annealing temperature is 61.7ºC for full-length amplification using the primers: p35S.PVX.GFP-CP_fwd primer and p35S.PVX.GFP-CP_rev primer. The expected product size is 9329 bp

.**b.** PCR amplifying the 4xcsy4.DsRed-2A insert.

Recommended annealing temperature is 57ºC for primer parts designed for overlapping ends and then upto 61.7ºC for full-length amplification using the primers: pTRA.PVX.csy4.DsR-CP_fwd primer and pTRA.PVX.csy4.DsR-CP_rev primer. The expected product size is ~1 kb.

c. PCR amplifying the the 30k insert.

Recommended annealing temperature is 57ºC for primer parts designed for overlapping ends and then upto 68ºC for full-length amplification using the primers:

JT1189a_fwd primer and JT1189a_rev primer. The expected product size is ~840 bp

The modified virus plasmid p35S.PVX.deltaTGBs.30K.4xCsy4.DsRED-2A-CP (or JTM003) are cloned in chemically-competent DH5alpha (Invitrogen "Library Efficiency") and bombarded into *N.benthamiana* followed by a detection analysis under UV ignition lamp and the confocal microscopy to check for their fluorescent infection. Clones (JTM003m and JTM003p) that show successful fluorescent infection are then sent to be sequenced using the following primers: 30kS68CF and 30kS163CR. These will cover the end of 165k through all of 30k to first csy4 stem

loop. Both of the JTM003m and JTM003p were correct and no errors found in either of them.

3.1.2. p35S.PVX.165k-2A-phiLOV2.1-mcherry-2A-CP

Using restriction free cloning (NEBuilder HiFi DNA Assembly Cloning Kit from New England Biolabs), p35S.PVX.165k-2A-phiLOV2.1-mcherry-2A-CP (or **JTM082**) construct is successfully assembled as nested PCRs followed by NEBuilder overlapping reaction.

a. PCR amplifying the p35S.PVX backbone

Recommended annealing temperature is 56ºC for for full-length amplification using the primers: fusePVXsgtbp_fwd primer and fuse165k_rev primer. The expected product size is ~11 kb.

b. Three nested PCRs constructing the 2A- phiLOV2.1 insert.

Recommended annealing temperature is 56ºC for primer parts designed for overlapping ends and then upto 70ºC for full-length amplification using three primer pairs: 2A1-phiLOVF primer and 2A-phiLOV_rev primer for the first PCR, 2A2F primer and 2A-phiLOV_rev primer pair for the second PCR and 2A-phiLOV_fwd primer and 2A-phiLOV_rev primer pair for the third PCR. The expected product size is ~400 bp.

The modified virus plasmids p35S.PVX.165k-2A-phiLOV2.1-mcherry-2A-CP (or (JTM082e) are cloned in chemically-competent DH5alpha (Invitrogen "Library Efficiency") and bombarded into *N.benthamiana* followed by a detection analysis under UV ignition lamp and the confocal microscopy to check for their fluorescent infection. Clones (JTM082e) that show successful fluorescent infection are then sent to be sequenced using GKEArev primer to check if 2A-phiLOV2.1 has been added to the end of 165k seamlessly exactly as planned.

3.1.3. PVX virus with internal philLOV2.1-tagged Replicase

Using restriction free cloning (NEBuilder HiFi DNA Assembly Cloning Kit from New England Biolabs), three PVX plasmids JTM858, JTM868 and JTM838 are constructed and assembled to have internally tagged replicases, from wild PVX pTRA , and p35PVX plasmids and the modified PVX with TGBps replaced by 30K MP JTM003, respectively.

These plasmids are successfully assembled as nested PCRs followed by NEBuilder overlapping reaction.

a. PCR amplifying the PVX backbone

Recommended annealing temperature is 61.7ºC for full-length amplification using the primers: GS-165F primer and GS-165R primer. The expected product size is 10-12 kb

b. PCR amplifying the phiLOV2.1 insert

Recommended annealing temperature is 55ºC for primer parts designed for overlapping ends and then upto 71ºC for full-length amplification using the primers:

GS-phiLOVF primer and GS-phiLOVR primer.The expected product size is ~500bp

The modified virus plasmids with internal phiLOV (JTM858, JTM868 and JTM838) are cloned in chemically-competent DH5alpha (Invitrogen "Library Efficiency") and bombarded into *N.benthamiana* followed by a detection analysis under UV ignition lamp and the confocal microscopy to check for their fluorescent infection. Clones (JTM868 BC, JTM858 AB and JTM838O) that show successful fluorescent infection are then sent to be sequenced using LINK-F and GS-phiLOVF. There will be NO NEED for 2A. 2As are not added in there because if the internal phiLOV kills the virus, the 2As will not rescue it: when 2A is active, a truncated

replicase is produced, when it is inactive an internally tagged one. There is no wild type replicase restored as in the fusions via 2A at termini.

3.1.4. PVX virus with frameshifted replicase.

Truncating part of the replicase using PVX plasmid/KpnI then ligating it as a delta 165k (defective replicase) will be a large deletion, potentially missing important regulatory RNA sequences. A frameshifted replicase will, however, result in an incorrect amino acid sequence by replacing few functional nucleotides but still keeping the rest of RNA sequences.

This frame-shifted *pTRA.PVX (*or *pTRA*)* is constructed by *AgeI* (5'A|CCGGT3') digestion at 37C /3h followed by the 5' overhang filling, 5'-to-3' polymerization activity of the *E.coli* DNA polymerase I *Klenow* fragment at 25C/15min and the T4-ligation at 4C/o.n, resulting in the new sequence 5'A**CCGG**CCGGT3' and a frame-shift in the replicase following the codon for Pro 385 (underlined). *it is co-bombarded*

The modified virus plasmids with frame-shifted *pTRA.PVX (*or *pTRA*)* are cloned in chemically-competent DH5alpha (Invitrogen "Library Efficiency"). To corroborate the loss of infectivity of *pTRA*, it is* co-bombarded with GFP-sporamin/19K into *N.benthamiana* followed by a detection analysis under UV ignition lamp and the confocal microscopy.

3.1.5. Fused (N- and C- terminal GFP-tagged) and unfused (165k-E) replicases.

Using gateway technology, three plasmids JTM010, JTM011 and JTM002 are constructed and assembled to have unfused replicases165K-E, and fused replicase GFP-165k and 165k-GFP, respectively.

These plasmids are successfully assembled as overlaping PCRs amplifying the full length PVX replicase followed by BP recombination into pDONR201and then LR recombination into a suitable gateway plasmid (pGWB405 (C-terminal GFP), pGWB402omega (unfused) and pGWB406 (N-terminal GFP)).

a. Two nested overlapped PCRs amplifying the PVX 165-nostopcodon

Recommended annealing temperature is 67ºC for primer parts complementary to gene-specific nested primers and then upto 72ºC for full-length adapters using the primer pair: attB-186 forward primer and attB-186 reverse primer for the first PCR. But 47ºC for primer parts complementary to gene-specific nested primers, 72ºC recommended for full-length adapters using the the primer pairs : attB1 adapter primer and attB2 adapter primer for the second PCR. The expected product size is 4.5kb.

b. Two nested overlapped PCRs amplifying the PVX 165-stopcodon

Recommended annealing temperature is 66ºC for primer parts complementary to gene-specific nested primers and then upto 72ºC for full-length adapters using the primer pair: attB-186 forward primer and attB-Stop-186 reverse primer for the first PCR. But 47ºC for primer parts complementary to gene-specific nested primers, 72ºC recommended for full-length adapters using the the primer pairs : attB1 adapter primer and attB2 adapter primer for the second PCR. The expected product size is 4.5kb.

The pDONR containing the 165K are fully sequenced, and the localization of the fusion proteins are then ecotopically expressed in the non-infected cell and during the infection context.

3.2. Plant Materials and Inoculations.

All *Nicotiana benthamiana* plants are grown in JHI greenhouse at 20°C with a 16 h/8 h light/dark cycle. For each treatment, identical plants at the two-leaf stage are used. 35S::PVX constructs are introduced into the plants via bombardment. However, pTRA-based and pGWB-based plasmids can be both agroinfiltrated and bombarded. Co-infiltration and/or co-bombardment of the virus plasmids and/or virally and ectopically expressed FP fusions are performed to study colocalizations and complementation in the infection context. The agroinfiltrations are carried out

2-3 days after the bombardments. The Agrobacterium tumefaciens strain AGL1-suspensions are diluted into 0.1A OD600 for 19K protein and 0.25 for the virus and other fusion proteins. A needless-syringe is used to agroinfiltrate the T-DNA binary plasmids in the lower abaxial surface of the leaf. The infiltration media is prepared according to Voinnet et al., 2003. Transient expression by bombardment 2–5 µg of the infectious DNA plasmid coated with gold particles (from Bio-Rad Laboratories) is achieved using a pressure delivery system at ~20 psi N-pressure with the nozzle around 5 cm distance to the surface of the leaf. All bombarded and infiltrated leaves are marked by a hole and only detached from plants on the day of imaging (Tilsner et al., 2009).

3.3. Confocal Microscopy

All imaging are performed on confocal laser scanning (CLS) microscope ZEISS. The microscopic power and detection range of the fluorophores GFP (488nm), TagRFP (561nm) and analine blue (405nm) are optimized for each individual image. On the microscope slides, every leaf is put with the lower epidermis facing upward. To mark the PD, leaves are immediately infiltrated with 0.1 mg/ml aniline blue solution before imaging.

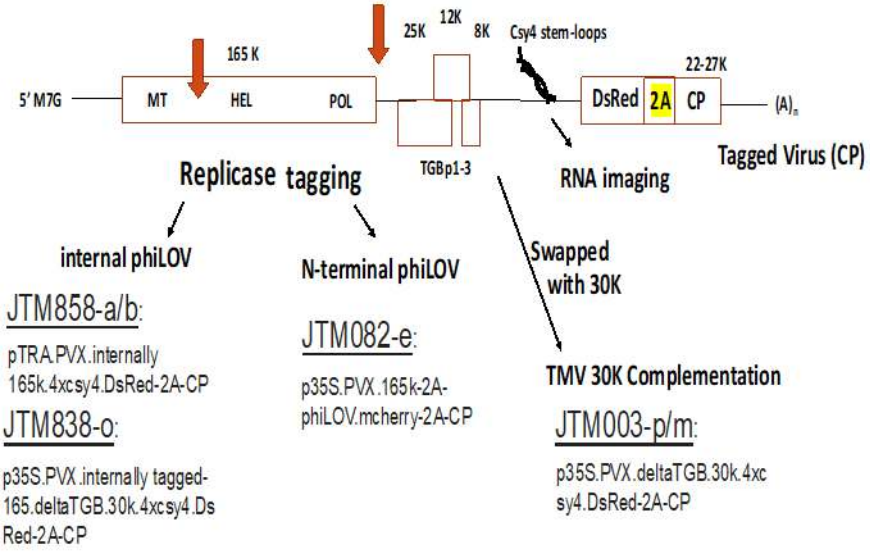

Figure 3.2. Schematic representation of all plasmid constructs used in that research

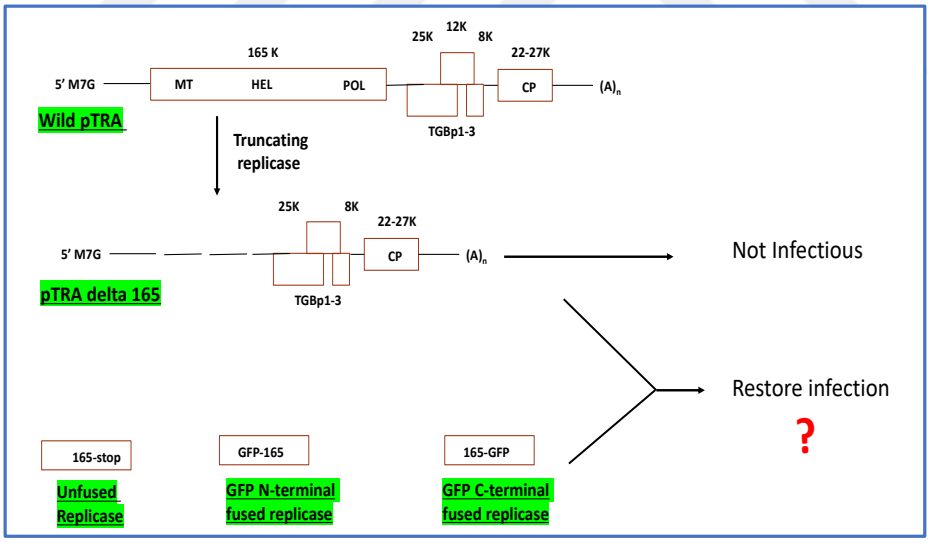

Figure 3.3. Schematic representation of complementation test between the PVX plasmid having a truncated replicase (delta pTRA) and the ectopic expression of fused and unfused replicase.

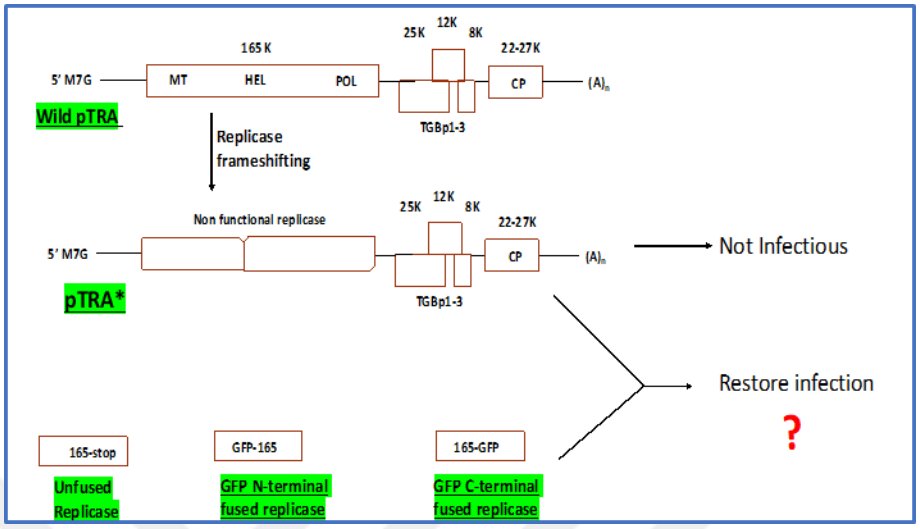

Figure 3.4. Schematic representation of complementation test between the PVX plasmid having a frameshifted replicase (pTRA*) and the ectopic expression of fused and unfused replicase.

4. RESULTS AND DISCUSSION

4.1. Cell-to-cell movement of the TGB-deficient PVX is rescued by the TMV MP together with P19.

It has been shown previously that the potexvirus MP mutants with a truncated TGB region are incapable of cell-to-cell movement (Morozov SY, et al., 1997). The cell-to-cell transport of MP mutatnts of many plant viruses has been previously observed to be rescued by TMV transport system components. Among them, the TGBps-deficient PVX genome has been initially restored when co-bombarded with the 30K gene that the two viral cDNA clones were drived under two 35S promoters (Morozov SY, et al., 1997). In here, to evaluate movement compatibility in regards to replication, one chimera virus cDNA clone is used, containing the TMV 30K MP instead of PVX MP. This p35S.PVX.deltaTGBs.30K.4xCsy4.DsRED-2A-CP (or JTM003) construct is successfully assembled (Figure 4.1.a and 4.1.b) to provide insights into the functionality of both movement and replication proteins in a cis complementation experiment, in which, the triple gene block TGBs responsible for the PVX movement are deleted and replaced with the TMV movement protein (30K). It also includes the fluorescent protein DsRED linked with the PVX capsid protein (CP) using 2A linker and therefore these virus particles, during a successful infection, can be visualised by confocal microscopy. In addition, the detection of its viral RNA (vRNA) progeny can be achieved as well, as the virus genome contains just upstream of the CP four csy4 stem-loops that are bound by the bacterial protein Csy4 fused to GFP for observation. Screening of sixteen clones of JTM003a-p using colony PCR (Figure 4.1.c, and 4.1.d) with JT1189a_fwd primer and pTRA.PVX.csy4.DsR-CP_rev primer, has verified the correct insertion in clones JTM003a-d, JTM003g-k, JTM003l-m and JTM003o-p (correct colony PCR product band size of 1.8 kb in Figure 4.1.c and 4.1.d). HindIII diagnostic digestion of JTM003m and JTM003p shows the correct pattern 6230, 1211, 1205, 973, 845, 570 bp (Figure 4.1.e). They are infectious/red fluorescent (showing that both the

replicase and DsRed are intact) and are able to cross two cell boundaries due to the correct insertion of the intact 30k and successful movement complementation. Two clones, JTM003m and JTM003p are sent to be sequenced (sequencing analysis is attached in the appendix section) using the following primers: 30kS68CF and 30kS163CR. These will cover the end of 165k through all of 30k to first csy4 stem loop. Both of the JTM003m and JTM003p were correct and no errors found in either of them.

Movement-deficient PVX can only produce bright fluorescent single cells. When bombarding JTM003p/m, the TMV 30K assisted in the movement of the TGB1-3-truncated PVX to only a maximum of one-to-two cell boundaries. Probably the infection of TGBp1-deficient virus is blocked by the cellular RNA silencing machinery, and the virus could not move further due to the loss of the TGBp1, which acts as an RNA silencing suppressor protein. Co-bombardment of these JTM003m/p constructs with an alternative RNA silencing suppressor protein such as 19K protein to compensate the loss of TGBp1 did not change the extend of the viral movement, and the virus still could not move further than 2-cell boundaries (Figure 4.1.f. and 4.1.g.). We argu that virus was restricted by the absence of the 19k in the surrounding cells. The ecotopic expression of 19K was therefore required into the plant tissue before bombarding with the JTM003m/p virus constructs. Bombardment of JTM003 into tissue already ecotopically expressing 19k silencing suppressor developed some bigger viral lesions (Figure 4.1.h. and 4.1.i.). The virus in those big lesions had crossed an average of 10 cell-boundaries, demonstrating the successful co-complementation of the PVX lacking TGBp1-3 by TMV30-MP together with 19K.

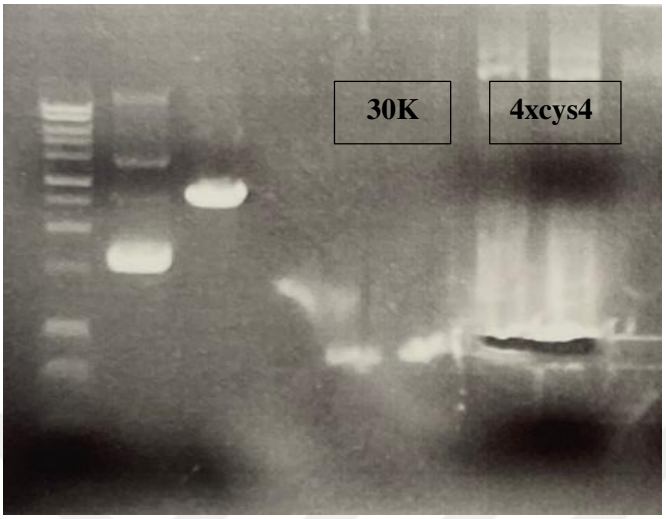

Figure 4.1. NESTED PCR amplifying the30k/4xcsy4.DsRed-2Afragments

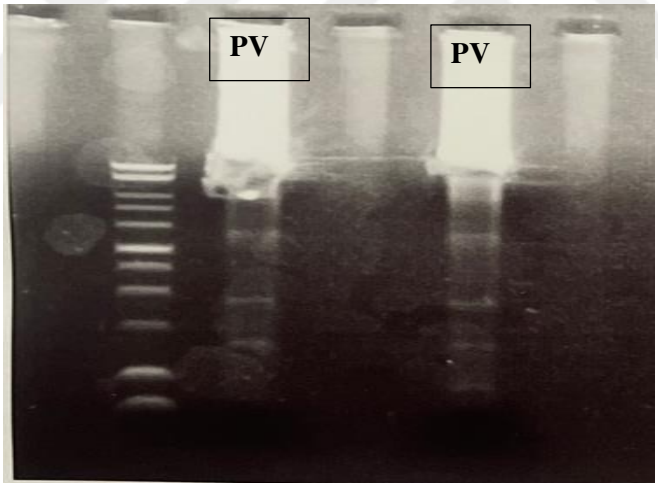

Figure 4.2. Nested PCR amplifying PVX plasmid backbone.

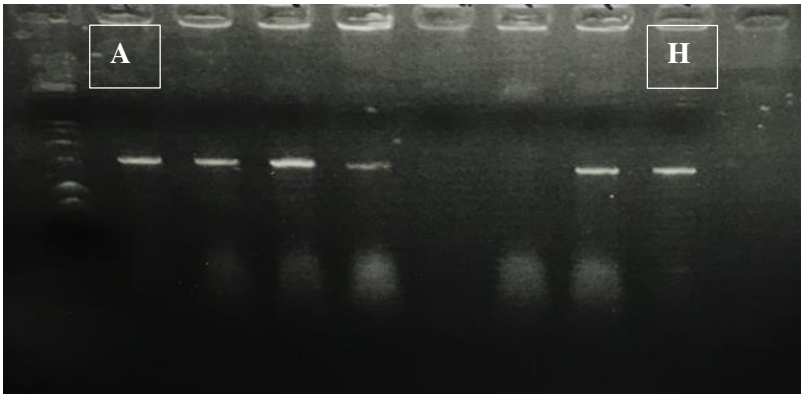

Figure 4.3. Colony PCR of JTM003A-H (from left to right) using DS JT1189a_fwd primer and pTRA.PVX.csy4.DsR-CP_rev primer. JTM003a-d and JTM003g-h had correct band size 1.8kb, but JTM003e-f had no PCR product (repeated in the coming PCR)

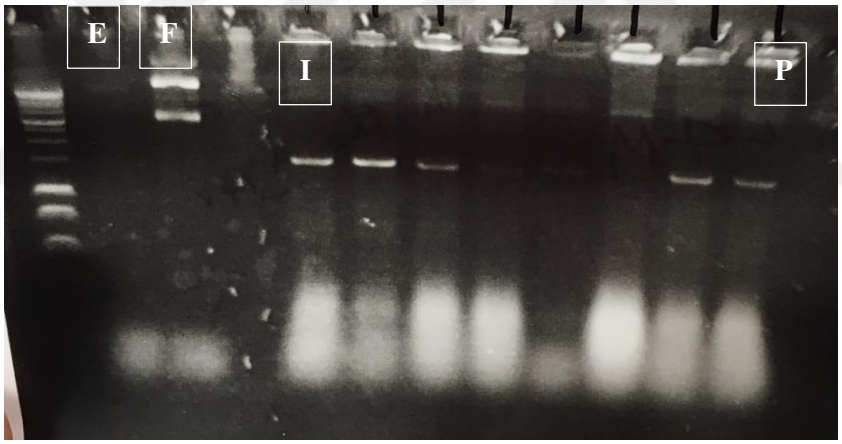

Figure 4.4. Colony PCR of JTM003E-F and JTM003I-P (from the left to to the right) using DS JT1189a_fwd primer and pTRA.PVX.csy4.DsR-CP_rev primer, JTM003i-k and JTM00o-p all had correct product size of 1.8 kb) and JTM003l-m had correct products as well, but very faint). However, JTM003e and JTM003n had no PCR product and JTM003f had two bands of incorrect size (10 kb and 6 kb).

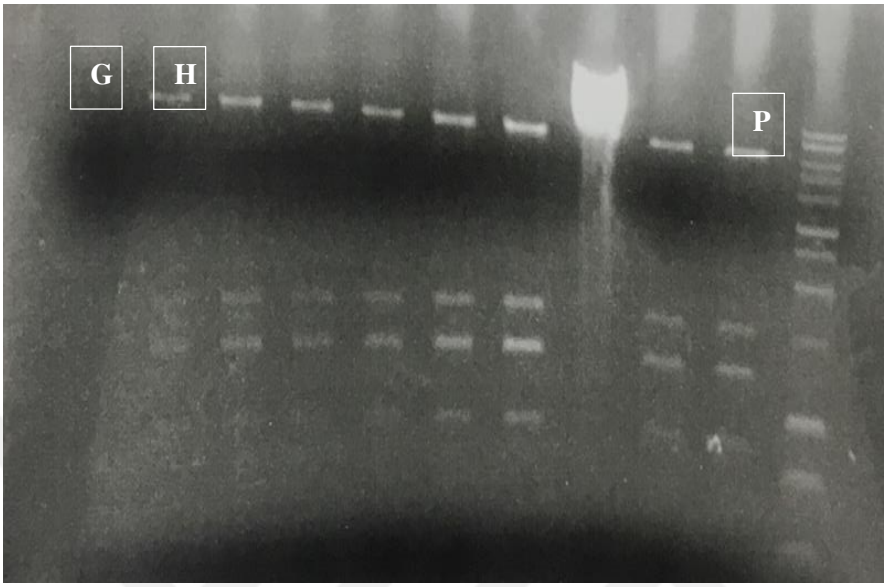

Figure 4.5. Diagnostic HindIII digestion of JTM003G-P, showing the correct expected patterns 6230, 1211, 1205, 973, 845, 570 bp.

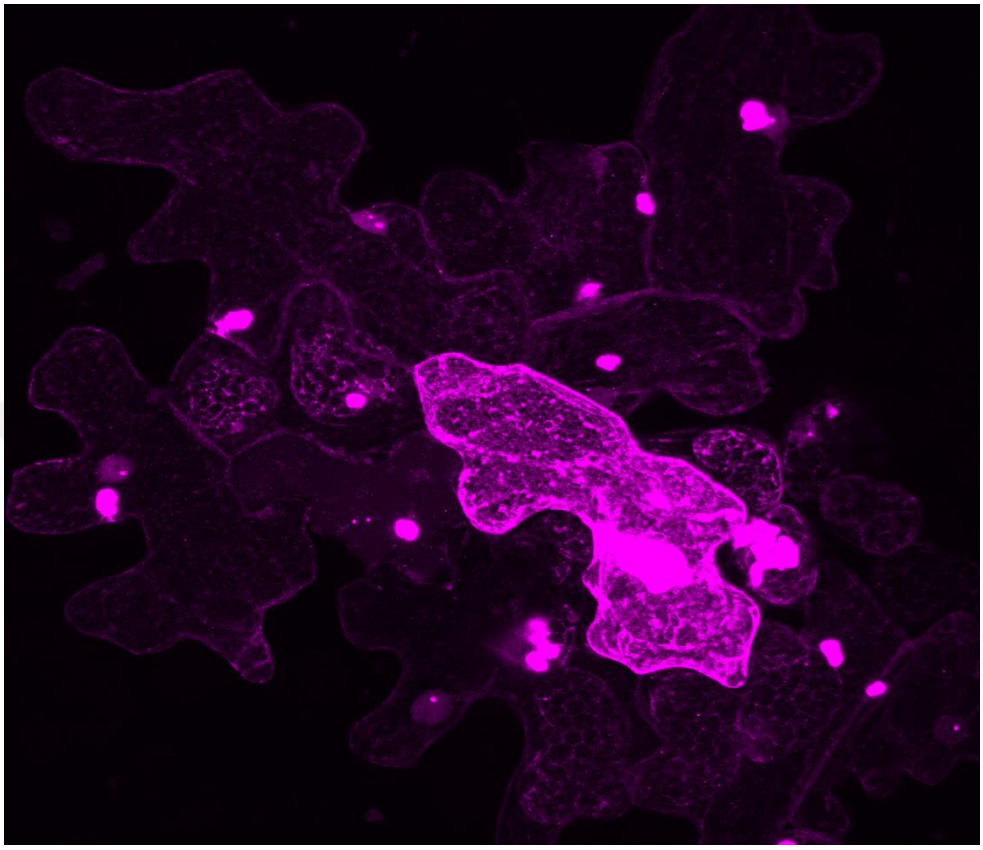

Figure 4.6. Co-bombardment of JTM003-m with 19K RNA silencing suppressor protein.

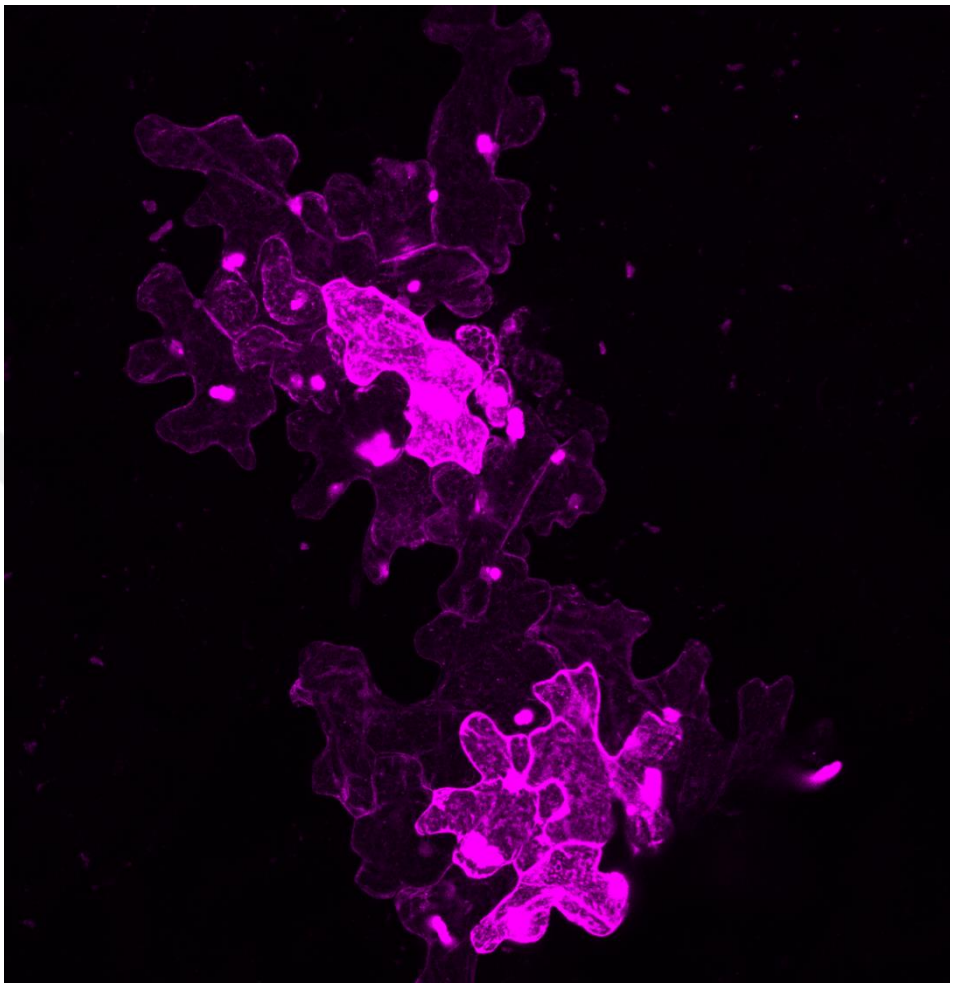

Figure 4.7. Co-bombardment of JTM003-p with 19K RNA silencing suppressor protein.

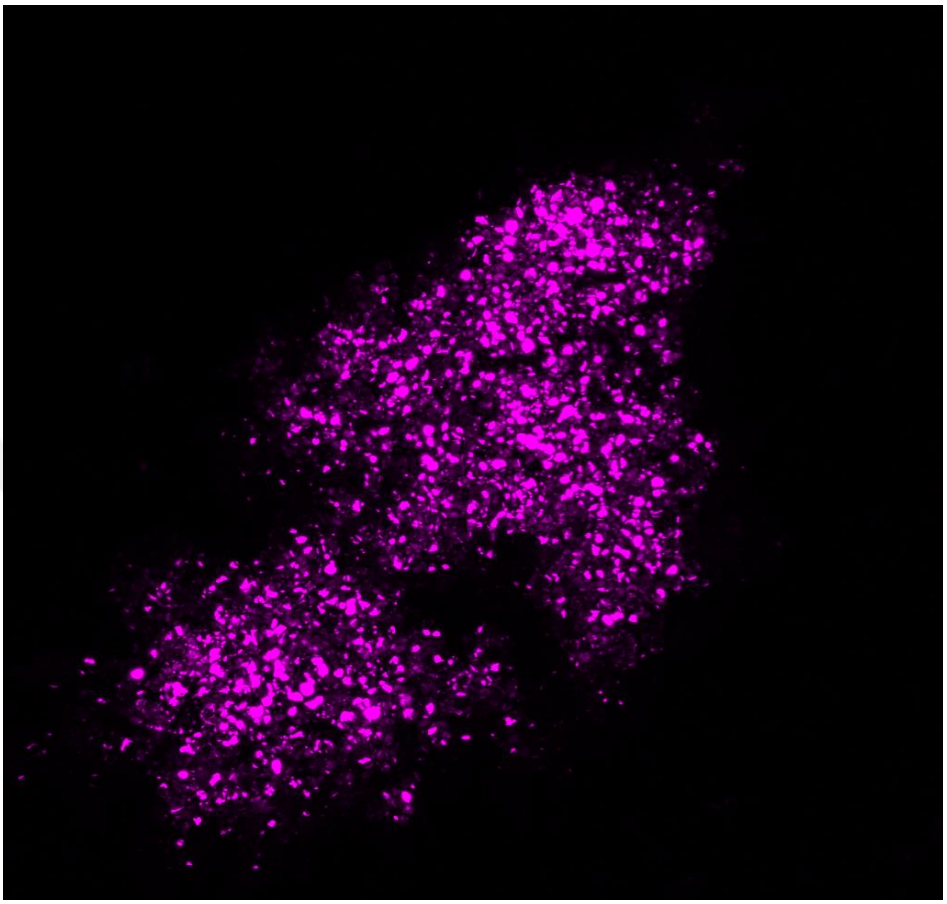

Figure 4.8. Bombardment of JTM003-p into tissue already expressing 19K RNA silencing suppressor protein

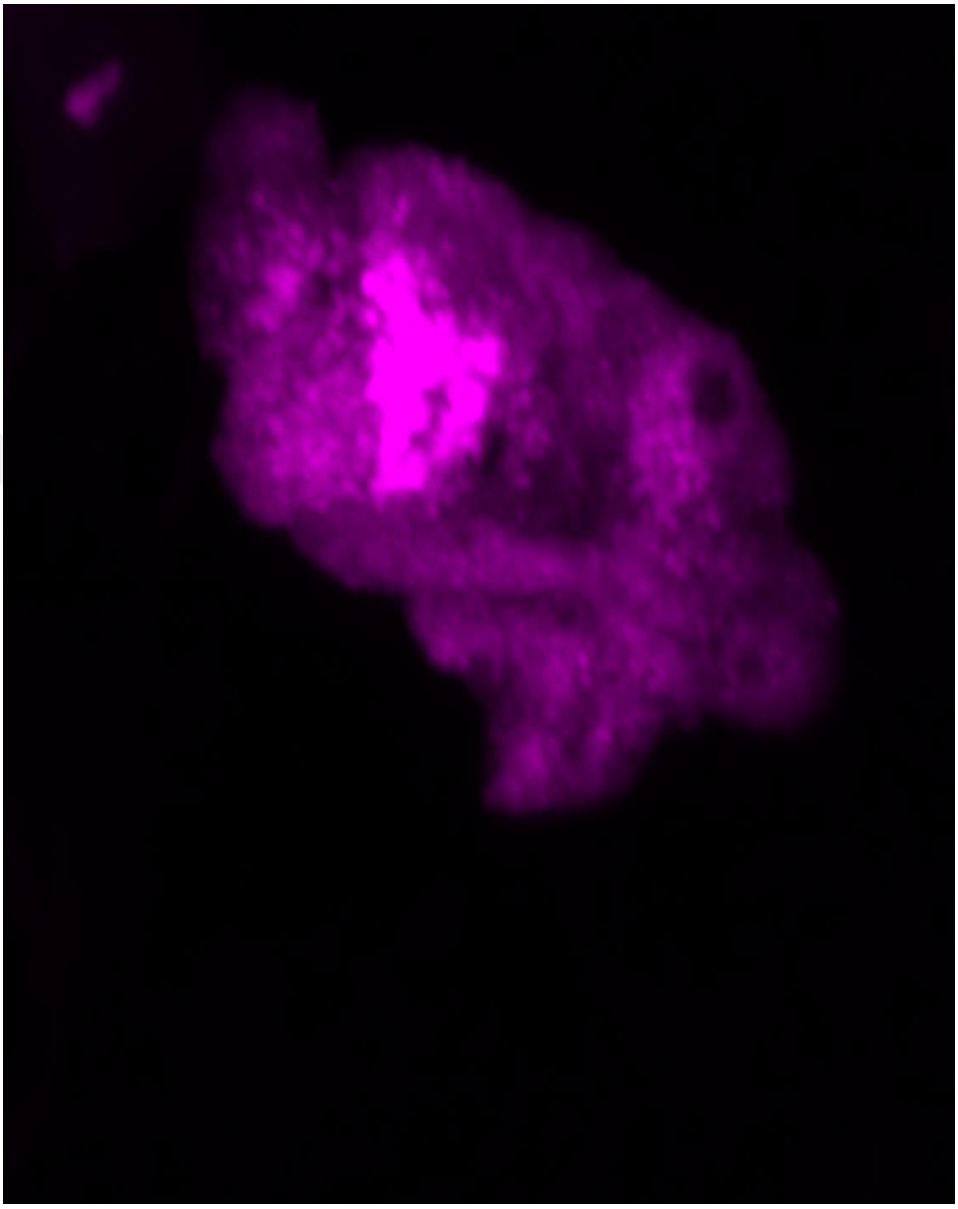

Figure 4.9. Virus aggregates of JTM003-p probably at factory when bombarded into tissue already expressing 19K RNA silencing suppressor protein, 40x magnification.

4.2. Imaging the full length 165K RdRP of PVX:

Tagging the full length PVX replicase (165K protein) at either the C- and N-terminal resulted in mainly nuclear fluorescence (and with the nucleolar exclusion) when the fusion protein is ecotopically expressed in the non-infected cell. In the infection context, the fusion was complexed into perinuclear amorphous structures. These structures are thought to be virus replication complexes VRC, however the ability to function of these non-native replicase tagged at either of its terminal is still a question to ask, especially when complexes of these intact proteins with their N- and C-GFP-tagged counterparts collapsed as aggregates inside the nucleus when infiltrated together with the untagged full length replicase (Figure 4.2.a., 4.2.b., 4.2.c. and 4.1.d.).

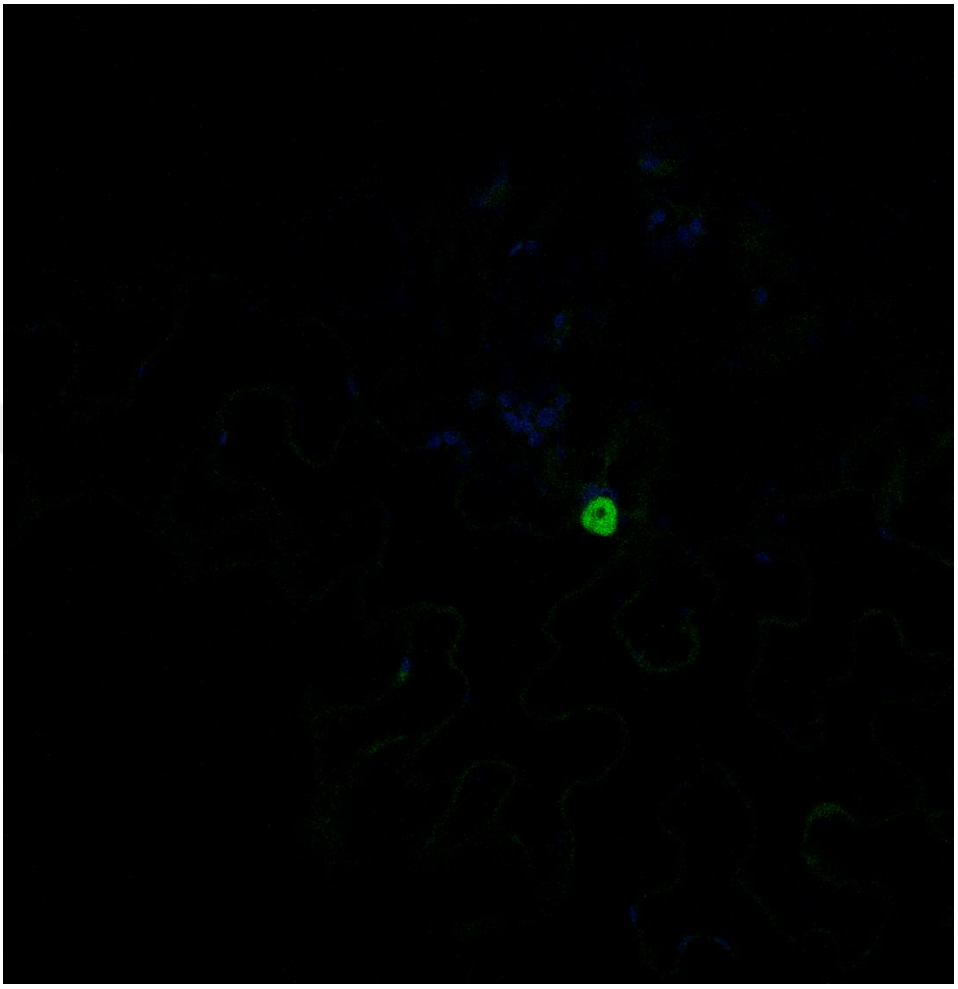

Figure 4.10. Ecotopic infiltration of replicase tagged at the C-terminal, without virus.

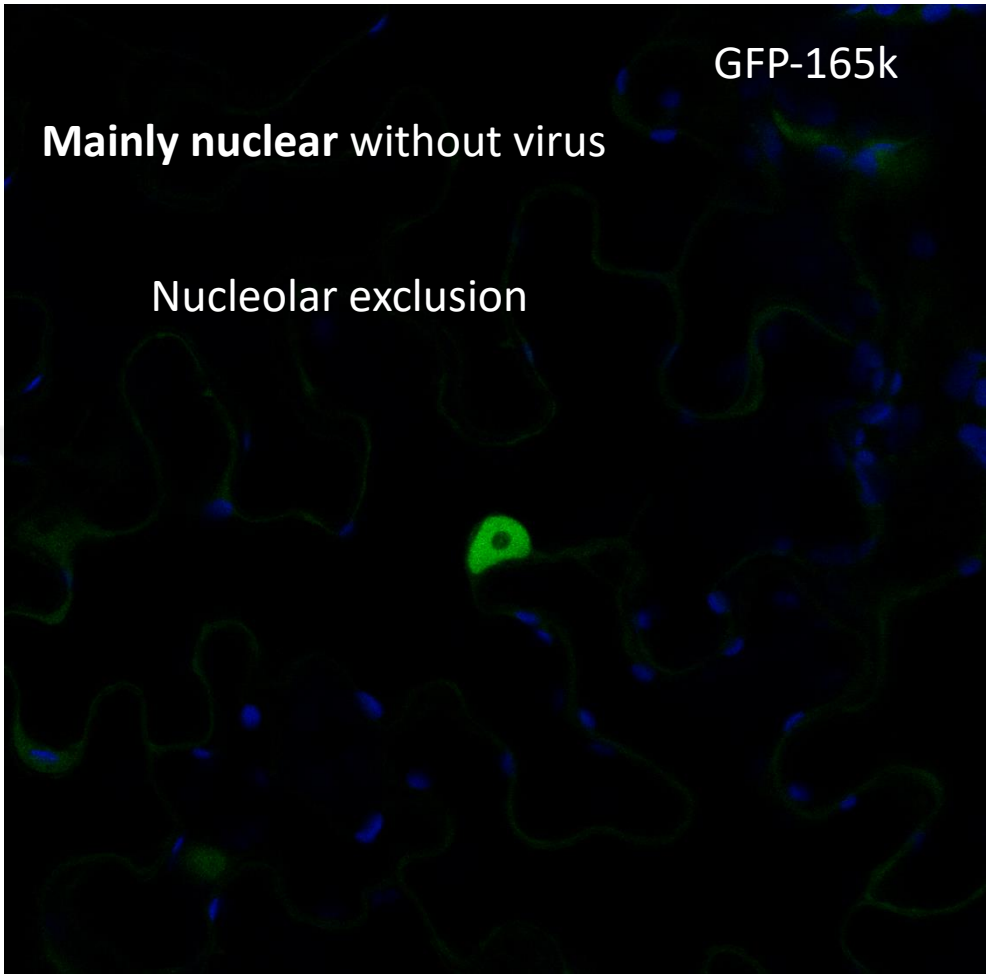

Figure 4.11. Ecotopic infiltration of replicase tagged at the N-terminal, without virus.

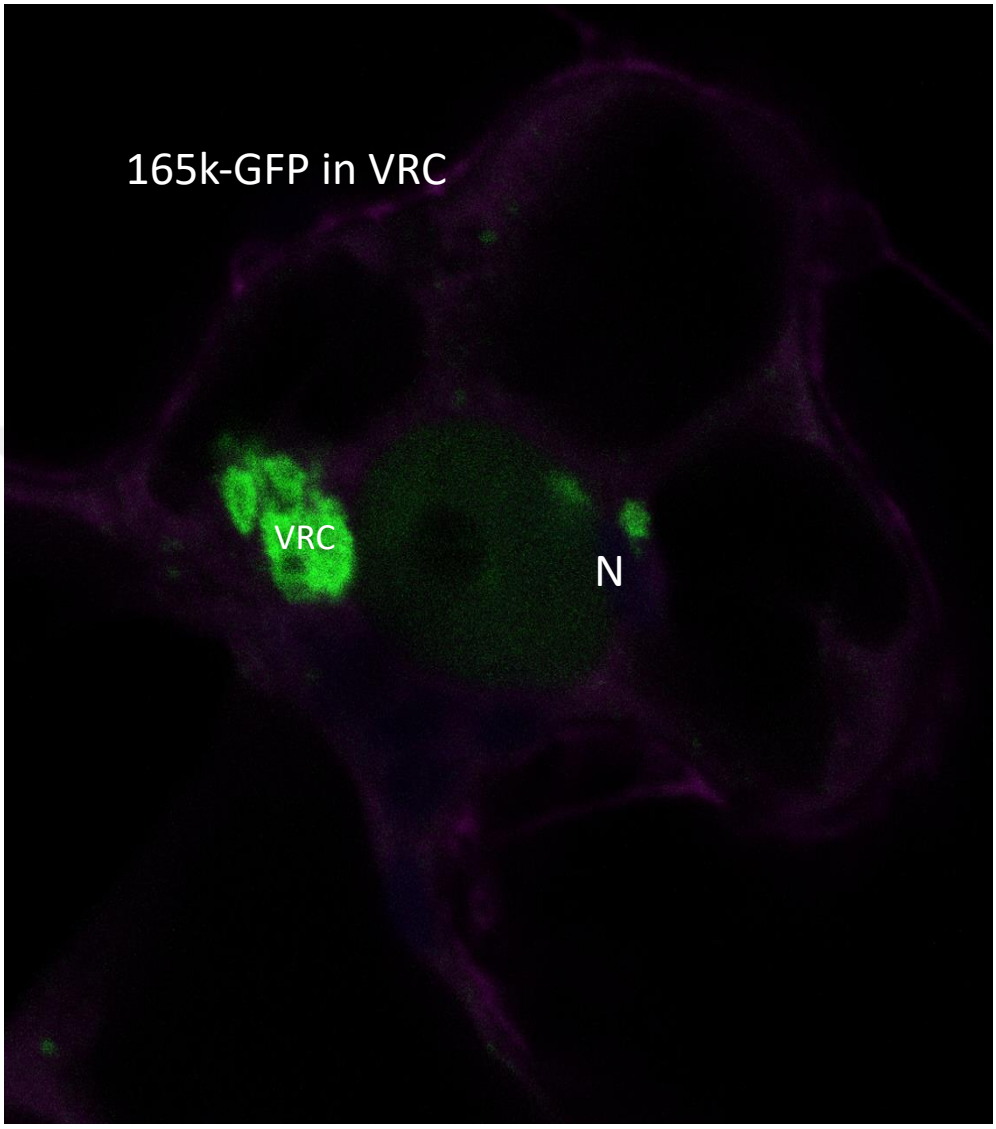

Figure 4.12. Ecotopic infiltration of replicase tagged at the C-terminal in the presence of virus. (VRC: viral replication complex; N: nucleus)

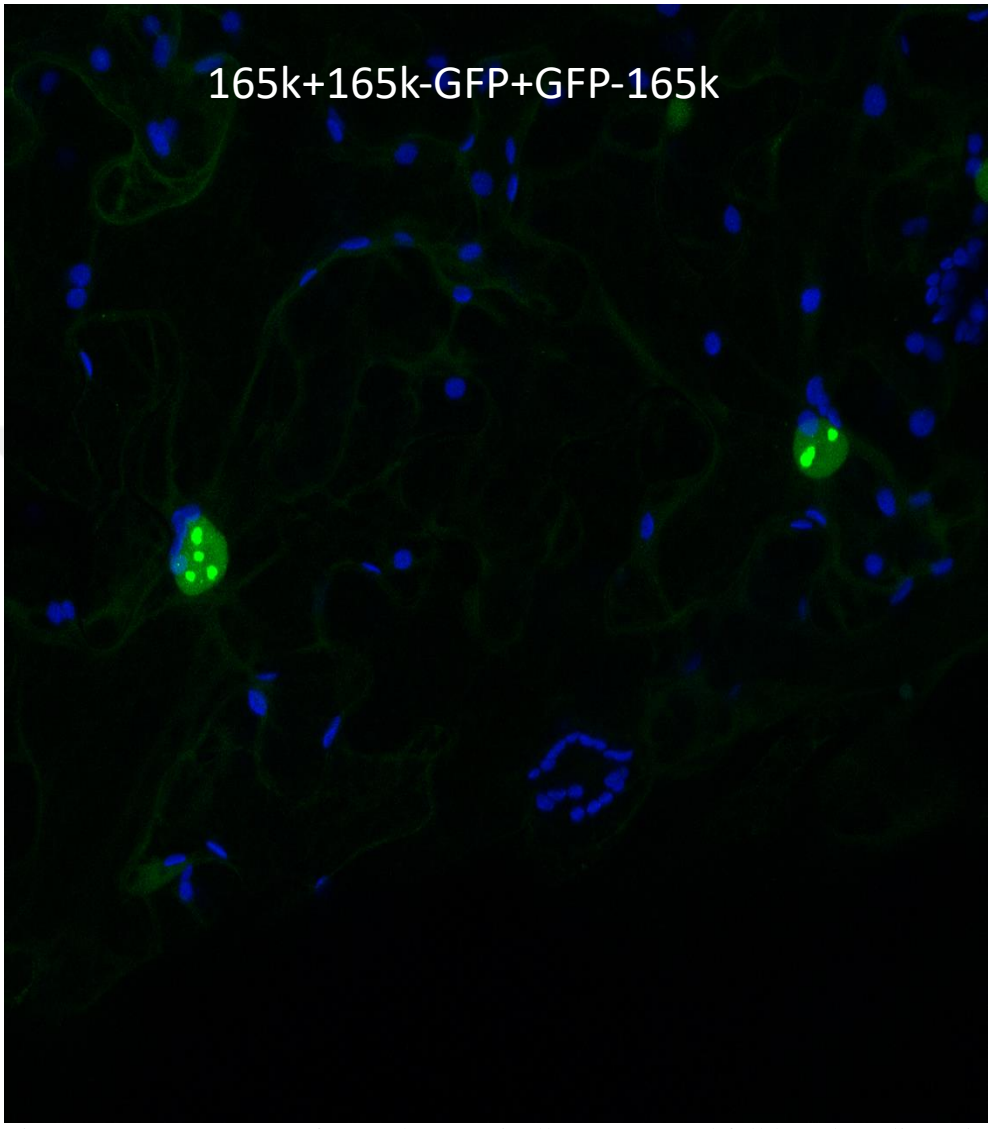

Figure 4.13. Aggregates of C- and N-terminally GFP-tagged full length replicase in the nucleus when infiltrated together with untagged replicase.

4.3. Localization of ectopic PVX Replicase

Virus replicates by hijacking several biological processes within the cell. For better understanding of viral replication and their ensuing events, it was important to

visualize the viral replicase that is typically associated with cellular membranes and to define subcellular regions where it is accumulated.

The confocal analysis was performed in N. benthamiana epidermal cells, and PVX-based vectors were used to produce infectious full-length clones of the virus where the replicase protein provided in cis (i.e. from the replicating virus) was attributed in this study as “authentic” while the one supplied in trans (i.e. from a separate expression vector) as “ectopic free”. At first, we determined the subcellular localizations of the C- and N-terminal fused replicase provided in trans with the virus and in non-infected cells that contained the unfused replicase version.

On tagging the replicase, the full length replicase ends with a stop codon and was amplified from the PVX virus expression vector JM24 (p35S.PVX.4xCys4.GFP-CP-David-A clone miniprepped from non-methylated E.coli strain JM109) with flanking attB sites and recombined into the attP sites of the pDONR201 mediated by the Gateway BP clonase. pDONR201/PVX 165k-stopcodon or JTM004a-c were tested by KpnI digestion releasing a 2.3kb fragment (Figure 4.3.a.). Clone JTM004-a was fully sequenced to reveal an error free replicase gene. Gateway LR recombination of JTM004-a into pGWB402 (unfused) and -406 (N-terminal GFP) resulted in JTM010/165k-E and JTM011/GFP-165k, respectively.

Similar to the 165k-GFP’s localization, the N-terminal GFP-tagged recombinant protein’s signal was also detected mainly in the nucleus in the absence of virus, with only weak cytoplasmic signal (Figure 4.3.b), and formed nuclear amorphous aggregates when co-expressed with the unfused replicase (Figure 4.3.d). However, in cells infected with the dsRED-tagged PVX, the GFP fluorescence of the N- and C-terminal fused ectopic replicase was observed diffusively distributed in the cytoplasm and co-localized within the perinuclear virus inclusions (Figure 4.3.h). The detailed observation of the infection periphery showed a few viral cap structures, near PD, with weak GFP signal from the fused ectopic replicase, emphasizing the possibility proposed by Tilsner et al. (2013) of PD-localized replication of the virus (Figures 4.3.k. and 4.3.l. showing the GFP-fused replicase

inside PVX cap near PD). The replicase is an RNA-binding protein, that specifically recognizes the virus, and can therefore be recruited into the cytoplasm where the virus is. We have confirmed in our findings obtained from CLS (confocal laser scanning) examination of N- and C-terminal fusions that it also appears more condensed inside perinuclear virus bodies and somewhat (=in very few cases) at PD-localized viral caps, when it is co-expressed with a viral RNA expressed from a plasmid with a 35S promoter, as there eventually should be quite a lot of viral RNA to encounter. However, especially when the vRNA is missing, the agroinfiltrated replicase may preferentially localise where there is abundant RNA, including the nucleus, hence the nuclear signal of the tagged replicase without the virus (Figure 4.3.b. and 4.3.c. showing the nuclear GFP-165k and 165k-GFP, respectively). The PVX polymerase may function as a multimer like other RNA virus RNA-dependent RNA polymerases and this may be the reason for its aggregation (Figure 4.3.d.-4.3.g., showing the nuclear aggregates of 165k-GFP and GFP-165k in combination with 165k-E) inside the nuclei of the non-infected cells (Wu et al, 2019). The question is does PVX replication protein accumulate first in the nucleus before it targets the vRNA in the cytoplasm? However, answering this requires more evidence to determine how it interacts in cytoplasmic replication.

Two models are proposed to describe the cell-to-cell movement of the PVX, either as a modified virion (TGBp1 associates with a fully/partially encapsidated virion modifies them to be more translatable) or a CP-containing RNP (partially encapsidated virion associates with TGBp1). But in these two models, replicase has not put into the picture until Tilsner et al. (2013) that has proposed co-insertional replicational model, where replication and movement are coupled in caps anchored in front of the PD orifice. Moving of the replicase with the viral cargo may complicate the picture, but unlike CP, replicase is not required for the virus intercellular spread. Nevertheless, including the replicase in the viral cargo, especially at the very early infection stages, may increase efficacy and specificity of

the infection spread. Furthermore, replicases are shown moving, colocalized with TGBp1 and found in caps of different sizes at different levels of movement.

Tilsner et al. (2013) propose that these caps (Figures 4.3.j-l) are smaller VRC, however they are only limited in numbers during the course of infection and their growth into bigger virus factory (X-body) is unlikely to happen. These caps are mainly TGBp2/3-induced vesicles that are not harboring the replicase to initiate replication, but rather anchoring replicase for transport towards PD. TGBp2/3 mutations which inhibit these vesicles' movement and the cap formation are unlikely to affect virus replication. This may mean that these caps are not the replication-competent sites when the virus is moving. These caps may look as transit ports (enforced by the narrowing of ER inside the PD channels) before the virus can exit the cell, rather than being dynamic replication sites. At early infection stages, replication is most likely transported into the caps than being actually done in there but it still needs to be furtherly studied.

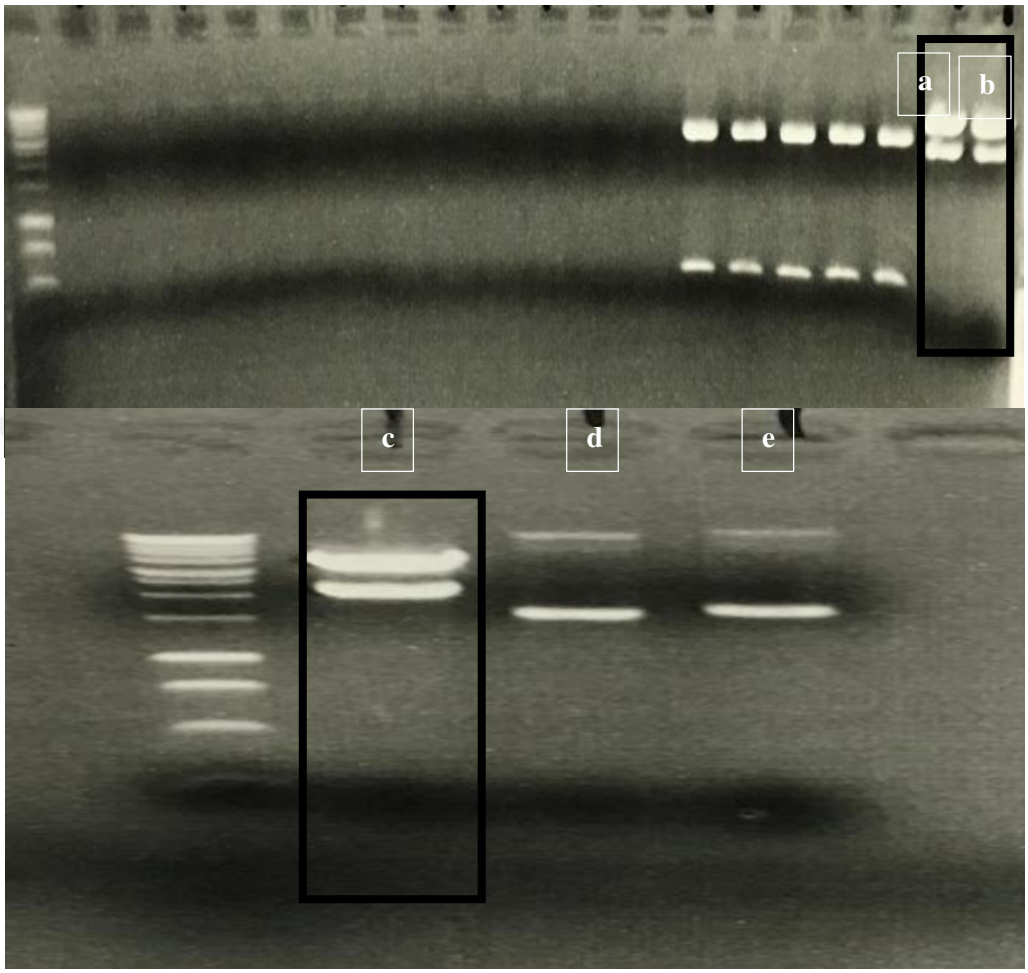

Figure 4.14. *lanes in the two rectangles are the KpnI* diagnostic digestion of JTM004a-e (or 165-Stop), only clones JTM004a-c released the 2.3k fragment, clones e-d did not have the correct plasmid backbone and were therefore discarded. Clone JTM004a was proved a correct 165k sequence via sequencing using the following primers: DONRfor, DONRrev, attB-L61_453Kpnfor, attB-MTrev, attB-HELfor, attB-L61_2800Kpnrev, attB-HELrev, attB-POLfor, attB-L61_3528for, attB-LINKfor, attB-LINKrev, L61-2648for

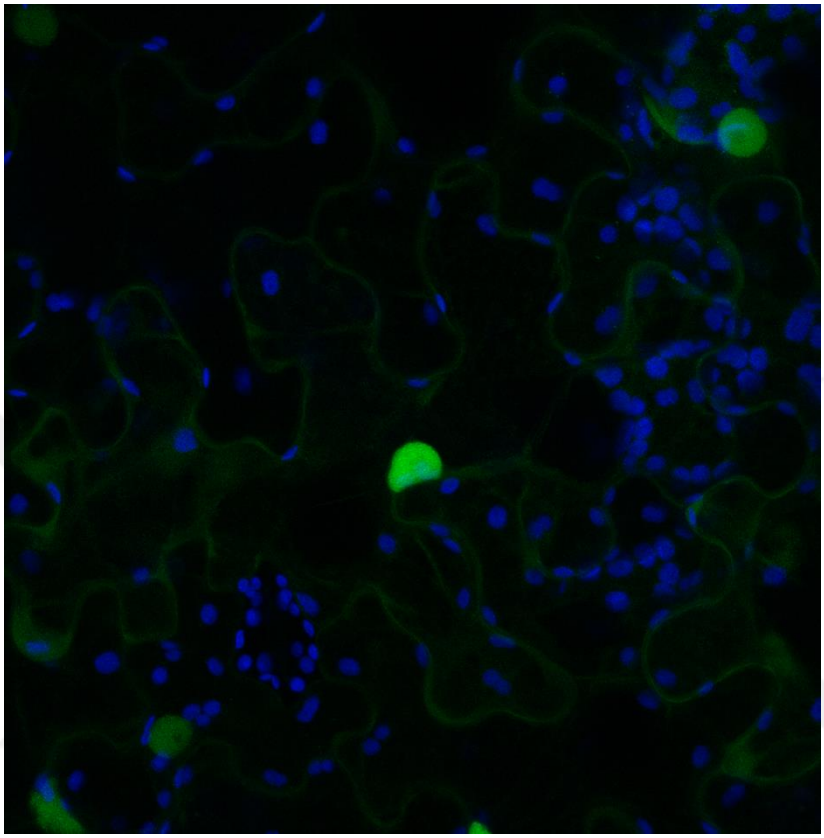

Figure 4.15. Maximum intensity projection showing the predominantly nuclear localization of GFP-165k.

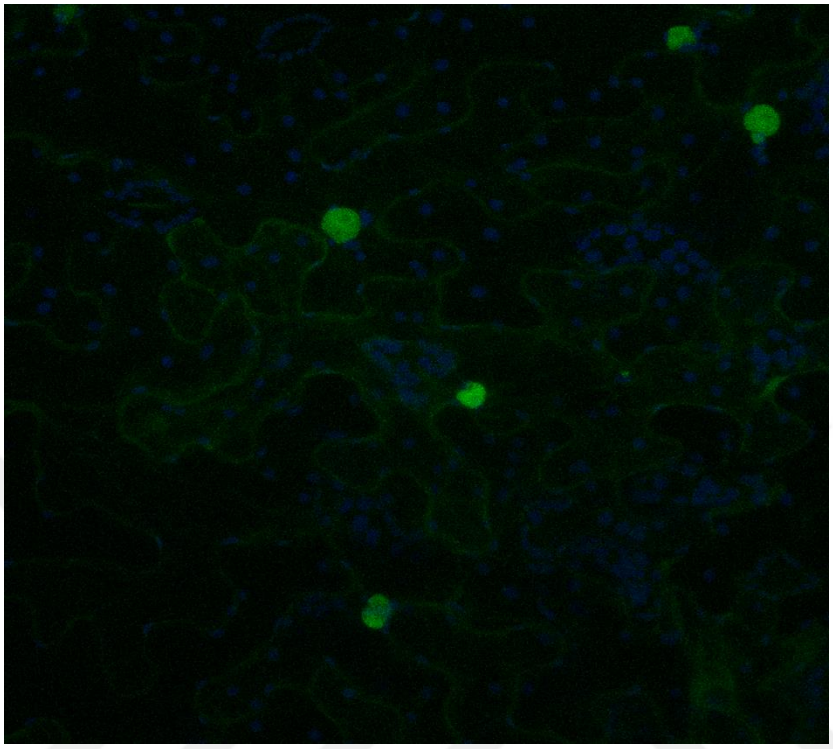

Figure 4.16. Maximum intensity projection showing the predominantly nuclear localization of 165k-GFP.

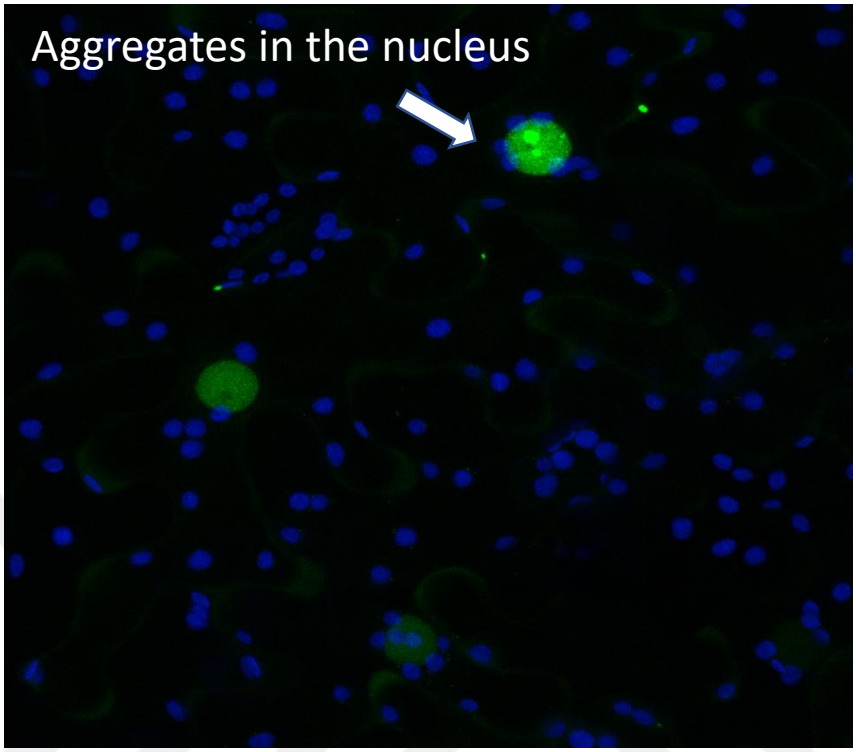

Figure 4.17. Nuclear localization of GFP-165k in combination with 165k-E showing the nucleolar exclusion and faint cytoplasmic signal and some aggregates (arrowhead) inside few nuclei.

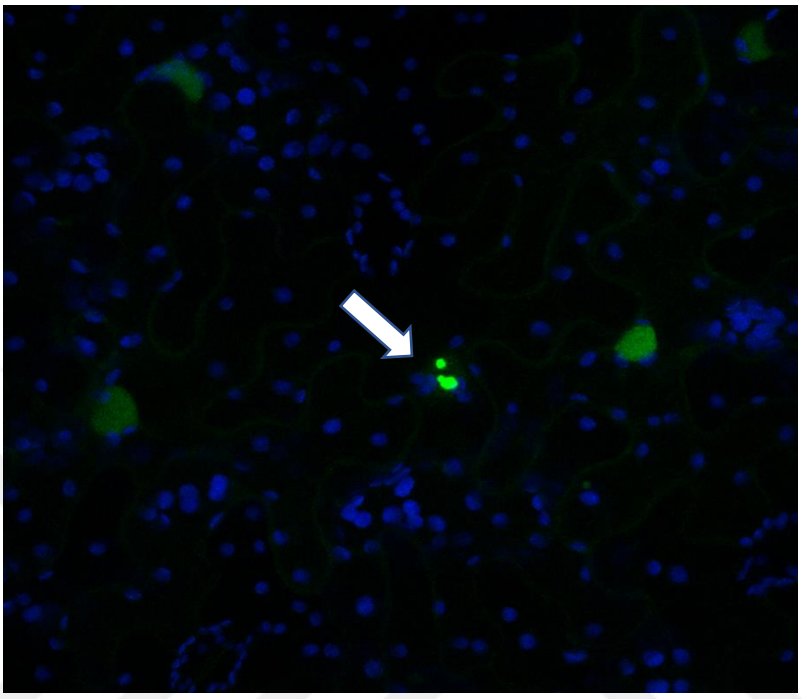

Figure 4.18. Nuclear localization of 165k-GFP in combination with 165k-E in the presence of the silencing suppressor 19k protein, showing the nucleolar exclusion and faint cytoplasmic signal and some aggregates (arrowhead) inside few nuclei.

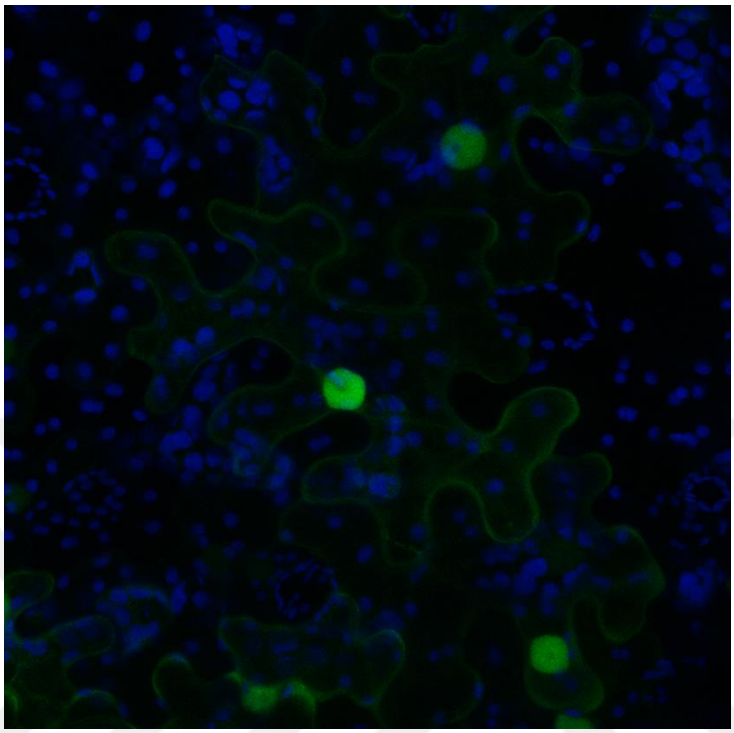

Figure 4.19. Maximum intensity projection showing the nuclear localization of GFP-165k and 165k-GFP in the presence of the helper 19k protein. Notice the nucleolar exclusion and faint cytoplasmic signal.

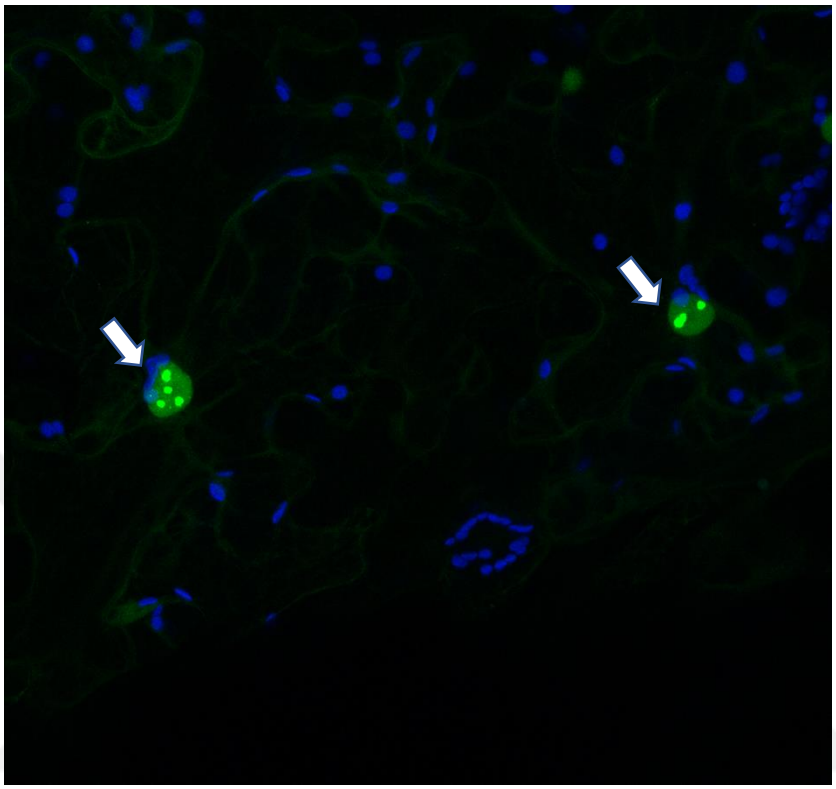

Figure 4.20. Maximum intensity projection showing the nuclear localization of GFP-165k and 165k-GFP in combination with 165k-E in presence of the helper 19k protein. Notice the aggregates (arrowhead) inside the nuclei.

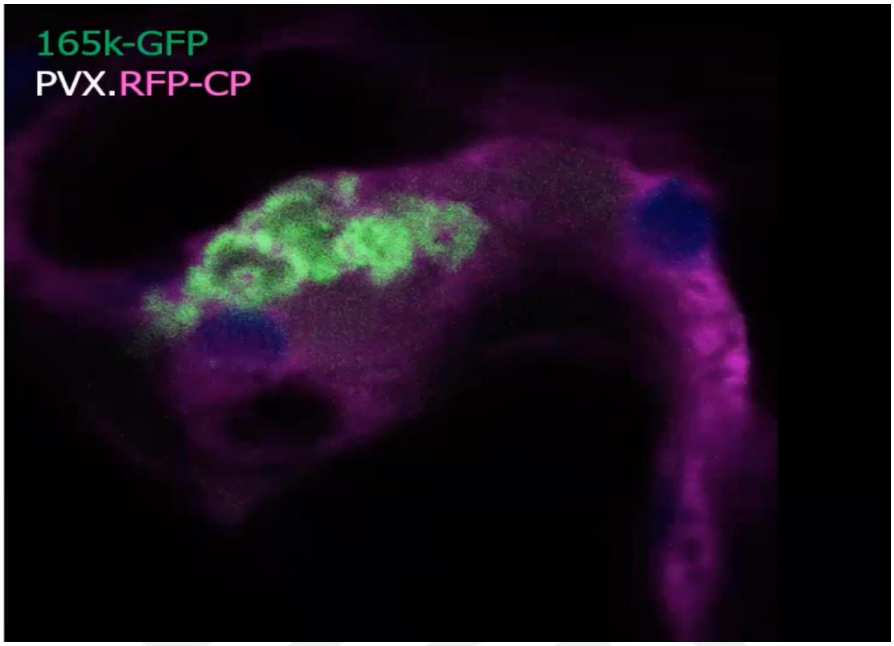

Figure 4.21. Maximum intensity projection showing the GFP-fused replicase inside PVX X-bodies

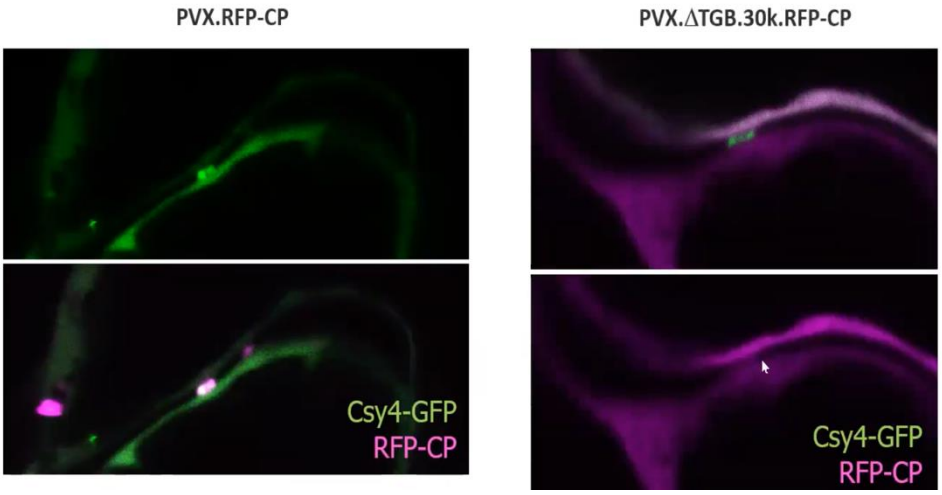

Figure 4.22. Maximum intensity projection showing Csy4 RNA-imaging of PVX movement complementation

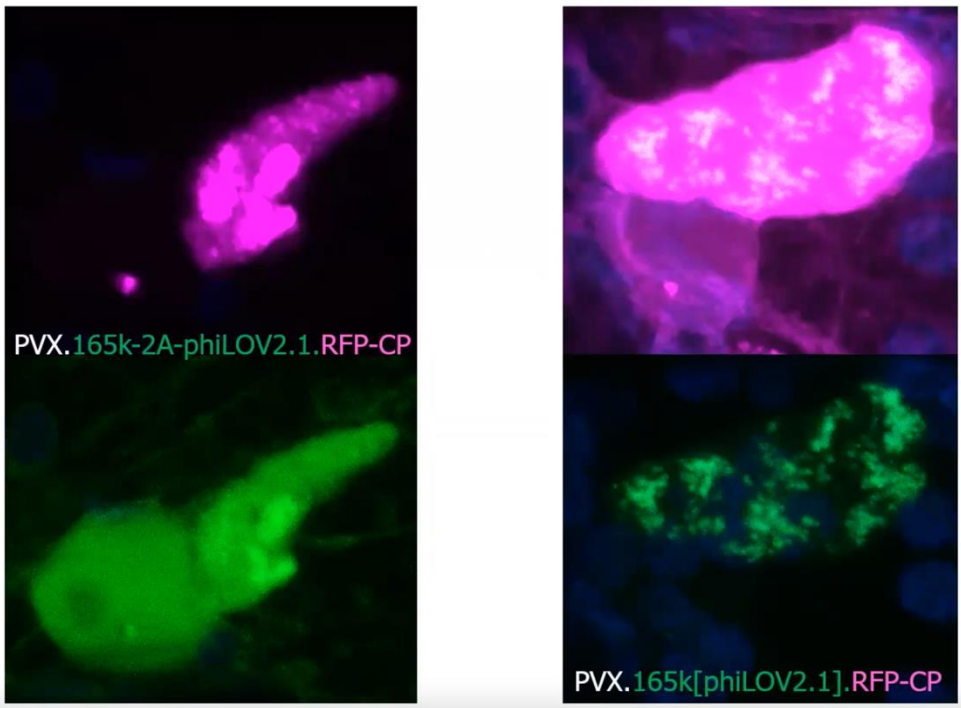

Figure 4.23. Maximum intensity projection showing in cis labelling of replicase. Native tagged viral replicase with internal phiLOV2.1 (left) and C-terminal phiLov2.1 (right).

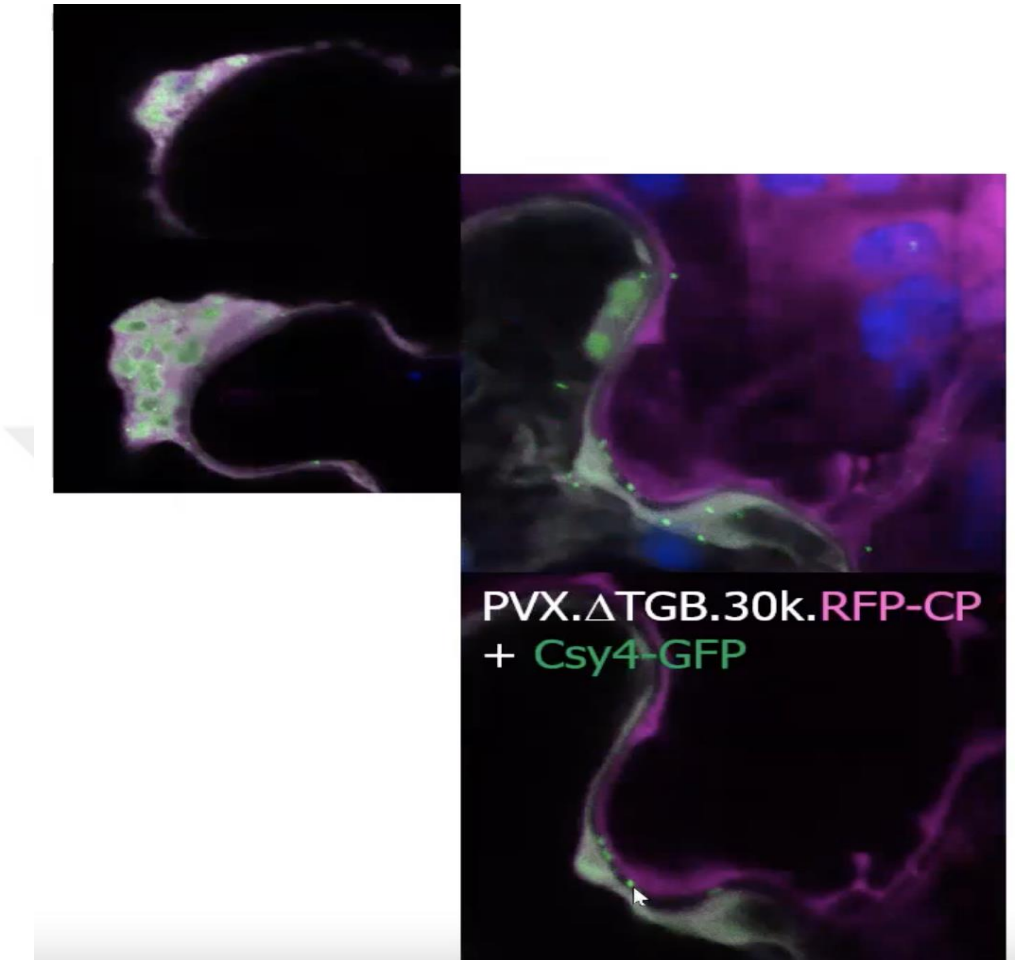

Figure 4.24. Maximum intensity projection showing viral RNAs (in green) in cap structures of a localized replication during movement complementation

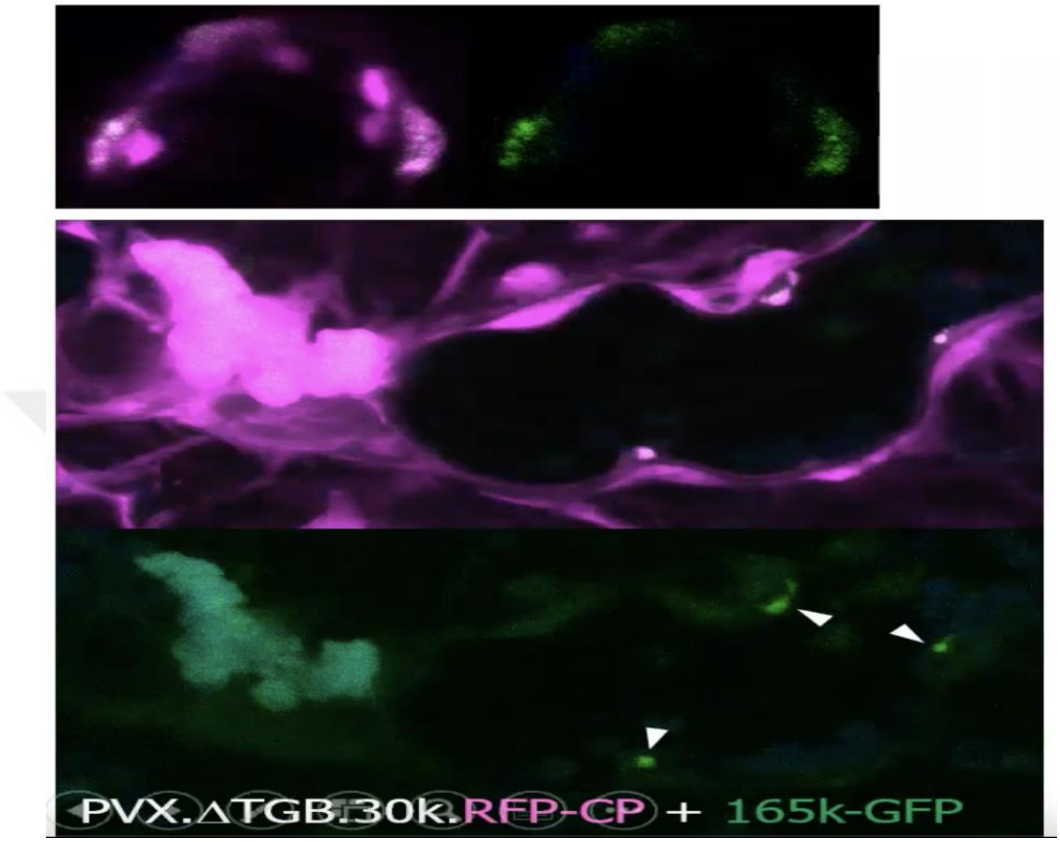

Figure 4.25. Maximum intensity projection showing viral replicases (in green) in cap structures of a localized replication during movement complementation

4.4. Incompatibility of Ectopic PVX Replicase

We also demonstrated that transient expression of the replicase protein failed to complement the replicase truncated PVX mutants, which raises the possibility that some cis information contained in the viral genome could be required for the enzyme to function during virus replication.

The first attempts had failed to complement a virus vector that lacks a functional replicase gene with 165k-E expressed from a plasmid vector in trans. The virus construct was pTRA.PVX delta 165k as constructed by the removal of part of the replicase open reading from from the virus genome by digesting the wild type

pTRA.PVX expression vector with the NcoI endonuclease at 37C for 2-3h (Figure 4.4.a. and 4.4.b.) and ligating the plasmid backbone into itself using T4-ligase at 16C o/n. Neither the co-infiltration of 165k-E with the pTRA.PVX delta 165k nor with the wild type pTRA.PVX did produce any infection. Infiltrating pTRA.PVX and its subsequent derivative vectors were known to be infectious in the past in a different lab. But, unfortunately, infectivity from agrobacterium infiltration appears to have been lost under growth conditions at JHI. Instead, we decided to bombard the virus vectors to assure successful infections. Co-bombardment of the two plasmid vectors pTRA.PVX delta 165k and 165k-E failed to get the virus restore its infectivity in the bombarded cells, even after co-infiltrating 165k-E and the helper protein 19k shortly after bombardment (summarized in Tables 1.2 and 1.3). There was a possibility that complementation of pTRA.PVX delta 165k by ectopic 165k-E failed, due to the loss of some RNA features of the viral genome contributing to replicase/RNA interaction. The NcoI.PVX.NcoI region of the PVX viral genome may participate in efficient vRNA replication, possibly by possessing some intra-structures or specific sequences that interact with replicase to function over the template vRNA (Choi et al. 2004) even though RVX RNA elements reported to be required for replication have mostly been located in the 5' and 3'UTRs.

Instead, we therefore designed the viral RNA to encode dysfunctional replicase by preserving the the majority of genomic sequences unaltered to represent suitable RNA features for any possible recognition by the replication elements. That was achieved by inserting four nucleotides at the AgeI site downstream the start codon of the first ORF of the pTRA.PVX expression vector. This frame-shifted pTRA.PVX (or pTRA*) was constructed by AgeI (5'A|CCGGT3') digestion at 37C /3h followed by the 5' overhang filling, 5'-to-3' polymerization activity of the E.coli DNA polymerase I Klenow fragment at 25C/15min and the T4-ligation at 4C/o.n, resulting in the new sequence 5'ACCGGCCGGT3' and a frame-shift in the replicase following the codon for Pro 385 (underlined). To corroborate the loss of infectivity of pTRA*, it was co-bombarded with GFP-sporamin/19K. None of the GFP-

expressing bombarded sites showed any sign of viral RFP expression indicative of infection, although they were marked and surrounded with faint green cells, as traces of GFP-sporamin leaked out into the neighboring cells (Figure 4.4.d). Here the GFP-sporamin was used to mark the bombarded cells, without changing their biology (The ideal marker would be ER-targeted GFP, as that cannot move cell-to-cell and thus definitely marks only the bombarded cell). As early as one day after the co-bombardment of pTRA.PVX/GFP-sporamin/ 19K, a successful introduction of both the GFP-sporamin and the dsRed virus vectors had been recorded in almost each bombardment site. In these viral lesions, the virus developed big virus factories and moved 2-3 boundaries within 3 days of bombardment, however the GFP-sporamin was only confined in the first bombarded cells. When 165k-E was co-bombarded into plant cells with pTRA* no expression of dsRed from a replicating virus was detected for up to 7 days after bombardment. Similarly, the N- or C-terminal GFP-fusions of the 165k protein could not complement the replication of the frame-shifted pTRA.PVX (pTRA*).

Based on these data, no virus amplification of the replicase-defective PVX mutants was rescued by the ectopic expression of 165k-E, suggesting that replicase may not function in trans, and that CLS images of 165k RdRP in the context of PVX infection, supplied as GFP fusions from ectopic expression may not directly participate in the virus subcellular replication. However, in the presence of authentic replicase encoded by the infectious viral RNA, they may highlight replication sites indirectly through 165k(ectopic, trans)-165k(viral, cis) interactions.

Nevertheless, this polymerase-polymerase binding of cis and trans-expressed replicases could affect the viral replication, with two possibilities: Either they may both compete for catalytic access to the vRNA causing the cis-expressed active replicase to slow down, which may result in some interrupted pauses along vRNA replication (Costa et al. 2013). Or, one leading replicase may act in cooperation with other oligomerized 165k molecules that in turn disengage nascent RNA molecules from escaping into the cytoplasm and bind them in proximity, resulting in multiple

rounds of replication over several strands of nascent RNAs. The former scenario would be reminiscent of the replicase-mediated resistance against many plant RNA viruses, such as PVX. In contrast, research has yet to be done to elucidate whether trans-expressed replicase may enhance cis replicase-mediated replication of positive sense RNA viruses.

There is no evidence that potexvirus 165k is cleaved like a potyvirus polyprotein that showed good results for trans-complementation. (cleaving may impose the meaning of trans-activity of these proteins brought into play a while after they were transcribed and translated, as if they were cloned separately on different vectors). Unlike to the PVX TGBps and CP, that can be complemented in trans being normally expressed from separate subgenomic vRNAs anyway, PVX replicase, is translated directly as a mature enzyme from the virus genome and its template-specific catalytic activity may therefore arise from regulatory steps at some events prior to the end of its synthesis. PVX replicase could be required to bind the vRNA as soon as it is translated so as to facilitate the commencement of replication. Co-translational replication might be a possible explanation, where the translating ribosome unwinds RNA secondary structure near the end of the 165k ORF, thereby opening up sequences that the replicase recognizes. This would then be impossible in PVX mutant constructs with frame-shifted or partially deleted replicase, where translation stops a long way before the end of the 165k ORF. Additionally, the PVX replicase cannot copy its plasmid-derived messenger RNA (165k-E) as that contains only the 165k ORF but no other viral sequences, in particular those mediating production of negative sense RNA. The viral RNA replicase is template specific, and its capability of making complementary RNA strands depends mainly on the 5'/3' UTRs present in the PVX RNA, that retains a conformational structure (i.e. binding/recognition sites) recognized by the enzyme. Trans-replication system is not shown to be feasible to study PVX viral RNA replication; some kind of missing regulation is more likely, which is what co-translational replication describes. It will be interesting to see if it affects replication of the whole genome, or just the

subcellular mRNA required for translation of TGBs and CP, and what are these regulations bits in the vRNA, necessary for functional replicase to commence replication? The potyvirus movement protein P3N-PIPO is expressed by transcriptional frameshifting, where the replicase “stutters” on a GAAAAAA sequence making a GAAAAAAA copy. (Olspert et al., 2015). The authors asked how is predominant replication of frameshifted genomes prevented and present a hypothesis based on data linking replication to translation. In potyviruses, which only encode a single long ORF on their genome, replication can only occur if the translating ribosome unwinds RNA secondary structure near the end of the ORF, thereby opening up sequences that the replicase recognises. A similar mechanism might operate in PVX, where the replicase only bind to sequences near the end of the 165k ORF when that ORF has been translated. This would then be impossible in the mutant constructs with frame-shifted or partially deleted replicase, where translation stops a long way before the end of the 165k ORF.

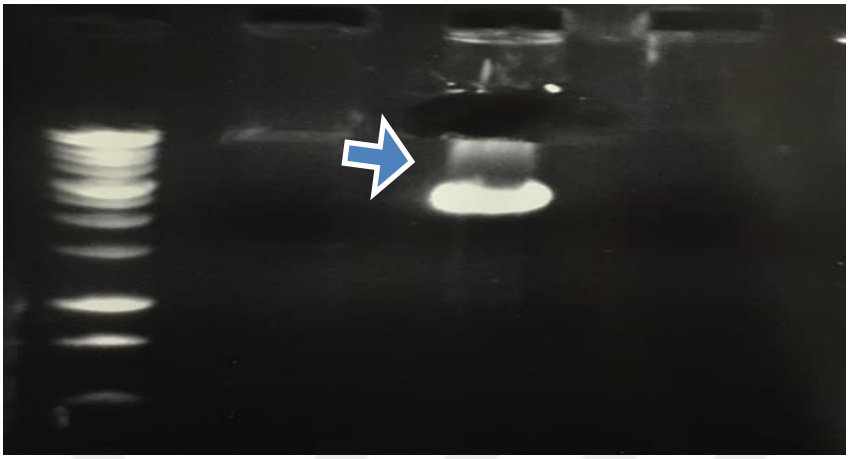

Figure 4. 26. NcoI digestion of pTRA.PVX plasmid releasing a 2.5kb fragment band, and the 11.1kb NcoI-digested pTRA plasmid backbone (arrowhead) was excised, purified and ligated into itself to produce pTRA.delta165k.

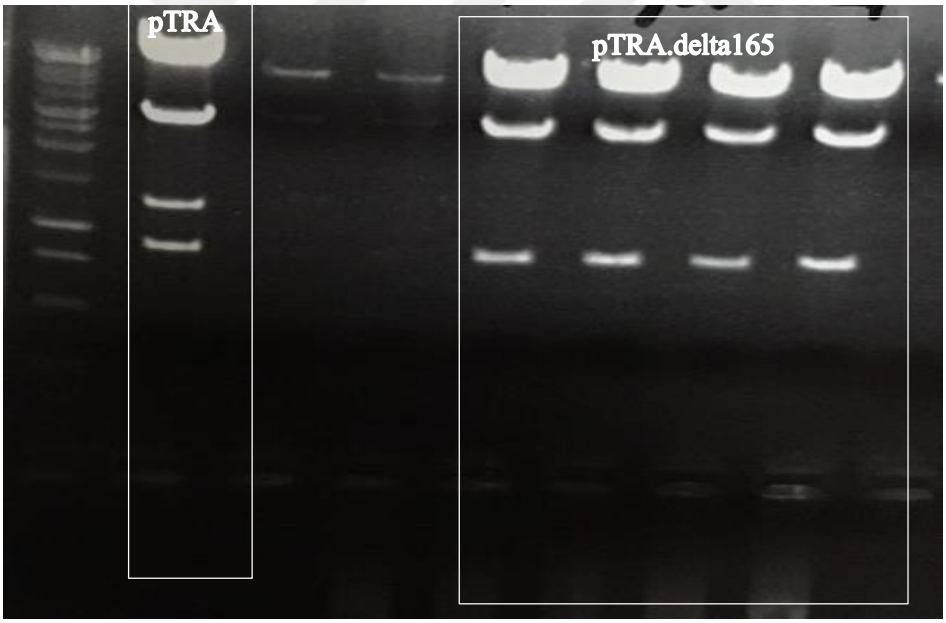

Figure 4.27. *HindIII digestion of the pTRA.PVX#10, and* pTRA.delta165k#1, 2, 6, 7. (from left to right).There is a 1.2 kb band in the original pTRA that is absent in all of the delta165k clones.

The expected HindIII patterns:

pTRA.PVX.4xcsy4.DsRed-CP/HindIII: 8552, 2460, **1205**, 857, 570 bp
pTRA.PVX.delta165k.4xcsy4.DsRed-CP/HindIII: 7255, 2460, 857, 570 bp

(The 570 bp band may be too weak for detection or the 2.5 kb band may instead be ~500 bp larger at 3 kb, due to inaccuracies in public sequence data for these large binary vectors.

Table 4.1. Co-infiltration of PVX different plasmids with ectopic replicase.

Co-infiltration	Disease analysis (7day post infiltration)
pTRA.PVX	No infection
pTRA.PVX.delta165k	No infection
165k-E + *pTRA.PVX.delta165k*	No infection
GFP-165k + *pTRA.PVX.delta165k*	No infection
165k-GFP + *pTRA.PVX.delta165k*	No infection

Table 4.2. Co-Bombardment of PVX different plasmids with ectopic replicase.

Co-bombardment	Disease analysis (7day post bombardment)
pTRA.PVX	Infection (CLS image 1.7)
pTRA.PVX.delta165k	No infection
165k-E + *pTRA.PVX.delta165k*	No infection
GFP-165k + *pTRA.PVX.delta165k*	No infection
165k-GFP + *pTRA.PVX.delta165k*	No infection

Table 4.3. Co-Bombardment of PVX different plasmids co-infiltrated with ectopic replicase and the expression booster, 19k.

Co-bombardment	Co-infiltration (shortly after the bombardment)	Disease analysis (7day post treatment)
pTRA.PVX	-	Infection (CLS image 1.7)
pTRA.PVX.delta165k	-	No infection
165k-E + pTRA.PVX.delta165k	*165k-E / 19K*	No infection
GFP-165k + pTRA.PVX.delta165k	*GFP-165k / 19K*	No infection
165k-GFP + pTRA.PVX.delta165k	*165k-GFP/ 19K*	No infection

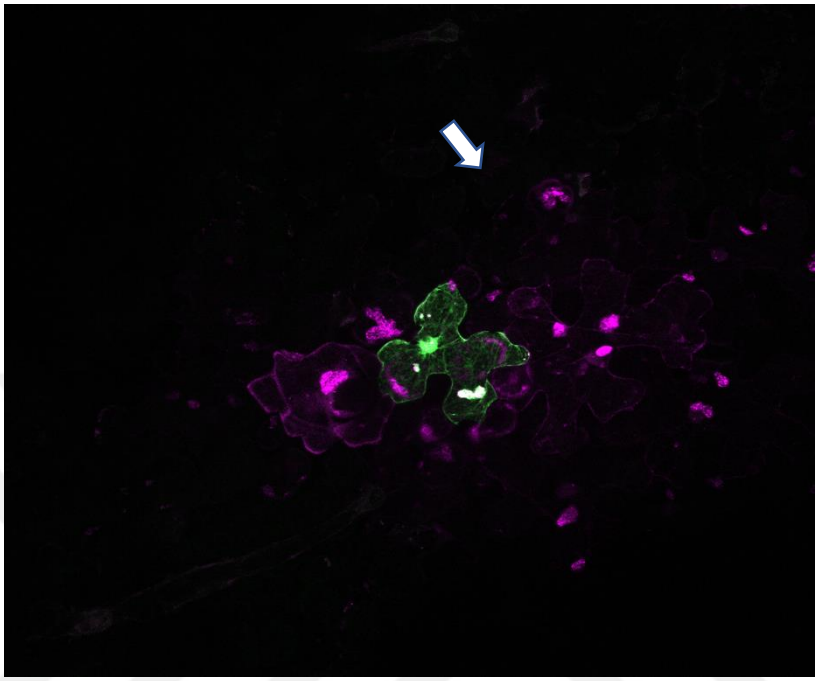

Figure 4.28. Maximum intensity projection showing the bombardment delivery of pTRA.DsR-CP & 19k & GFP-sporamin into the epidermal cells of *N.benthamiana*. Notice the GFP-sporamin (arrowhead) inside the first bombarded cell. The infection moved for about 3-cell layers within 3 days post bombardment (dpb).

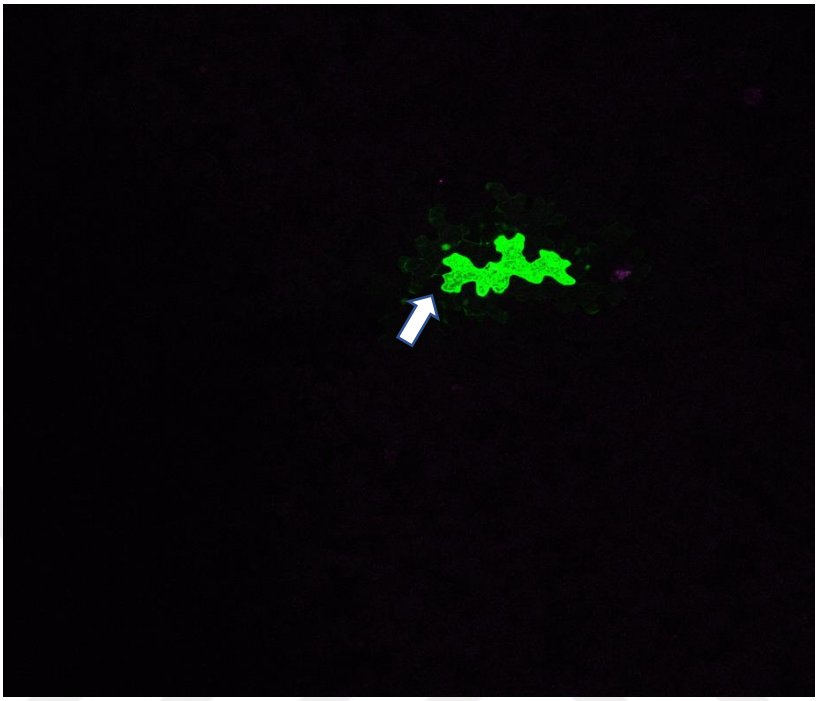

Figure 4.29. Maximum intensity projection showing the bombardment delivery of pTRA* & 19k & GFP-sporamin into the epidermal cells of N.benthamiana. Notice the loss of infection of pTRA* and the GFP-sporamin (arrowhead) is confined inside the first bombarded cell.

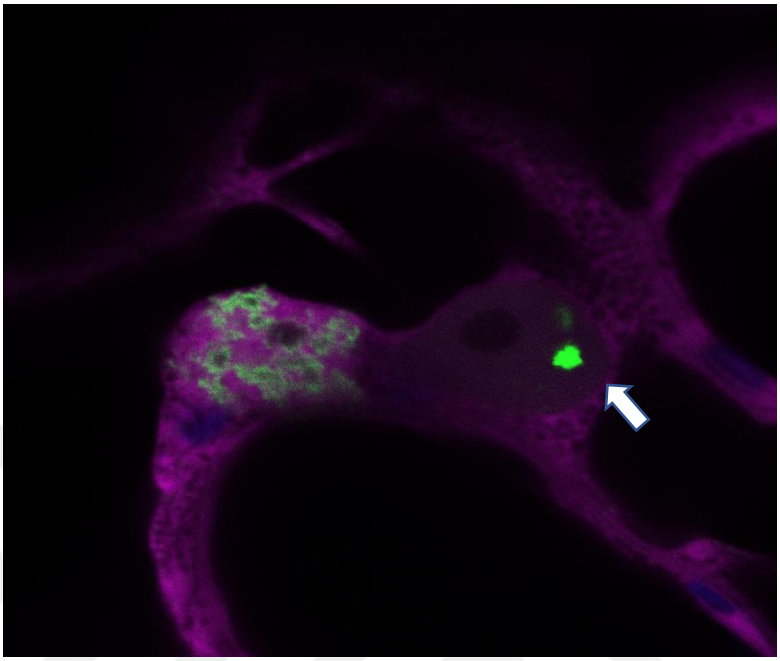

Figure 4.30. The localization of GFP-fused replicase inside perinuclear X-body (arrowhead) of PVX infected cells. 165k-GFP+19k 3dpi & PVX.cherry-CP 5 dpi

5. CONCLUSIONS AND RECOMMENDATIONS

PVX based plasmids are useful tools for gene expression, functional manipulation of plants, vaccine production and nanotechnology. For all these uses, we modify viral genomes according to human needs. Often this results in loss of or reduction of infectivity. Understanding in greater detail how these viruses work enables us to overcome such obstacles. For instance many processes in the viral life cycle seem to be linked, e.g. replication-encapsidation and replication-movement. RNA-protein interactions and RNA secondary structures are important for these processes.

Both PVX and TMV have shown localised replication at PD. There are more reasons of using PVX-30K complementation system, but not with other TGBS: TMV 30k is the simplest MP known (one protein can do anything, without requiring CP for local movement) and is the most promiscuous in complementation experiments, there are no instances when it has failed to complement, and it can even introduce insect viruses into plants. Thus, chances were high that complementation would work. By contrast, almost all TGB systems need CP to some extent, so much greater chance they simply would not work in PVX. Also, in TGB systems, TGB2/3 are expressed from a second sub-genomic messenger RNA separate from TGB1. This requires a sub-genomic promoter located within the TGB1 ORF to be active. If we had replaced with a different TGB, we would not know whether that subgenomic promoter works, and would have had to test if TGB2/3 are even expressed, which is tricky as they are small proteins expressed at very low levels in natural infections.

Complementation only works in cis for replicase but in both cis and trans for MP. The requirement in cis has something to do with privileged access to the viral RNA. When the replicase is translated from the viral genome, it may be able to bind its 3' end immediately, whilst still being translated. When mutated genome and replicase are expressed separately, they may never 'see' each other because the RNA is bound by cellular proteins whilst the replicase gets 'stuck' on some cellular RNA

it cannot use as a template (hence its nuclear/nucleolar localisation). But this is all still rather speculative and requires more investigation; as to repeat the experiment with a virus that has a frame shift in the replicase immediately after its start codon, i.e. not even a fragment of replicase is expressed. This is to exclude the possibility that a virus-expressed partial replicase has an inhibitory function. Also, to introduce csy4 stem-loops into the replicase frame-shifted viral RNA, so as to image its localization whilst in trans-expressed replicase fails to complement. Does the ectopically expressed replicase affect RNA localisation at all?

PVX and other (+) ssRNA viruses can recombine genomes by replicase template switching, resulting in a chimeric offspring with increased mutations. Lethal mutations are eliminated but in areas of low information content, the mutations are tolerated and the recombinant chimeric virus survives These hot spot in the replicase linker region were used for tagging. Internal replicase tagging was successful and functional.

At early PVX infiction, there are ‘caps’ at PD containing vRNA, replicase and MPs. The MPs are responsible for the PD-targeting as neither the replicase nor the CP can do it. The possiblity that MPs recruit it directly is very low, because of the ability of MPs to complement unrelated viruses. The recruitment must be indirect, likely via the RNA. Whether the MP recruits an RNA alone and replicase is then translated from it at caps, or whether MP recruits an RNA that has a replicase attached to it, is a question to be experimentally.elaborated. So, Replicase could be translated after RNA recruitment, but the important result is that replicase is unlikely to be recruited directly.

REFERENCES

Aaziz R, Dinant S, Epel BL. Plasmodesmata and plant cytoskeleton. Trends in Plant Science. 2001 Jul 1;6(7):326-30.

Agbeci M, Grangeon R, Nelson RS, Zheng H, Laliberté JF. Contribution of host intracellular transport machineries to intercellular movement of turnip mosaic virus. PLoS Pathogens. 2013 Oct 3;9(10):e1003683.

Akpınar, G., (2009). Türkiye'de Trakya Bölgesi'nde Güllerde Görülen Virüslerin Biyolojik Ve Serolojik Yöntemlerle Saptanması Üzerine Araştırmalar. Namık Kemal Üniversitesi Fen Bilimleri Enstitüsü Dergisi, (32), (26-28).

Ali I, Yang WC. The functions of kinesin and kinesin-related proteins in eukaryotes. Cell Adhesion & Migration. 2020 Jan 1;14(1):139-52.

Amari K, Di Donato M, Dolja VV, Heinlein M. Myosins VIII and XI play distinct roles in reproduction and transport of tobacco mosaic virus. PLoS pathogens. 2014 Oct 16;10(10):e1004448.

Amari K, Lerich A, Schmitt-Keichinger C, Dolja VV, Ritzenthaler C. Tubule-guided cell-to-cell movement of a plant virus requires class XI myosin motors. PLoS Pathogens. 2011 Oct 27;7(10):e1002327.

Ananthakrishnan R, Ehrlicher A. The forces behind cell movement. International journal of biological sciences. 2007;3(5):303.

Avisar D, Prokhnevsky AI, Dolja VV. Class VIII myosins are required for plasmodesmatal localization of a closterovirus Hsp70 homolog. Journal of virology. 2008 Mar 15;82(6):2836-43.

Barton DA, Cole L, Collings DA, Liu DY, Smith PM, Day DA, Overall RL. Cell-to-cell transport via the lumen of the endoplasmic reticulum. The Plant Journal. 2011 Jun;66(5):806-17

Bayer EM, Mongrand S, Tilsner J. Specialized membrane domains of plasmodesmata, plant intercellular nanopores. Frontiers in plant science. 2014 Sep 30;5:507.

Bidhendi AJ, Geitmann A. Relating the mechanics of the primary plant cell wall to morphogenesis. Journal of experimental botany. 2016 Jan 1;67(2):449-61.

Blackman LM, Overall RL. Immunolocalisation of the cytoskeleton to plasmodesmata of Chara corallina. The Plant Journal. 1998 Jun;14(6):733-41.

Brett C, Waldron K. The cell wall and intercellular transport. InPhysiology and biochemistry of plant cell walls 1990 (pp. 114-136). Springer, Dordrecht.

Brunkard JO, Runkel AM, Zambryski PC. Plasmodesmata dynamics are coordinated by intracellular signaling pathways. Current opinion in plant biology. 2013 Oct 1;16(5):614-20.

Celler K, Fujita M, Kawamura E, Ambrose C, Herburger K, Holzinger A, Wasteneys GO. Microtubules in plant cells: strategies and methods for immunofluorescence, transmission electron microscopy, and live cell imaging. InCytoskeleton Methods and Protocols 2016 (pp. 155-184). Humana Press, New York, NY.

Chen C, Vanneste S, Chen X. Membrane tethers control plasmodesmal function and formation. Plant Science. 2021 Mar 1;304:110800.

Collings DA. Crossed-wires: interactions and cross-talk between the microtubule and microfilament networks in plants. Plant microtubules. 2008:47-79.

Cotton S, Grangeon R, Thivierge K, Mathieu I, Ide C, Wei T, Wang A, Laliberté JF. Turnip mosaic virus RNA replication complex vesicles are mobile, align with microfilaments, and are each derived from a single viral genome. Journal of virology. 2009 Oct 15;83(20):10460-71.

Cui X, Wei T, Chowda-Reddy RV, Sun G, Wang A. The Tobacco etch virus P3 protein forms mobile inclusions via the early secretory pathway and traffics along actin microfilaments. Virology. 2010 Feb 5;397(1):56-63.

Dashevskaya S, Kopito RB, Friedman R, Elbaum M, Epel BL. Diffusion of anionic and neutral GFP derivatives through plasmodesmata in epidermal cells of Nicotiana benthamiana. Protoplasma. 2008 Dec;234(1):13-23.

Diao M, Huang S. An Update on the Role of the Actin Cytoskeleton in Plasmodesmata: A Focus on Formins. Frontiers in Plant Science. 2021 Feb 15;12:647123.

Dong X, Hong Z, Chatterjee J, Kim S, Verma DP. Expression of callose synthase genes and its connection with Npr1 signaling pathway during pathogen infection. Planta. 2008 Dec;229(1):87-98.

Eckardt NA. Membrane rafts and virus movement in plant cells. The Plant Cell. 2009 May;21(5):1326-.

Epel BL. Plant viruses spread by diffusion on ER-associated movement-protein-rafts through plasmodesmata gated by viral induced host β-1, 3-glucanases. InSeminars in cell & developmental biology 2009 Dec 1 (Vol. 20, No. 9, pp. 1074-1081). Academic Press.

Farvardin A, González-Hernández AI, Llorens E, García-Agustín P, Scalschi L, Vicedo B. The apoplast: a key player in plant survival. Antioxidants. 2020 Jul 10;9(7):604.

Feng Z, Chen X, Bao Y, Dong J, Zhang Z, Tao X. Nucleocapsid of Tomato spotted wilt tospovirus forms mobile particles that traffic on an actin/endoplasmic reticulum network driven by myosin XI-K. New Phytologist. 2013 Dec;200(4):1212-24.

Fridborg I, Grainger J, Page A, Coleman M, Findlay K, Angell S. TIP, a novel host factor linking callose degradation with the cell-to-cell movement of Potato virus X. Molecular plant-microbe interactions. 2003 Feb;16(2):132-40.

Gallagher KL, Sozzani R, Lee CM. Intercellular protein movement: deciphering the language of development. Annual review of cell and developmental biology. 2014 Oct 6;30:207-33.

Geitmann A, Nebenführ A. Navigating the plant cell: intracellular transport logistics in the green kingdom. Molecular Biology of the Cell. 2015 Oct 1;26(19):3373-8.

Geng C, Cong QQ, Li XD, Mou AL, Gao R, Liu JL, Tian YP. Developmentally regulated plasma membrane protein of Nicotiana benthamiana contributes to potyvirus movement and transports to plasmodesmata via the early secretory pathway and the actomyosin system. Plant physiology. 2015 Feb;167(2):394-410.

Gicking AM, Swentowsky KW, Dawe RK, Qiu W. Functional diversification of the kinesin-14 family in land plants. FEBS letters. 2018 Jun;592(12):1918-28.

Harries PA, Park JW, Sasaki N, Ballard KD, Maule AJ, Nelson RS. Differing requirements for actin and myosin by plant viruses for sustained intercellular movement. Proceedings of the National Academy of Sciences. 2009 Oct 13;106(41):17594-9.

Harries PA, Schoelz JE, Nelson RS. Intracellular transport of viruses and their components: utilizing the cytoskeleton and membrane highways. Molecular plant-microbe interactions. 2010 Nov;23(11):1381-93.

Haupt S, Cowan GH, Ziegler A, Roberts AG, Oparka KJ, Torrance L. Two plant–viral movement proteins traffic in the endocytic recycling pathway. The Plant Cell. 2005 Jan;17(1):164-81.

He F, Chen H, Han R. The plant cytoskeleton and crosslinking factors. CellBio. 2020 May 29;9(02):85.

Ho-Jong J, Samuels TD, Wang YS, Blancaflor E. The Potato Virus X TGBp2 Movement Protein Associates with Endoplasmic Reticulum-Derived Vesicles during Virus Infection1. Plant Physiology. 2005 Aug 1;138(4):1877.

Iglesias VA, Meins Jr F. Movement of plant viruses is delayed in a β-1, 3-glucanase-deficient mutant showing a reduced plasmodesmatal size exclusion limit and enhanced callose deposition. The Plant Journal. 2000 Jan;21(2):157-66.

Karasev AV, Kashina AS, Gelfand VI, Dolja VV. HSP70-related 65 kDa protein of beet yellows closterovirus is a microtubule-binding protein. FEBS letters. 1992 Jun 8;304(1):12-4.

Kawakami S, Watanabe Y, Beachy RN. Tobacco mosaic virus infection spreads cell to cell as intact replication complexes. Proceedings of the National Academy of Sciences. 2004 Apr 20;101(16):6291-6.

Kost B, Chua NH. The plant cytoskeleton: vacuoles and cell walls make the difference. Cell. 2002 Jan 11;108(1):9-12.

Kost B, Spielhofer P, Chua NH. A GFP-mouse talin fusion protein labels plant actin filaments in vivo and visualizes the actin cytoskeleton in growing pollen tubes. The Plant Journal. 1998 Nov;16(3):393-401.

Krasavina MS, Ktitorova IN, Burmistrova NA. Electrical conductance of cell-to-cell junctions and the cytoskeleton of plant cells. Russian Journal of Plant Physiology. 2001 Nov;48(6):741-8.

Krishnamurthy K, Heppler M, Mitra R, Blancaflor E, Payton M, Nelson RS, Verchot-Lubicz J. The Potato virus X TGBp3 protein associates with the ER network for virus cell-to-cell movement. Virology. 2003 Apr 25;309(1):135-51.

Kwok EY, Hanson MR. In vivoanalysis of interactions between GFP-labeled microfilaments and plastid stromules. BMC plant biology. 2004 Dec;4(1):1-9.

Laporte C, Vetter G, Loudes AM, Robinson DG, Hillmer S, Stussi-Garaud C, Ritzenthaler C. Involvement of the secretory pathway and the cytoskeleton in intracellular targeting and tubule assembly of Grapevine fanleaf virus movement protein in tobacco BY-2 cells. The Plant Cell. 2003 Sep;15(9):2058-75.

Lev-Yadun S. Intrusive Growth. The Plant Analog of Dendrite and Axon Growth in Animals. New Phytologist. 2001 Jun 1:508-12.

Lev-Yadun S. Plant development: Cell movement relative to each other is both common and very important. Plant signaling & behavior. 2015 Mar 4;10(3):e991566.

Levy A, Zheng JY, Lazarowitz SG. The tobamovirus turnip vein clearing virus 30-kilodalton movement protein localizes to novel nuclear filaments to enhance virus infection. Journal of virology. 2013 Jun 1;87(11):6428-40.

Liu JZ, Blancaflor EB, Nelson RS. The tobacco mosaic virus 126-kilodalton protein, a constituent of the virus replication complex, alone or within the complex aligns with and traffics along microfilaments. Plant Physiology. 2005 Aug;138(4):1853-65.

Lu L, Wu G, Xu X, Luan H, Zhi H, Cui J, Cui X, Chen X. Soybean actin-depolymerizing factor 2 interacts with Soybean mosaic virus-encoded P3 protein. Virus Genes. 2015 Apr;50(2):333-9.

Lucas WJ, Bouché-Pillon S, Jackson DP, Nguyen L, Baker L, Ding B, Hake S. Selective trafficking of KNOTTED1 homeodomain protein and its mRNA through plasmodesmata. Science. 1995 Dec 22;270(5244):1980-3.

Martens HJ, Roberts AG, Oparka KJ, Schulz A. Quantification of plasmodesmatal endoplasmic reticulum coupling between sieve elements and companion cells using fluorescence redistribution after photobleaching. Plant Physiology. 2006 Oct;142(2):471-80.

McLean BG, Zupan J, Zambryski PC. Tobacco mosaic virus movement protein associates with the cytoskeleton in tobacco cells. The Plant Cell. 1995 Dec;7(12):2101-14.

Morozov SY, Fedorkin ON, Jóttner G, Schiemann J, Baulcombe DC, Atabekov JG. Complementation of a potato virus X mutant mediated by bombardment of plant tissues with cloned viral movement protein genes. Journal of General Virology. 1997 Aug 1;78(8):2077-83.

Nebenführ A, Dixit R. Kinesins and myosins: molecular motors that coordinate cellular functions in plants. Annual Review of Plant Biology. 2018 Apr 4;69:329.

Niehl A, Heinlein M. Cellular pathways for viral transport through plasmodesmata. Protoplasma. 2011 Jan;248(1):75-99.

Niehl A, Peña EJ, Amari K, Heinlein M. Microtubules in viral replication and transport. The Plant Journal. 2013 Jul;75(2):290-308.

Olesen P. The neck constriction in plasmodesmata. Planta. 1979 Jan;144(4):349-58.

Olspert A, Chung BY, Atkins JF, Carr JP, Firth AE. Transcriptional slippage in the positive-sense RNA virus family Potyviridae. EMBO reports. 2015 Aug;16(8):995-1004.

Overall RL, Blackman LM. A model of the macromolecular structure of plasmodesmata. Trends in plant science. 1996 Sep 1;1(9):307-11.

Porter K, Day B. From filaments to function: the role of the plant actin cytoskeleton in pathogen perception, signaling and immunity. Journal of integrative plant biology. 2016 Apr;58(4):299-311.

Prokhnevsky AI, Peremyslov VV, Dolja VV. Actin cytoskeleton is involved in targeting of a viral Hsp70 homolog to the cell periphery. Journal of Virology. 2005 Nov 15;79(22):14421-8.

Reddy AS. Molecular motors and their functions in plants. 2001: 97-178.

Riedl J, Crevenna AH, Kessenbrock K, Yu JH, Neukirchen D, Bista M, Bradke F, Jenne D, Holak TA, Werb Z, Sixt M. Lifeact: a versatile marker to visualize F-actin. Nature methods. 2008 Jul;5(7):605-7.

Rim Y, Huang L, Chu H, Han X, Cho WK, Jeon CO, Kim HJ, Hong JC, Lucas WJ, Kim JY. Analysis of Arabidopsis transcription factor families revealed extensive capacity for cell-to-cell movement as well as discrete trafficking patterns. Molecules and cells. 2011 Dec;32(6):519-26.

Schneider R, Persson S. Connecting two arrays: the emerging role of actin-microtubule cross-linking motor proteins. Frontiers in Plant Science. 2015 Jun 2;6:415.

Serazev TV, Nadezhdina ES, Shanina NA, Leshchiner AD, Kalinina NO, Morozov SY. Virions and the coat protein of the potato virus X interact with microtubules and induce tubulin polymerization in vitro. Molecular Biology. 2003 Nov;37(6):919-25.

Sevilem I, Yadav SR, Helariutta Y. Plasmodesmata: channels for intercellular signaling during plant growth and development. Plasmodesmata. 2015:3-24.

Sheahan MB, Staiger CJ, Rose RJ, McCurdy DW. A green fluorescent protein fusion to actin-binding domain 2 of Arabidopsis fimbrin highlights new features of a dynamic actin cytoskeleton in live plant cells. Plant physiology. 2004 Dec;136(4):3968-78.

Southworth D, Cresti M. Comparison of flagellated and nonflagellated sperm in plants. American journal of botany. 1997 Sep;84(9):1301-11.

Spiegelman Z, Lee CM, Gallagher KL. KinG is a plant-specific kinesin that regulates both intra-and intercellular movement of SHORT-ROOT. Plant Physiology. 2018 Jan;176(1):392-405.

Stadler R, Wright KM, Lauterbach C, Amon G, Gahrtz M, Feuerstein A, Oparka KJ, Sauer N. Expression of GFP-fusions in Arabidopsis companion cells reveals non-specific protein trafficking into sieve elements and identifies a novel post-phloem domain in roots. The Plant Journal. 2005 Jan;41(2):319-31.

Su S, Liu Z, Chen C, Zhang Y, Wang X, Zhu L, Miao L, Wang XC, Yuan M. Cucumber mosaic virus movement protein severs actin filaments to increase the plasmodesmal size exclusion limit in tobacco. The Plant Cell. 2010 Apr;22(4):1373-87.

Sun Y, Huang D, Chen X. Dynamic regulation of plasmodesmatal permeability and its application to horticultural research. Horticulture Research. 2019 Dec 1;6.

Sun Y, Huang D, Chen X. Dynamic regulation of plasmodesmatal permeability and its application to horticultural research. Horticulture Research. 2019 Dec 1;6.

Takemoto D, Hardham AR. The cytoskeleton as a regulator and target of biotic interactions in plants. Plant Physiology. 2004 Dec;136(4):3864-76.

Tilsner J, Linnik O, Wright KM, Bell K, Roberts AG, Lacomme C, Santa Cruz S, Oparka KJ. The TGB1 movement protein of Potato virus X reorganizes actin

and endomembranes into the X-body, a viral replication factory. Plant physiology. 2012 Mar;158(3):1359-70.

Tominaga M, Nakano A. Plant-specific myosin XI, a molecular perspective. Frontiers in plant science. 2012 Sep 10;3:211.

Tominaga M, Nakano A. Plant-specific myosin XI, a molecular perspective. Frontiers in plant science. 2012 Sep 10;3:211.

Ueda K, Matsuyama T, Hashimoto T. Visualization of microtubules in living cells of transgenicArabidopsis thaliana. Protoplasma. 1999 Mar;206(1):201-6.

Ueki S, Citovsky V. Plasmodesmata-associated proteins: Can we see the whole elephant?. Plant signaling & behavior. 2014 Feb 1;9(2):e27899.

Wei T, Huang TS, McNeil J, Laliberté JF, Hong J, Nelson RS, Wang A. Sequential recruitment of the endoplasmic reticulum and chloroplasts for plant potyvirus replication. Journal of virology. 2010 Jan 15;84(2):799-809.

White RG, Barton DA. The cytoskeleton in plasmodesmata: a role in intercellular transport?. Journal of Experimental Botany. 2011 Nov 1;62(15):5249-66.

Yan F, Lu Y, Lin L, Zheng H, Chen J. The ability of PVX p25 to form RL structures in plant cells is necessary for its function in movement, but not for its suppression of RNA silencing. (2012): e43242

Yang HC, Pon LA. Actin cable dynamics in budding yeast. Proceedings of the National Academy of Sciences. 2002 Jan 22;99(2):751-6.

Yuan Z, Chen H, Chen Q, Omura T, Xie L, Wu Z, Wei T. The early secretory pathway and an actin-myosin VIII motility system are required for plasmodesmatal localization of the NSvc4 protein of Rice stripe virus. Virus research. 2011 Jul 1;159(1):62-8.

BIOGRAPHY

I hold a Bsc degree in Science from Alexandria University, Faculty of Science and an Msc student in Plant protection department at the University of Cukurova, faculty of Agriculture, in Adana, Turkey

I have gained lots of opportunites while studying in Turkey. Firstly, being an International student in Turkey helped me a lot be an independent student and get used to the life abroad, so it will not take much time for me to adapt and get used to new environment anywhere else. Secondly, through their Erasmus programs, I got an opportunity to visit Europe as a student. I have succeeded to do some training at Copenhagen University in Denmark and to do part of my Msc. Studies at the university of Lleida in Spain. I have done as well some training courses in Bonn University in Germany.

At the University of Copenhagen, I have done the analysis of **Cerato-platanin gene** from different *Septoria tritici* isolates. About 15 resistance genes (Stb1-Stb15) were recently identified in wheat. Though none of the Stb genes is effective to **all** *Siptoria tritici* isolates, the ***Stb*6**, is known to be an effective gene against **IPO323** isolates. Two cultivars were identified for the plant-fungus gene interaction, cv Stakado (resistant cultivar, incompatible interaction) and cv Sivan (susceptible cultivar, compatible interaction). Previous studies at Prof Dr. Hans Theodral team indicated that in the compatible interaction the fungus produces a proteinous toxin that is thought to switch the nutrition mode of the fungus from being biotrophic (extracellular mycelium, latent infection) into necrotrophic (pycnidia formation associated with appearance of lesion of the **speckled leaf blotch**). The hypothesis of experiment was that the isolates (collected from almost 50 infected wheat in Denmark), which overcome *Stb6*-mediated resistance, express **altered versions of the toxin**, preventing its binding. During my stay, I isolate the fungus from the infected leaves and inoculating a single mycelium into PDA (for further studies by the department). I followed CTAB protocol to have fungal DNA isolation. Then

Together with Dr. Cartsen, we designed primers for the amplification of the cerato-platanin gene (the toxin gene) in PCR. The toxin gene was amplified in the isolates by PCR and the product sequenced to reveal whether there are differences in the sequence which can explain differences in susceptibility to the fungus. As expected, there was no significant difference in the isolates screened for the Cerato-platanian gene.

My work in MSc thesis was under the supervision of Associate Professor Muharrem Arap Kamberoglu. For practical experience and study, I have attended lectures and practical training courses such as Virology of Citrus, molecular virology, Taxonomy of plant weeds, and I am planning of getting some courses to cover the areas of gene function, scientific research methods, plant biochemistry and I plan in the future to check the pathogen progress (by QPCR).

I am so keen to learn anything new, since I get the school soul anywhere I go. I may learn from anybody, at any time. My life is school and I hope to seek knowledge till the end and practice upon them.

APPENDICES

Appendix 1. Plasmid map of pTRA.PVX.4xcsy4.DsRed-CP

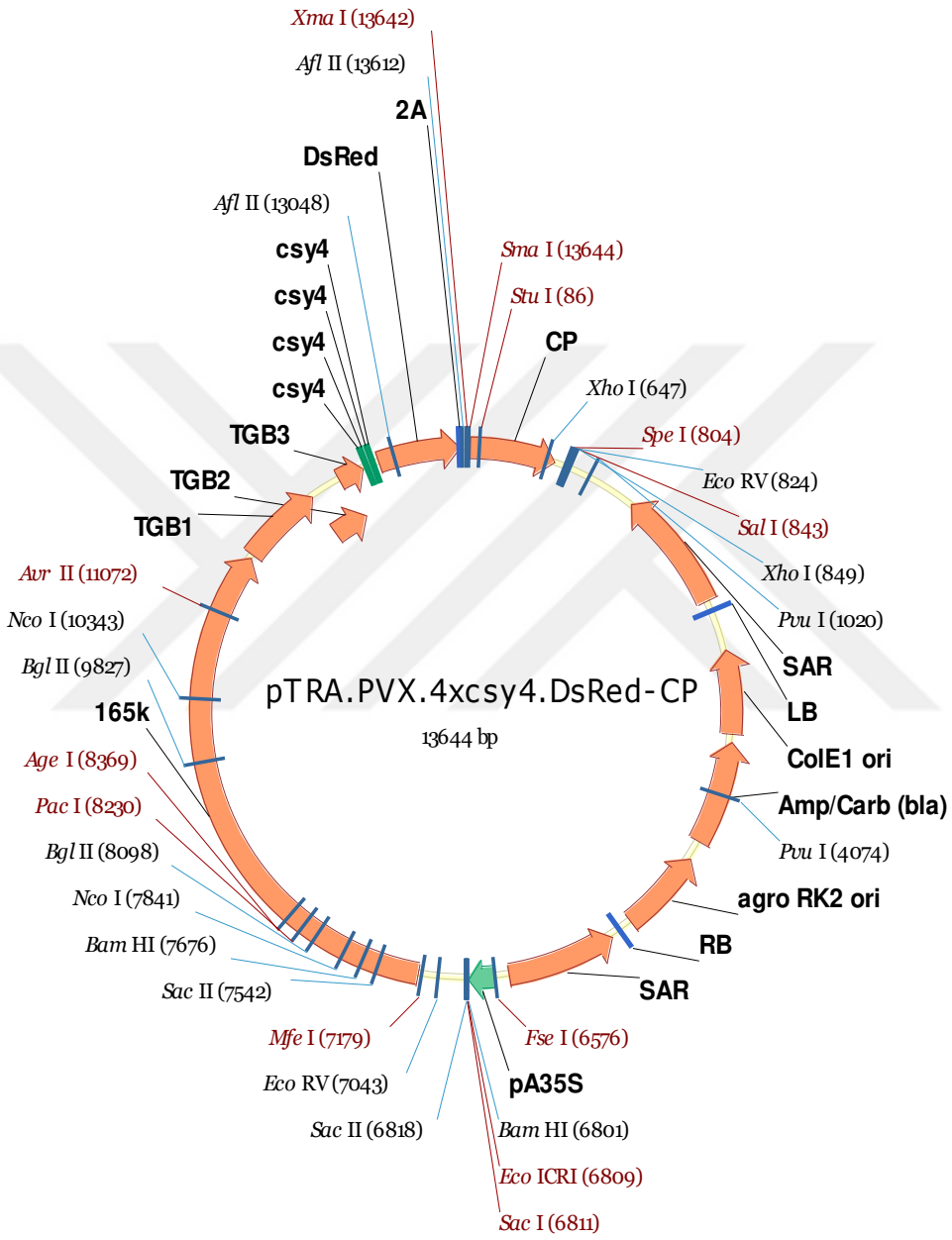

Appendix 2. Plasmid map of p35S.PVX.GFP-CP

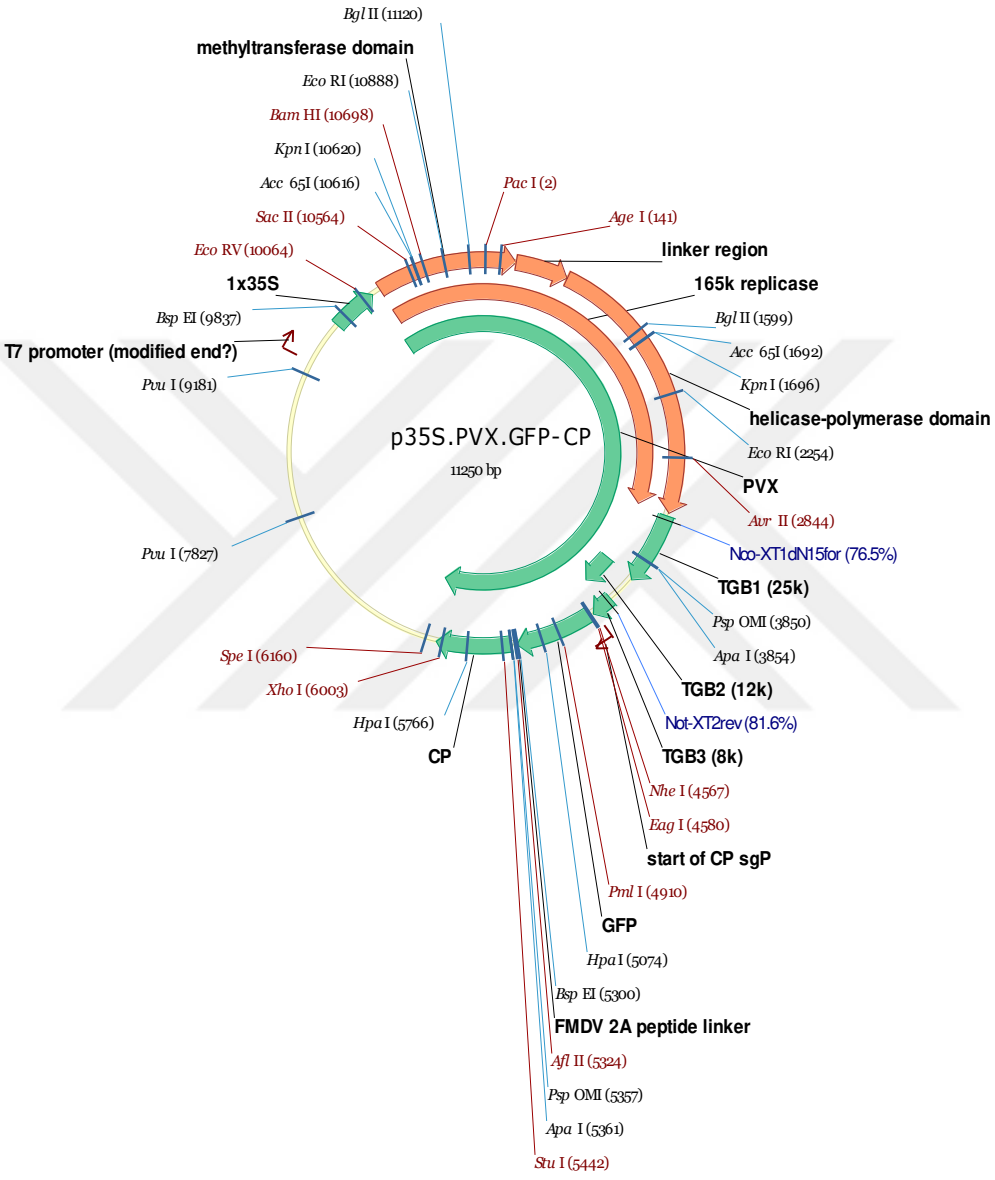

Appendix 3. Plasmid map of p35S.PVX.deltaTGB.xcsy4.DsR-2A-CP

Appendix 4. Plasmid map of p35S.PVX.deltaTGB.xcsy4.DsR-2A-CP

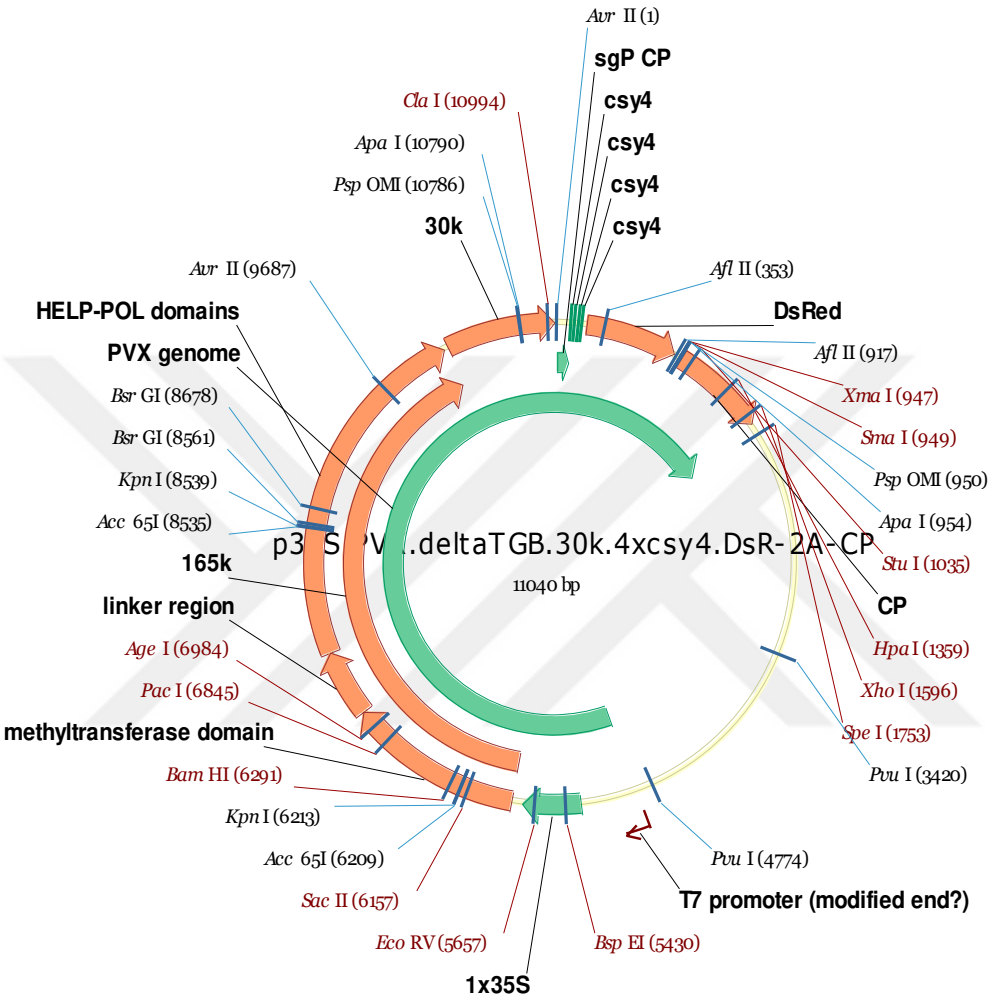

Appendix 5. PCR amplifying the p35S.PVX backbone

PCR#1 vector backbone (p35S.PVX backbone)
0.5 µl template* 10 µl 5x Q5 buffer 1 µl 10 mM dNTPs 2.5 µl 10 µM p35S.PVX.GFP-CP_fwd primer 2.5 µl 10 µM p35S.PVX.GFP-CP_rev primer 0.5 µl Q5 polymerase ad 50 µl H2O *p35S.PVX.GFP-CP
98ºC 30 sec ---------- 98ºC 15 sec 61.7ºC 15 sec* 72ºC 4 min x20 ---------- 72ºC 2 min 4ºC hold *NEB Tm Calculator: 61.7ºC recommended for full-length amplification. No overlap to other sequences (the overlaps are generated on the inserts), so annealing temperature is 61.7 C throughout.
Expected product size is 9329 bp.

Appendix 6. PCR amplifying the 4xcsy4.DsRed-2A insert.

PCR#2 insert fragment (4xcsy4.DsRed-2A)
0.5 µl template* 10 µl 5x Q5 buffer 1 µl 10 mM dNTPs 2.5 µl 10 µM pTRA.PVX.csy4.DsR-CP_fwd primer 2.5 µl 10 µM pTRA.PVX.csy4.DsR-CP_rev primer 0.5 µl Q5 polymerase ad 50 µl H2O * pTRA.PVX.4xcsy4.DsRed-2A.CP
98ºC 30 sec ---------- 98ºC 15 sec 57ºC 15 sec* 72ºC 30 sec x3 ---------- 98ºC 15 sec* 66ºC 15 sec* 72ºC 30 sec x17 ---------- 72ºC 2 min 4ºC hold *NEB Tm Calculator: 57ºC recommended for primer parts designed for overlapping ends, 66ºC recommended for full-length amplification.
Expected product size is ~1 kb

Appendix 7. PCR amplifying the 30k insert.

PCR#3 insert fragment (30k)
0.5 µl template* 10 µl 5x Q5 buffer 1 µl 10 mM dNTPs 2.5 µl 10 µM JT1189a_fwd primer 2.5 µl 10 µM JT1189a_rev primer 0.5 µl Q5 polymerase ad 50 µl H2O * JT1189 (pDONR201.30k-stop)
98ºC 30 sec ---------- 98ºC 15 sec 57ºC 15 sec* 72ºC 30 sec x3 ---------- 98ºC 15 sec* 68ºC 15 sec* 72ºC 30 sec x17 ---------- 72ºC 2 min 4ºC hold *NEB Tm Calculator: 57ºC recommended for primer parts designed for overlapping ends, 68ºC recommended for full-length amplification.
Expected product size is ~840 bp

Appendix 8. NEBuilder overlapping reaction of p35S.PVX/30k/4xcsy4.DsRed-2A fragments.

NEBuilder Overlapping (p35S.PVX/30k/4xcsy4.DsRed-2Afragments overlapping)
4 µl reactions 2 µl backbone-insert PCR fragments* mix** + 2 µl NEB-Enzyme mix 2x 15 min 50ºC → stored -20 *PCR products, if not gel-purified, are digested by **DpnI**. ** Quantification of PCR/DpnI digests. PCR fragments are diluted into 50 ng/µl (eq. 0.01 pmol.) for the vector fragment (~9000 bp) and 13 ng/µl (eq. 0.02 pmol.; i.e. double fold the vector amount) for each insert fragment (each ~1000 bp). pmols = (weight in ng) x 1,000 / (base pairs x 650 daltons) Simply pmols = wt ng / (0.65 x bps)
DpnI digestion (To break down methylated pDNA template but not PCR DNA product) 8 µl PCR DNA + 1 µl 10x bu. + 1 µl DpnI (NEB) total 10 µl Rxn → 30 min. 37ºC → 20 min. 80ºC

Appendix 9. Purification and bulking of the cloned modified virus plasmid p35S.PVX.deltaTGBs.30K.4xCsy4.DsRED-2A-CP (or JTM003).

E.coli transformations
2 µl NEB into 50 µl chemically-competent DH5alpha (Invitrogen "Library Efficiency"), incubated on ice in 0.5 ml tube for 30 min, heat-shock at 42ºC for 45 sec, re-suspended in 200 µl SOC → 1h 37ºC → plated 50 µl, 100 µl on LB-AMP
<u>Culture growth for plasmid minipreps</u> 2 picked colonies of JTM003 inoculated in 4 ml LB-AMP→ o/n 37ºC with shaking. *colony-PCR
<u>Colony PCR</u> Tested 2 colonies each of JTM003 4 µl l 5 x GoTaq green buffer 1 µl 10 mM dNTPs 1 µl 10 µM DS JT1189a_fwd primer 1 µl 10 µM pTRA.PVX.csy4.DsR-CP_rev primer 0.2 µl GoTaq polymerase ad 20 µl H2O 98°C 30 min ---------- 98°C 15 sec 55°C 15 sec 72°C 2 min x25 ---------- 72°C 2 min 4°C hold <u>Entire PCR on gel</u> Expected product size is 1.8 kb
<u>Plasmid minipreps of JTM003</u> QIAgen kit, eluted in 50 µl EB → JTM003m and JTM003p
<u>Glycerol preservation of DH5alpha-JTM003m and DH5alpha-JTM003p</u> 800 µl bacterial growth + 300 µl 100% autoclaved glycerol → Vortex → thrown in Liq. N → stored at -80ºC

Appendix 10 Diagnostic digestion of the cloned modified virus plasmid p35S.PVX.deltaTGBs.30K.4xCsy4.DsRED-2A-CP (or JTM003).

Diagnostic HindIII digestion
2.5 µl DNA + 2 µl 10x bu. + 0.2 µl BSA + 0.5 µl HindIII (NEB), ad 20 µl H2O → 1.5 h 37ºC → all on gel
JTM003/HindIII: Correct patterns are: 6230, 1211, 1205, 973, 845, 570 bp.

Appendix 11. Biolistic particle bombardment of the cloned modified virus plasmid p35S.PVX.deltaTGBs.30K.4xCsy4.DsRED-2A-CP (or JTM003).

Biolistic bombardment of JTM003 clones 5 dpi
10 µl DNA particle solution → loaded into the nozzle → shot twice/each leaf → two leaves/ plant. DNA particle solution: 2 µl DNA plasmid template {JTM003} + 5 µl 70%ETOH + 11 µl gold beads suspended in ETOH

Appendix 12. PCR amplifying the p35S.PVX backbone

PCR#1 vector backbone (p35S.PVX backbone)
0.5 µl template* 10 µl 5x Q5 buffer 1 µl 10 mM dNTPs 2.5 µl 10 µM fusePVXsgtbp_fwd primer 2.5 µl 10 µM fuse165k_rev primer 0.5 µl Q5 polymerase ad 50 µl H2O *p35S.PVX.mcherry-CP (JT1096)
98ºC 30 sec ---------- 98ºC 15 sec 56ºC 15 sec* 72ºC 5:15 min x20 ---------- 72ºC 2 min 4ºC hold *NEB Tm Calculator: 56ºC recommended for full-length amplification. No overlap to other sequences (the overlaps are generated on the inserts), so annealing temperature is 56ºC throughout.
Expected product size is 11 kb.

Appendix 13. Three nested PCRs constructing the 2A- phiLOV2.1 insert.

PCR#2 insert fragment (2A-phiLOV2.1)
Step1 00.5 µl template* 5 µl 5x Q5 buffer 0.5 µl 10 mM dNTPs 1.25 µl 10 µM 2A1-phiLOVF primer 1.25 µl 10 µM 2A-phiLOV_rev primer 0.25 µl Q5 polymerase ad 25 µl H2O *JTM40 (phiLove2.1 provided from Glasgow lab)
98ºC 30 sec ---------- 98ºC 15 sec 56ºC 15 sec* 72ºC 30 sec x3 ---------- 98ºC 15 sec* 70ºC 15 sec* 72ºC 30 sec x10 ---------- 72ºC 2 min 4ºC hold *NEB Tm Calculator: 56ºC recommended for primer parts designed for overlapping ends, 70ºC recommended for full-length amplification.
Step2 00.5 µl template* 5 µl 5x Q5 buffer 0.5 µl 10 mM dNTPs 1.25 µl 10 µM 2A2F primer 1.25 µl 10 µM 2A-phiLOV_rev primer 0.25 µl Q5 polymerase ad 25 µl H2O

*JTM40 (phiLove2.1 template plasmid provided from Glasgow lab)
98ºC 30 sec ---------- 98ºC 15 sec 56ºC 15 sec* 72ºC 30 sec x3 ---------- 98ºC 15 sec* 70ºC 15 sec* 72ºC 30 sec x10 ---------- 72ºC 2 min 4ºC hold *NEB Tm Calculator: 56ºC recommended for primer parts designed for overlapping ends, 70ºC recommended for full-length amplification.
<u>Step3</u> 0.5 µl template* 10 µl 5x Q5 buffer 1 µl 10 mM dNTPs 2.5 µl 10 µM 2A-phiLOV_fwd primer 2.5 µl 10 µM 2A-phiLOV_rev primer 0.5 µl Q5 polymerase ad 50 µl H2O *1st and 2nd PCR products (no need to purify the PCR products before the use, as the subsequent reverse primers can only bind to previous PCR products, not the phiLOV2.1 template plasmid.)
98ºC 30 sec ---------- 98ºC 15 sec 56ºC 15 sec* 72ºC 30 sec x3 ---------- 98ºC 15 sec* 70ºC **15** sec* 72ºC 30 sec x22 ----------

72ºC 2 min 4ºC hold *NEB Tm Calculator: 56ºC recommended for primer parts designed for overlapping ends, 70ºC recommended for full-length amplification.
Expected product size is ~400 bp.

Appendix 14. NEBuilder overlapping reaction of p35S.PVX and 1652A-phiLOV2.1.

NEBuilder Overlapping (p35S.PVX and 1652A-phiLOV2.1 overlapping)
4 µl reactions 2 µl backbone-insert PCR fragments* mix** + 2 µl NEB-Enzyme mix 2x 15 min 50ºC → stored -20 *PCR products, if not gel-purified, are digested by **DpnI**. ** Quantification of PCR/DpnI digests. PCR fragments are diluted into 71.5 ng/µl (eq. 0.01 pmol.) for the vector fragment (~11000 bp) and 5.2 ng/µl (eq. 0.02 pmol.; i.e. double fold the vector amount) for insert fragment (each ~400 bp). pmols = (weight in ng) x 1,000 / (base pairs x 650 daltons) Simply pmols = wt ng/ (0.65 x bps)
DpnI digestion (To break down methylated pDNA template but not PCR DNA product) 8 µl PCR DNA + 1 µl 10x bu. + 1 µl DpnI (NEB) total 10 µl Rxn → 30 min. 37ºC → 20 min. 80ºC

Appendix 15. Purification and bulking of the cloned modified virus plasmid p35S.PVX.1652A-phiLOV-mcherry-2A (or JTM082).

E.coli transformations
2 µl NEB into 50 µl chemically-competent DH5alpha (Invitrogen "Library Efficiency"), incubated on ice in 0.5 ml tube for 30 min, heat-shock at 42ºC for 45 sec, re-suspended in 200 µl SOC → 1h 37ºC → plated 50 µl, 100 µl on LB-AMP
<u>Culture growth for plasmid minipreps</u> 2 picked colonies of JTM082 are inoculated in 4 ml LB-AMP→ o/n 37ºC with shaking.
<u>Plasmid minipreps of JTM082</u> QIAgen kit, eluted in 50 µl EB → JTM082e
<u>Glycerol preservation of DH5alpha-JTM082e</u> 800 µl bacterial growth + 300 µl 100% autoclaved glycerol → Vortex → thrown in Liq. N → stored at -80ºC

Appendix 16. Diagnostic digestion of the cloned modified virus plasmid p35S.PVX.1652A-phiLOV-mcherry-2A (or JTM082).

Diagnostic HindIII digestion
2.5 µl DNA + 2 µl 10x bu. + 0.2 µl BSA + 0.5 µl HindIII (NEB), ad 20 µl H2O → 1.5 h 37ºC
JTM082/HindIII: Correct patterns are: 6230, 2338, 1205, 1016, 845 bp

Appendix 17. Biolistic particle bombardment of the cloned virus plasmid p35S.PVX.1652A-phiLOV-mcherry-2A (or JTM082). Upon bombardment seeing red fluorescence will prove that replicase is OK, because mCherry-CP will only be expressed from a replicating virus (as it is the 5th ORF on the viral RNA). Failing to have red fluorescence will leave require a sequencing to answer check if it is because the phiLOV fusion is the problem, or because the PCRs created mutations in 165k ORF.

Biolistic bombardment of JTM0082e clones
10 µl DNA particle solution → loaded into the nozzle → shot twice/each leaf → two leaves/ plant. DNA particle solution: 2 µl DNA plasmid template {JTM082e} + 5 µl 70%ETOH + 11 µl gold beads suspended in ETOH

Appendix 18. PCR amplifying the PVX backbone

PCR#1 vector backbone (PVX backbone)
0.5 µl template* 10 µl 5x Q5 buffer 1 µl 10 mM dNTPs 2.5 µl 10 µM GS-165F primer 2.5 µl 10 µM GS-165R primer 0.5 µl Q5 polymerase ad 50 µl H2O *JT1096 (p35S.PVX.mCherry-2A-CP), JTM003 and pTRA.DsRed-2A-CP p35S.PVX.GFP-CP
98ºC 30 sec ---------- 98ºC 15 sec 58ºC 15 sec* 72ºC 30 sec x4 ---------- 98ºC 15 sec* 72ºC 6 min* 72ºC 30 sec x21 ---------- 72ºC 2 min 4ºC hold *NEB Tm Calculator: 58ºC recommended for primer parts designed for overlapping ends, 72ºC recommended for full-length amplification
Expected product size is 10-12 kb.

Appendix 19. PCR amplifying the phiLOV2.1 insert.

PCR#2 insert fragment (phiLOV2.1, without adding 2A linker)
0.5 µl template* 10 µl 5x Q5 buffer 1 µl 10 mM dNTPs 2.5 µl 10 µM GS-phiLOVF primer 2.5 µl 10 µM GS-phiLOVR primer 0.5 µl Q5 polymerase ad 50 µl H2O * phiLOV2.1 template
98ºC 30 sec ---------- 98ºC 15 sec 55ºC 15 sec* 72ºC 30 sec x3 ---------- 98ºC 15 sec* 71ºC 15 sec* 72ºC 30 sec x17 ---------- 72ºC 2 min 4ºC hold *NEB Tm Calculator: 55ºC recommended for primer parts designed for overlapping ends, 71ºC recommended for full-length amplification.
Expected product size is ~500bp

Appendix 20. NEBuilder overlapping reaction of plasmids of PVX and phiLOV2.1.

NEBuilder Overlapping (PVX plasmids and phiLOV2.1 overlapping)
4 µl reactions 2 µl backbone-insert PCR fragments* mix** + 2 µl NEB-Enzyme mix 2x 15 min 50ºC → stored -20 *PCR products, if not gel-purified, are digested by **DpnI**. ** Quantification of PCR/DpnI digests. PCR fragments are diluted into 71.5 ng/µl (eq. 0.01 pmol.) for the vector fragment (~11000 bp) and 5.2 ng/µl (eq. 0.02 pmol.; i.e. double fold the vector amount) for insert fragment (each ~400 bp). pmols = (weight in ng) x 1,000 / (base pairs x 650 daltons) Simply pmols = wt ng/ (0.65 x bps)
DpnI digestion (To break down methylated pDNA template but not PCR DNA product) 8 µl PCR DNA + 1 µl 10x bu. + 1 µl DpnI (NEB) total 10 µl Rxn → 30 min. 37ºC → 20 min. 80ºC

Appendix 21. Purification and bulking of the cloned PVX virus plasmid with internally phiLOV-tagged replicases (JTM858, JTM868 and JTM838).

E.coli transformations
2 µl NEB into 50 µl chemically-competent DH5alpha (Invitrogen "Library Efficiency"), incubated on ice in 0.5 ml tube for 30 min, heat-shock at 42ºC for 45 sec, re-suspended in 200 µl SOC → 1h 37ºC → plated 50 µl, 100 µl on LB-AMP
Culture growth for plasmid minipreps 2 picked colonies of *JTM858, JTM868 and JTM838* are inoculated in 4 ml LB-AMP→ o/n 37ºC with shaking. *colony-PCR
Colony PCR 2 colonies each plate 4 µl l 5 x GoTaq green buffer 1 µl 10 mM dNTPs 1 µl 10 µM GS-phiLOVF primer (or LINK-F primer) 1 µl 10 µM GS-phiLOVR primer (or GS-phiLOVR primer) 0.2 µl GoTaq polymerase ad 20 µl H2O 98°C 30 min ---------- 98°C 15 sec 55°C 15 sec 72°C 2 min x25 ---------- 72°C 2 min 4°C hold Entire PCR on gel Expected product size is 1.3 kb.
Plasmid minipreps of JTM868 BC, JTM858 AB and JTM838O QIAgen kit, eluted in 50 µl EB → JTM868 BC, JTM858 AB and JTM838O
Glycerol preservation of DH5alpha-JTM868 BC, DH5alpha-JTM858 AB and DH5alpha- JTM838O 800 µl bacterial growth + 300 µl 100% autoclaved glycerol → Vortex → thrown in Liq. N → stored at -80ºC

Appendix 22. Diagnostic digestion of the cloned PVX virus plasmid with internally phiLOV-tagged replicases (JTM858, JTM868 and JTM838).

Diagnostic HindIII digestion
2.5 µl DNA + 2 µl 10x bu. + 0.2 µl BSA + 0.5 µl HindIII (NEB), ad 20 µl H2O → 1.5 h 37ºC
JTM838/HindIII: Correct patterns are: 6230, 1211, 1205, 973, 845, 570 bp JTM868 /HindIII: Correct patterns are: 6230, 2970, 1205, 845 bp JTM858/HindIII: Correct patterns are: 8552, 2460, 1205, 857, 570 bp

Appendix 23. Biolistic particle bombardment of the cloned PVX virus plasmid with internally phiLOV-tagged replicases (JTM858, JTM868 and JTM838).

Biolistic bombardment of JTM868 BC, JTM858 AB and JTM838O clones
10 µl DNA particle solution → loaded into the nozzle → shot twice/each leaf → two leaves/ plant. DNA particle solution: 2 µl DNA plasmid template {JTM868 BC, JTM858 AB and JTM838O } + 5 µl 70%ETOH + 11 µl gold beads suspended in ETOH

Appendix 24. Digestion-ligation reaction of the pTRA.PVX virus plasmid to produce a frameshifted replicases (pTRA*).

Preparative AgeI (5' overhang) digestion
2.5 µl DNA + 2 µl 10x bu. + 0.2 µl BSA + 0.5 µl AgeI-HF (NEB), 0.5 µl Klenow (NEB), ad 20 µl H2O → 2-3 h 37ºC (reaction activation) → 20 min. 65ºC (reaction inactivation) DNA: pTRA plasmid template As an alternative, PacI (3' overhang) can be used. heat-inactivate
Klenow 5' overhang fill-in
50 µl DNA digest + 0.5 µl 10 mM dNTPs + 0.5 µl Klenow (NEB) → 15 min 25ºC (reaction activation) → + 1 µl 0.5 M EDTA (to stop reaction) → 20 min. 75ºC (reaction inactivation) DNA digest: the digest reaction with the inactivated enzyme. Klenow 5' overhang fill-in can also 3' overhang digestion NOTE1: for fill-in, NEB Klenow enzyme works in all NEB restriction buffers NOTE2: for 3' overhang removal, Klenow works in all NEB buffers except 1, 1.1. (Buffer 2 is optimal). If buffer 1 or 1.1 is used for restriction digest, the reaction needs to be spin-dialysed and buffer 2 added before blunting
PCR cleanup QIAquick kit, eluted in 30 µl TE → AgeI/Klenow/PCR-Cleanup
Ligation: 5 µl linearized plasmid with blunt ends (AgeI/Klenow/PCR-Cleanup)* + 2 ul 10x ligation buffer + 1 µl ligase, water to 20 µl → o/n 16 ºC *As a negative control to check for undigested plasmid coming through, set up a "ligation" without ligase enzyme.
Transformation of ligations: 40 µl C2987 + 1.5 µl ligation reactions (positive and negative), incubated on ice in 0.5 ml tube for 30 min, heat-shock at 42ºC for 45 sec, re-suspended in 200 µl SOC → 1h 37ºC → plated 50 µl, 100 µl on LB-AMP → compare colony numbers

Diagnostic AgeI/NcoI digestion

2.5 µl DNA + 2 µl 10x bu. + 0.2 µl BSA + 0.5 µl AgeI (NEB) + 0.5 µl NcoI (NEB), ad 20 µl H2O → 1.5 h 37ºC

AgeI/NcoI/ pTRA: 11142, 1974 and 528
AgeI/NcoI/ frame-shifted pTRA: 11142 and 1974

Alternative digestions

AgeI/ AvrII / pTRA: 2.7 kb fragment release
AgeI/ AvrII / frame-shifted pTRA: nothing.

AgeI/ SacI / pTRA: 1.55 kb fragment release.
AgeI/ SacI / frame-shifted pTRA: nothing.

AgeI/ EcoICRI / pTRA: 1.56 kb fragment release.
AgeI/ EcoICRI / frame-shifted pTRA: nothing.

Appendix 25. Biolistic particle co-bombardment of the pTRA.PVX virus plasmid with frameshifted replicases (pTRA*) with GFP/sporamin.

Biolistic co-bombardment of pTRA*/GFP-spramin/19k
10 µl DNA particle solution → loaded into the nozzle → shot twice/each leaf → two leaves/ plant. DNA particle solution: 2 µl DNA plasmid template { pTRA*/GFP-spramin/19k } + 5 µl 70%ETOH + 11 µl gold beads suspended in ETOH

Appendix 26. PCR amplifying the PVX 165-stopcodon

PCR#1
0.5 µl template* 5 µl 5x Q5 buffer 0.5 µl 10 mM dNTPs 1.25 µl 10 µM attB-186 forward primer 1.25 µl 10 µM attB-Stop-186 reverse primer 0.25 µl Q5 polymerase ad 25 µl H2O * p35S.PVX.4xCys4.CP-GFP
98ºC 30 sec ---------- 98ºC 15 sec 66ºC 15 sec* 72ºC 2:30 sec x4 ---------- 98ºC 15 sec* 72ºC 2:30 min x10 ---------- 72ºC 2 min 4ºC hold *NEB Tm Calculator: 66ºC recommended for primer parts complementary to gene-specific nested primers, 72ºC recommended for full-length adapters.
PCR#2
0.5 µl PCR#1 10 µl 5x Q5 buffer 1 µl 10 mM dNTPs 2.5 µl 10 µM attB1 adapter primer 2.5 µl 10 µM attB2 adapter primer 0.5 µl Q5 polymerase ad 50 µl H2O
98ºC 30 sec ----------

98ºC 15 sec 47ºC 15 sec* 72ºC 2:15 min x3 ---------- 98ºC 15 sec* 72ºC 2:30 min x17 ---------- 72ºC 2 min 4ºC hold *NEB Tm Calculator: 47ºC recommended for primer parts complementary to gene-specific nested primers, 72ºC recommended for full-length adapters
Expected product size is 4.5 kb.
PCR cleanup QIAquick kit, eluted in 30 µl TE → attB1-165k(non-stop)-attB2

Appendix 27. BP recombination of PVX 165-stopcodon into pDONR201.

BP recombination
5 µl reactions 3 µl undiluted insert* + 1 µl 1:3** pDONR201 (7.6.16, 210 ng/µl) o/n 25ºC → 30 min 70ºC → kept on 4ºC *PCR product purified and eluted in TE pH8 buffer, **diluted in TE pH8 buffer

Appendix 28. Purification and bulking of the pDONR201/ PVX 165-stopcodon (JTM004, 165k-E).

E.coli transformations
1 µl BP into 50 µl electro-competent DH10B (Invitrogen "Library Efficiency"), incubated on ice in cuvette for 30 min before zapping, slight click when zapped at 1800 V, resuspended in 900 µl LB → 2 h 37ºC → plated 30 µl, 200 µl, 720 µl on LB-Kan
Culture growth for plasmid minipreps 3 picked colonies of *JTM004(a,b and c)* are inoculated in 4 ml LB-Kan→ o/n 37ºC with shaking. *no colony-PCR
Plasmid minipreps of JTM004 QIAgen kit, eluted in 50 µl EB → JTM001
Glycerol preservation of DH10B-JTM004 800 µl bacterial growth + 300 µl 100% autoclaved glycerol → Vortex → thrown in Liq. N → stored at -80ºC
Diagnostic KpnI digestion
2.5 µl DNA + 2 µl 10x bu. + 0.2 µl BSA + 0.5 µl HindIII (NEB), ad 20 µl H2O → 1.5 h 37ºC Expected fragments: JTM004-a/ *Kpn*I: 5.2, 2.3 kb; uncut 4.4 kb plasmid if empty pDONR201
Sequencing of JTM004-a JHI in-house*; primers DONRfor, DONRrev, attB-L61_453Kpnfor, attB-MTrev, attB-HELfor, attB-L61_2800Kpnrev, attB-HELrev, attB-POLfor, attB-L61_3528for, attB-LINKfor, attB-LINKrev, L61-2648for * 6µl pDNA (100-200 ng/µl) submitted per each 2 ul primer

***Appendix 29.. LR recombination of* PVX 165-stopcodon *into* pGWB402omega (unfused) and pGWB406 (N-terminal GFP)**

LR recombination
5 µl reactions 0.5 µl undiluted entry clone* + 0.5 µl undiluted destination vector** + 3 µl TE pH8 buffer + 1 µl LR recombinase. o/n 25ºC → 30 min 70ºC → kept on 4ºC * JTM004-b (~75 ng/ diluted using TE pH8 buffer), **into pGWB402omega (unfused) and pGWB406 (N-terminal GFP)

Appendix 30. Purification and bulking of the pGWB402omega/PVX 165-stopcodon 165-E or JTM010 and pGWB406/(GFP-)PVX 165-stopcodon GFP-165k or JTM011.

E.coli transformations
1 µl LR into 50 µl chemically-competent DH5alpha (Invitrogen "Library Efficiency"), incubated on ice in 0.5 ml tube for 30 min, heat-shock at 42ºC for 45 sec, re-suspended in 200 µl SOC → 1h 37ºC → plated 50 µl, 100 µl on LB-Spec.
Culture growth for plasmid minipreps 2 picked colonies of *JTM010(a and b), JTM011(a and b)* are inoculated in 4 ml LB-Spec→ o/n 37ºC with shaking. *no colony-PCR
Plasmid minipreps of JTM010 and JTM011 QIAgen kit, eluted in 50 µl EB → JTM010 and JTM011.
Glycerol preservation of DH5alpha-JTM010 and DH5alpha-JTM011 800 µl bacterial growth + 300 µl 100% autoclaved glycerol → Vortex → thrown in Liq. N → stored at -80ºC

Appendix 31. Agrobacterium transformation of JTM010 and JTM011

AGL1 transformations
2 µl Plasmid DNA* into 40 µl electroporant AGL1 (home-made Aliquots), incubated on ice in cuvette for 30 min before zapping, slight click when zapped at 1800 V**, resuspended in 900 µl LB → 2 h 37ºC → plated 30 µl on LB-SPEC *JTM010 and JTM011 **And at zapped at 2800 V*
Glycerol preservation of AGL1-JTM010 and AGL1-JTM011 800 µl bacterial growth + 300 µl 100% autoclaved glycerol → Vortex to homogenate → thrown in Liq. N → stored at -80ºC
Culture growth for agroinoculation a colony is inoculated in 5 ml LB-Spec/Rif→ 2 days 28ºC with shaking.

Appendix 32. Agroinoculation of JTM010 and JTM011.

Agroinoculation
Agrobacteria culture → spin 4000rpm 15 min → resuspend pellets → 2 ml infiltration* → 1h in dark → dilute in 10 ml up to OD600 of 0.25A for most fusion proteins, and 0.1A for P19k Measuring OD600 for AGL1 infiltrate using the UV-Spectrometer: 50 µl of infiltration solution as blank read. Dilute the bacterial growth 1/10 (5ul bacterial growth + 45ul infiltration medium). Measure OD 600 of the dilutes which calculates for a "real" OD600 of 10X of the measurement values. *Infiltration medium: (bacterial suspensions in this infiltration media are kept in dark) 100 µl 1M MgCl2 + 200 µl 0.5M MES + 15µl Acetosyringone, ad 10 ml H2O

Appendix 33. PCR amplifying the PVX 165-nostopcodon

PCR#1
0.5 µl template* 5 µl 5x Q5 buffer 0.5 µl 10 mM dNTPs 1.25 µl 10 µM attB-186 forward primer 1.25 µl 10 µM attB-186 reverse primer 0.25 µl Q5 polymerase ad 25 µl H2O * p35S::PVX.mCherry
98ºC 30 sec ---------- 98ºC 15 sec 67ºC 15 sec* 72ºC 2:15 sec x4 ---------- 98ºC 15 sec* 72ºC 2:30 min x10 ---------- 72ºC 2 min 4ºC hold *NEB Tm Calculator: 67ºC recommended for primer parts complementary to gene-specific nested primers, 72ºC recommended for full-length adapters
PCR#2
0.5 µl PCR#1 10 µl 5x Q5 buffer 1 µl 10 mM dNTPs 2.5 µl 10 µM attB1 adapter primer 2.5 µl 10 µM attB2 adapter primer 0.5 µl Q5 polymerase ad 50 µl H2O
98ºC 30 sec ----------

98ºC 15 sec 47ºC 15 sec* 72ºC 2:15 min x3 ---------- 98ºC 15 sec* 72ºC 2:30 min x17 ---------- 72ºC 2 min 4ºC hold *NEB Tm Calculator: 47ºC recommended for primer parts complementary to gene-specific nested primers, 72ºC recommended for full-length adapters
Expected product size is 4.5 kb.
PCR cleanup QIAquick kit, eluted in 30 µl TE → attB1-165k(non-stop)-attB2

Appendix 34. BP recombination of PVX 165-nostopcodon into pDONR201.

BP recombination
5 µl reactions 3 µl undiluted insert* + 1 µl 1:3** pDONR201 (7.6.16, 210 ng/µl) o/n 25ºC → 30 min 70ºC → kept on 4ºC *PCR product purified and eluted in TE pH8 buffer, **diluted in TE pH8 buffer

Appendix 35. Purification and bulking of the pDONR201/ PVX 165-nostopcodon (JTM001).

E.coli transformations
1 µl BP into 50 µl chemically-competent DH5alpha (Invitrogen "Library Efficiency"), incubated on ice in 0.5 ml tube for 30 min, heat-shock at 42ºC for 45 sec, re-suspended in 200 µl SOC → 1h 37ºC → plated 50 µl, 100 µl on LB-Kan.
Culture growth for plasmid minipreps 4 picked colonies of *JTM001(a,b,c and d)* are inoculated in 4 ml LB-Kan→ o/n 37ºC with shaking. *no colony-PCR
Plasmid minipreps of JTM001 QIAgen kit, eluted in 50 µl EB → JTM001
Glycerol preservation of DH5alpha-JTM001 800 µl bacterial growth + 300 µl 100% autoclaved glycerol → Vortex → thrown in Liq. N → stored at -80ºC
Diagnostic KpnI digestion
2.5 µl DNA + 2 µl 10x bu. + 0.2 µl BSA + 0.5 µl HindIII (NEB), ad 20 µl H2O → 1.5 h 37ºC Expected fragments: JTM001-a/ *Kpn*I: 5.2, 2.3 kb; uncut 4.4 kb plasmid if empty pDONR201
Sequencing of JTM001-b JHI in-house*; primers** DONRfor, DONRrev, attB-MTrev, attB-HELfor, attB-HELrev, attB-POLfor, L61-453Kpnfor, L61-2800Kpnrev, L61-3520for, attB-LINKrev and attB-LINKfor * 6µl pDNA (100-200 ng/µl) submitted per each 2 ul primer

Appendix 36. LR recombination of PVX 165-nostopcodon into pGWB405

LR recombination
5 µl reactions 0.5 µl undiluted entry clone* + 0.5 µl undiluted destination vector** + 3 µl TE pH8 buffer + 1 µl LR recombinase. o/n 25ºC → 30 min 70ºC → kept on 4ºC * JTM001-b (~75 ng/ diluted using TE pH8 buffer), **into pGWB405 (C-terminal GFP)

Appendix 37. Purification and bulking of the pGWB405/PVX 165-nostopcodon(-GFP) 165k-GFP or JTM002.

E.coli transformations
1 µl LR into 50 µl chemically-competent DH5alpha (Invitrogen "Library Efficiency"), incubated on ice in 0.5 ml tube for 30 min, heat-shock at 42ºC for 45 sec, re-suspended in 200 µl SOC → 1h 37ºC → plated 50 µl, 100 µl on LB-Spec.
Culture growth for plasmid minipreps 4 picked colonies of *JTM002(a,b,c and d)* are inoculated in 4 ml LB-Spec→ o/n 37ºC with shaking. *no colony-PCR
Plasmid minipreps of JTM002 QIAgen kit, eluted in 50 µl EB → JTM002
Glycerol preservation of DH5alpha-JTM002 800 µl bacterial growth + 300 µl 100% autoclaved glycerol → Vortex → thrown in Liq. N → stored at -80ºC
Diagnostic KpnI digestion
2.5 µl DNA + 2 µl 10x bu. + 0.2 µl BSA + 0.5 µl HindIII (NEB), ad 20 µl H2O → 1.5 h 37ºC Expected fragments: JTM002-c/ *Kpn*I: 12792 + 2326 bp fragment release pGWB405 does not have any KpnI sites so empty vector will not be digested at all. pGWB405.165k recombinants should fragment into 12792 + 2326 bp.

Appendix 38. Agrobacterium transformation of JTM002

AGL1 transformations
2 µl Plasmid DNA* into 40 µl electroporant AGL1 (home-made Aliquots), incubated on ice in cuvette for 30 min before zapping, slight click when zapped at 1800 V**, resuspended in 900 µl LB → 2 h 37ºC → plated 30 µl on LB-SPEC *JTM002-c **And at zapped at 2800 V*
Glycerol preservation of AGL1-JTM002c 800 µl bacterial growth + 300 µl 100% autoclaved glycerol → Vortex to homogenate → thrown in Liq. N → stored at -80ºC
Culture growth for agroinoculation a colony is inoculated in 5 ml LB-Spec/Rif→ 2 days 28ºC with shaking.

Appendix 39. Agroinoculation of JTM002

Agroinoculation
Agrobacteria culture → spin 4000rpm 15 min → resuspend pellets → 2 ml infiltration* → 1h in dark → dilute in 10 ml up to OD600 of 0.25A for most fusion proteins, and 0.1A for P19k Measuring OD600 for AGL1 infiltrate using the UV-Spectrometer: 50 µl of infiltration solution as blank read. Dilute the bacterial growth 1/10 (5ul bacterial growth + 45ul infiltration medium). Measure OD 600 of the dilutes which calculates for a "real" OD600 of 10X of the measurement values. *Infiltration medium: (bacterial suspensions in this infiltration media are kept in dark) 100 µl 1M MgCl2 + 200 µl 0.5M MES + 15µl Acetosyringone, ad 10 ml H2O